

MEDIAN NERVE DEFORMATION AND DISPLACEMENT INCREASE IN CONCERT
DURING GRIP TASKS IN THE TRANSVERSE PLANE OF THE CARPAL TUNNEL

Gabrielle Racine

Master of Science in Kinesiology
Nipissing University
2021

MEDIAN NERVE DEFORMATION AND DISPLACEMENT INCREASE IN CONCERT
DURING GRIP TASKS IN THE TRANSVERSE PLANE OF THE CARPAL TUNNEL

by

GABRIELLE RACINE

BPHE, Nipissing University, 2017

A THESIS SUBMITTED IN PARTIAL FULFILLMENT OF THE
REQUIREMENTS FOR THE DEGREE OF

MASTER OF SCIENCE IN KINESIOLOGY

in

THE SCHOOL OF GRADUATE STUDIES

NIPISSING UNIVERSITY

May 2021

© Gabrielle Racine, 2021

Certificate of Examination**Supervisor(s):**

Dr. Aaron Kociolek

Examiner(s)

Dr. Nicholas La Delfa

Supervisory Committee:

Dr. Dean Hay

Dr. Alison Schinkel-Ivy

The _____ thesis _____ by

Gabrielle Racine

entitled

MEDIAN NERVE DEFORMATION AND DISPLACEMENT INCREASE IN CONCENTRIC DURING GRIP
TASKS IN THE TRANSVERSE PLANE OF THE CARPAL TUNNEL

is accepted in partial fulfillment of the requirements for the degree of

Master of Science in Kinesiology

January 22, 2021

Date

Dr. Mark Bruner

Chair of the Examination Committee

Signature

Abstract

Introduction: Finger exertions involved in gripping tasks cause the flexor tendons in the carpal tunnel to migrate palmarly, thus decreasing the distances between the flexor tendons and transverse carpal ligament. This interaction may also influence passive carpal tunnel structures, including the median nerve (MN). However, it remains unclear as to what extent deformation of the nerve is related to tendon dynamics. **Objective:** We evaluated the effect of gripping on both MN deformation and displacement relative to the flexor tendons in the carpal tunnel. **Methods:** Fourteen right-handed participants ramped isometric force up to 50% of maximum voluntary effort (MVE) before ramping force back down to 0% MVE in 3 grip types (power, chuck, and pulp). Grip forces were measured with a digital dynamometer while the transverse plane of the carpal was imaged via ultrasonography. MN images were analyzed in increments of 10% MVE during both the ramp up and ramp down phases of the trials to determine its cross-sectional area, circularity, width, and height as well as relative displacement between the MN and flexor digitorum superficialis tendon of the middle finger (FDS_M) in both the radial-ulnar (X-) and palmar-dorsal (Y-) axes. **Results:** While there was very little change in cross-sectional area of the MN, deformation was observed including time-dependent changes in width, height, and circularity. For example, there was a significant interaction between grip force level and ramp force direction on width ($F_{5,55}=3.78, p=0.005$). During the ramp up phase, MN width decreased from 0% to 20% MVE with very little change from 20% to 50% MVE, which was best described by a quadratic trend ($p<0.001$). However, during the ramp down phase, MN width gradually increased from 50% to 0% MVE, which best fit a linear trend ($p=0.014$). Relative changes were also particularly interesting, since the width decrease during ramping force up from 0%-50% MVE did not correspond to the width increase during ramping force down from 50%-0% MVE

(ramp up – 9.2% decrease; ramp down – 5.6% increase). While time-dependent effects were also observed for height, the trends were reversed; height increased during the ramp up phase and decreased during the ramp down phase. Accordingly, the MN became more circular when grip force was ramped up from 0% to 50% MVE and less circular when grip force was ramped down from 50% to 0% MVE ($F_{2,22}=9.95, p=0.001$). Interestingly, MN displacement also changed in a time-dependent manner, and these results generally mirrored those observed for deformation metrics. For example, there was a significant interaction between grip force level and ramp force direction on relative displacement between the MN and FDS_M in the palmar-dorsal axis ($F_{2.08,22.88}=4.15, p=0.028$). During ramp up, MN position was 1.07 ± 0.21 mm palmar to the FDS_M at 0% MVE, and subsequently migrated dorsally with a MN position of 0.60 ± 0.22 mm palmar to the FDS_M at 20% MVE, corresponding to a positional change of 80%. There was no further change from 20% to 50% MVE, representing a quadratic trend with grip force level during the ramp up phase ($p<0.001$). Conversely, the nerve migrated palmarly during the ramp down ($p=0.001$). However, the percent change was considerably smaller (39%), such that the nerve did not return to its original position at the beginning of the trial. **Conclusions:** MN deformation and displacement metrics both changed in a time-dependent manner, including differences in ramping force up versus down. This suggests MN deformation is linked to its displacement within the carpal tunnel. In addition, the time-dependent trends observed in the transverse plane of the carpal tunnel mirror previous research demonstrating viscoelastic characteristics of flexor tendon and surrounding subsynovial connective tissue. This finding lends further support for an injury mechanism related to subsynovial fibrosis, thereby altering MN dynamics within the carpal tunnel, resulting in increased local strain and eventually nerve entrapment.

Acknowledgments

There are so many people I would like to thank that have helped me tremendously throughout my time completing my Master of Science in Kinesiology. First and foremost, I would like to thank Dr. Aaron Kociolek. Thank you for giving me this opportunity and for all your guidance over the years. I can truly say I would not be where I am today without your mentorship. You have been an amazing supervisor and I feel very fortunate to have worked with you. I cannot thank you enough! All faculty members in the Bachelor of Physical and Health Education and the Master of Science in Kinesiology programs, thank you so much for your support over the years. I truly enjoyed learning from all of you. Dr. Michael Holmes, thank you for hosting us at Brock University and for allowing us to use your lab space and research equipment. Dr. Alison Shinkel-Ivy and Dr. Dean Hay, thank you for your continued guidance on my research. Dr. Nicholas La Delfa, thank you for serving as the external thesis examiner and your insights at my defense. Kevin O'Reilly, thank you for all your help with my project, but most of all thank you for always making a pot of coffee in the lab. Kaylyn Turcotte, thank you for your companionship during conferences and our trips to Brock. It would not have been the same experience without you! Finally, I would like to dedicate this project to my grandfather who passed earlier in the year. I know he would be very proud of this achievement.

Table of Contents

Certificate of Examination.....	iii
Abstract.....	iv
Acknowledgments.....	vi
Table of Contents.....	vii
List of Tables.....	ix
List of Figures.....	x
List of Abbreviations.....	xiv
 Chapter 1: Introduction.....	 1
Chapter 2: Review of Literature.....	4
2.1 Wrist and Hand Musculoskeletal Disorders.....	4
2.2 Anatomy of the Carpal Tunnel.....	6
2.3 Injury Mechanisms of Carpal Tunnel Syndrome.....	10
2.4 Occupational Risk Factors.....	11
2.5 Longitudinal Ultrasound Studies of the Carpal Tunnel.....	12
2.6 Transverse Ultrasound Studies of the Carpal Tunnel.....	13
2.7 Grip Types in Occupational Settings.....	18
 Chapter 3: Summary of Literature.....	 20
Chapter 4: Purposes and Hypotheses.....	22
4.1 Purposes.....	22
4.2 Hypotheses.....	22
Chapter 5: Methods.....	23
5.1 Participants.....	23
5.2 Experimental Set-up.....	24
5.3 Experimental Protocol.....	26
5.3.1 Maximum Voluntary Efforts.....	26
5.3.2 Grip Force Ramp Trials.....	27
5.4 Data Collection.....	29
5.5 Data Analysis.....	30
5.6 Statistical Analysis.....	31
Chapter 6: Results.....	33
6.1 Maximum Voluntary Efforts (MVEs) and Grip Forces.....	33
6.2 Median Nerve Deformation.....	33
6.2.1 Cross-Sectional Area (CSA).....	33
6.2.2 Perimeter.....	35
6.2.3 Width.....	38
6.2.4 Height.....	41
6.2.5 Circularity.....	44
6.3 Median Nerve Relative Displacement.....	48

6.3.1	Radial-Ulnar (X-) Axis.....	48
6.3.2	Palmar-Dorsal (Y-) Axis.....	52
Chapter 7:	Discussion.....	57
Chapter 8:	Conclusion.....	68
Chapter 9:	References.....	69
Appendix A:	Nipissing University and Brock University Research Ethics Certificates.....	77
Appendix B:	Participant Information Letter and Informed Consent.....	86
Appendix C:	Screening Questionnaire.....	91
Appendix D:	Grip Forces During the Experimental Trials.....	95
Appendix E:	Within Subject Effects from Repeated Measures ANOVA.....	97
Appendix F:	Median Nerve and Flexor Tendon Positions in the Carpal Tunnel.....	102
Appendix G:	Copyright Permission for Figure 2.1.....	109

List of Tables

Table 2.1	Methodological considerations for ultrasound imaging studies of the carpal tunnel in the transverse plane.....	16
Table 5.1	Mean (SD) participant characteristics.....	23
Table 6.1	Mean (\pm standard error of the mean) of the MVEs for the 3 grip types (N).....	33
Table D.1	Mean (\pm standard error of the mean) grip forces extracted in both absolute (N) and relative (%) terms while ramping force up from 0%-50% MVE and ramping force down from 50%-0% MVE during the 6-second trapezoidal force profiles (2-second ramp up, 2-second plateau, 2-second ramp down).....	96
Table E.1	Tests of within-subject effects for median nerve cross-sectional area.....	98
Table E.2	Tests of within-subject effects for median nerve perimeter.....	98
Table E.3	Tests of within-subject effects for median nerve width.....	99
Table E.4	Tests of within-subject effects for median nerve height.....	99
Table E.5	Tests of within-subject effects for median nerve circularity.....	100
Table E.6	Tests of within-subject effects for median nerve position relative to the flexor digitorum superficialis tendon of the middle finger in the radial-ulnar (X-) axis.....	100
Table E.7	Tests of within-subject effects for median nerve position relative to the flexor digitorum superficialis tendon of the middle finger in the palmar-dorsal (Y-) axis.....	101

List of Figures

Figure 2.1	Transverse section of the carpal tunnel within the left wrist at the hamate level. Note: N – Median Nerve, FDS – Flexor digitorum superficialis, SSCT – subsynovial connective tissue, FPL – Flexor pollicis longus, FDP – Flexor digitorum profundus, FR – Flexor retinaculum, CB – Carpal bones, VS – Visceral synovium, PS – Parietal synovium. <i>Note: Image reproduced from Ettema et al., 2007 (page 293) with the permission of John Wiley and Sons.....</i>	8
Figure 2.2	Theoretical model of gliding patterns between the flexor digitorum superficialis (FDS) tendon and surrounding subsynovial connective tissue (SSCT) inside the carpal tunnel during the loading phase with proximal tendon displacement (wrist/finger flexion) and the unloading phase with distal tendon displacement (wrist/finger extension). <i>Note: FDS tendon – Solid blue line, Visceral synovium – Dashed blue line, SSCT layers and interconnecting fibrils – Gray lines; Image belongs to the author.....</i>	9
Figure 2.3	Common grip types used to complete various occupational tasks. The pulp pinch involves the index and opposing thumb. The chuck pinch involves the index, middle and opposing thumb. The power grip involves the use of all the digits to form a fist. <i>Note: Images belong to the author.....</i>	19
Figure 5.1	Custom built testing apparatus supporting the right distal upper limb of the participant. Adjustable features allowed the grip dynamometer to translate in 3 axes (superior-inferior, proximal-distal, medial-lateral) and rotate about 1 axis (medial-lateral) to enable interaction with the participant. The ultrasound probe was positioned at the base of the wrist using a three-prong clamp attached to a locking ball and socket joint. <i>Note: Image belongs to the author.....</i>	25
Figure 5.2	Experimental set-up with the wrist in the 0° neutral wrist position and the 30° flexed wrist position (inset). <i>Note: Images belong to the author.....</i>	26
Figure 5.3	Online display of the force matching task. For each gripping trial, participants received real-time force feedback (white) while tracing trapezoidal force profiles (red). <i>Note: Image belongs to the author.....</i>	28
Figure 5.4	Online display of the force matching task. The X's represent where ultrasound images were extracted along the gripping trials. <i>Note: Image belongs to the author.....</i>	31
Figure 6.1	Mean (\pm standard error of the mean) MN CSA during the ramp up and ramp down phases of force for the three grip types. <i>Note: Asterisk indicates a significant difference.....</i>	34
Figure 6.2	Mean (\pm standard error of the mean) MN perimeter during the three grip types. <i>Note: Asterisk indicates a significant difference.....</i>	35

Figure 6.3	Mean (\pm standard error of the mean) MN perimeter with grip force production..	36
Figure 6.4	Mean (\pm standard error of the mean) MN perimeter during the ramp up and ramp down phases throughout grip force production.....	37
Figure 6.5	Mean (\pm standard error of the mean) MN width during the three grip types. <i>Note: Asterisk indicates a significant difference</i>	38
Figure 6.6	Mean (\pm standard error of the mean) MN width during grip force production.....	39
Figure 6.7	Mean (\pm standard error of the mean) MN width during the ramp up and ramp down phases throughout grip force production.....	40
Figure 6.8	Mean (\pm standard error of the mean) MN height during the three grip types. <i>Note: Asterisk indicates a significant difference</i>	41
Figure 6.9	Mean (\pm standard error of the mean) MN height during grip force production...	42
Figure 6.10	Mean (\pm standard error of the mean) MN height while ramping force up and ramping force down for the three grip types. <i>Note: Asterisk indicates a significant difference</i>	43
Figure 6.11	Mean (\pm standard error of the mean) MN circularity during the three grip types. <i>Note: Asterisk indicates a significant difference</i>	45
Figure 6.12	Mean (\pm standard error of the mean) MN circularity during grip force production.....	46
Figure 6.13	Mean (\pm standard error of the mean) MN circularity during the ramp up and ramp down phases throughout grip force production.....	47
Figure 6.14	Mean (\pm standard error of the mean) median nerve (MN) position relative to the flexor digitorum superficialis tendon of the middle finger (FDS _M) in the X-axis during grip force production. <i>Note: + indicates ulnar position; – indicates radial position</i>	49
Figure 6.15	Mean (\pm standard error of the mean) median nerve (MN) position relative to the flexor digitorum superficialis tendon of the middle finger (FDS _M) in the X-axis during ramp up versus ramp down. <i>Note: Asterisk indicates a significant difference; + indicates ulnar position; – indicates radial position</i>	50
Figure 6.16	Mean (\pm standard error of the mean) median nerve (MN) position relative to the flexor digitorum superficialis tendon of the middle finger (FDS _M) in the X-axis during the ramp up and ramp down phases throughout grip force production. <i>Note: + indicates ulnar position; – indicates radial position</i>	51

Figure 6.17	Mean (\pm standard error of the mean) median nerve (MN) position relative to the flexor digitorum superficialis tendon of the middle finger (FDS _M) in the Y-axis with different grip types. <i>Asterisk indicates a significant difference; Note: + indicates palmar position; – indicates dorsal position</i>	52
Figure 6.18	Mean (\pm standard error of the mean) median nerve (MN) position relative to the flexor digitorum superficialis tendon of the middle finger (FDS _M) in the Y-axis during grip force production. <i>Note: + indicates palmar position; – indicates dorsal position</i>	53
Figure 6.19	Mean (\pm standard error of the mean) median nerve (MN) position relative to the flexor digitorum superficialis tendon of the middle finger (FDS _M) in the Y-axis during three different grip types throughout grip force production. <i>Note: + indicates palmar position; – indicates dorsal position</i>	55
Figure 6.20	Mean (\pm standard error of the mean) median nerve (MN) position relative to the flexor digitorum superficialis tendon of the middle finger (FDS _M) in the Y-axis during the ramp up and ramp down phases throughout grip force production. <i>Note: + indicates palmar position; – indicates dorsal position</i>	56
Figure F.1	Mean position of the median nerve (red x) located ulnarly to the flexor digitorum superficialis tendons of the index and middle fingers (purple +) and dorsally to the transverse carpal ligament (blue •) while ramping force up to (a) 0% MVE, (b) 10% MVE, (c) 20% MVE, (d) 30% MVE, (e) 40% MVE, and (f) 50% MVE during the pulp pinch gripping condition.....	103
Figure F.2	Mean position of the median nerve (red x) located ulnarly to the flexor digitorum superficialis tendons of the index and middle fingers (purple +) and dorsally to the transverse carpal ligament (blue •) while ramping force down to (a) 50% MVE, (b) 40% MVE, (c) 30% MVE, (d) 20% MVE, (e) 10% MVE, and (f) 0% MVE during the pulp pinch gripping condition.....	104
Figure F.3	Mean position of the median nerve (red x) located ulnarly to the flexor digitorum superficialis tendons of the index and middle fingers (purple +) and dorsally to the transverse carpal ligament (blue •) while ramping force up to (a) 0% MVE, (b) 10% MVE, (c) 20% MVE, (d) 30% MVE, (e) 40% MVE, and (f) 50% MVE during the chuck pinch gripping condition.....	105
Figure F.4	Mean position of the median nerve (red x) located ulnarly to the flexor digitorum superficialis tendons of the index and middle fingers (purple +) and dorsally to the transverse carpal ligament (blue •) while ramping force down to (a) 50% MVE, (b) 40% MVE, (c) 30% MVE, (d) 20% MVE, (e) 10% MVE, and (f) 0% MVE during the chuck pinch gripping condition.....	106
Figure F.5	Mean position of the median nerve (red x) located ulnarly to the flexor digitorum superficialis tendons of the index and middle fingers (purple +) and dorsally to the transverse carpal ligament (blue •) while ramping force up to (a) 0% MVE, (b) 10%	

MVE, (c) 20% MVE, (d) 30% MVE, (e) 40% MVE, and (f) 50% MVE during the power gripping condition.....107

Figure F.6 Mean position of the median nerve (red x) located ulnarly to the flexor digitorum superficialis tendons of the index and middle fingers (purple +) and dorsally to the transverse carpal ligament (blue •) while ramping force down to (a) 50% MVE, (b) 40% MVE, (c) 30% MVE, (d) 20% MVE, (e) 10% MVE, and (f) 0% MVE during the power gripping condition.....108

List of Abbreviations

ANOVA:	Analysis of variance
CSA:	Cross-sectional area
CTD:	Cumulative trauma disorder
CTP:	Carpal tunnel pressure
CTS:	Carpal tunnel syndrome
FDP:	Flexor digitorum profundus
FDS _I :	Flexor digitorum superficialis of index finger
FDS _M :	Flexor digitorum superficialis of middle finger
MN:	Median nerve
MSD:	Musculoskeletal disorder
MVE:	Maximum voluntary effort
MVR:	Maximum velocity ratio
NIOSH:	National Institute for Occupational Safety and Health
RSI:	Repetitive strain disorder
SSCT:	Subsynovial connective tissue
TCL:	Transverse carpal ligament
WMSD:	Work-related musculoskeletal disorder
WSIB:	Workers Safety Insurance Board

Chapter 1

Introduction

Musculoskeletal disorders (MSDs) of the wrist and hand are common in the workplace and have a profound impact on worker performance as well as quality of life outside the workplace (Zambrosky et al., 2017). Hand impairment, in particular, negatively influences quality of life due to the use of the hands in essential quotidian tasks. Wrist and hand MSDs burden not only individual workers, but also employers and insurers due to recurring symptoms and the percentage of claims that require surgery and rehabilitation (Manktelow et al., 2004; Silverstein et al., 1998). Numerous epidemiologic studies have associated physical workplace factors with the prevalence of wrist and hand MSDs, such as forceful exertions, repetitive motions, and non-neutral postures (Armstrong & Chaffin, 1979; Bernard & Putz-Anderson, 1997; Kutluhan et al., 2001; Palmer et al., 2007; Silverstein et al., 1987). While these physical factors are known to increase the risk of MSDs, underlying injury pathways are still not well understood for even well-defined disorders such as carpal tunnel syndrome (CTS).

CTS is the most frequently reported peripheral neuropathy of the upper limb and is often preceded by finger flexor tendinopathies. A common pathology in these patients is non-inflammatory fibrosis and thickening of the subsynovial connective tissue (SSCT) that surrounds the tendons and median nerve (MN) within the carpal tunnel (Ettema et al., 2008). SSCT fibrosis increases the volume of carpal tunnel contents, which alters carpal tunnel mechanics, including tendon and nerve displacement (Ettema et al., 2008; Ghasemi-rad et al., 2014; van Doesburg et al., 2012a; van Doesburg et al., 2012b). Physical risk factors in ergonomics are also known to alter tendon and nerve motion (Kociolek & Keir, 2015; Kociolek et al., 2015; Kociolek & Keir, 2016;

Tat et al., 2013; Tat et al., 2015). Therefore, the accumulation of SSCT strain and shear over time may account for the fibrotic changes observed in patients with CTS.

Several studies have used ultrasound to observe changes in the carpal tunnel during different wrist and finger movements. Researchers have investigated movement and deformation of carpal tunnel structures, both longitudinally (Kociolek & Keir, 2015; Korstanje et al., 2010a; Korstanje et al., 2010b; Korstanje et al., 2012; Soeters et al., 2004; Tat et al., 2015) and in the transverse plane of the carpal tunnel (Cowley et al., 2017; Filius et al., 2013; Gabra et al., 2016; Greening et al., 2001; Loh & Muraki, 2015; Lopes et al., 2011; Nanno et al., 2015; van Doesburg et al., 2010; Wang et al., 2014; Yoshii et al., 2009). A particularly large focus in the literature compares CTS patients to healthy controls performing different finger movements. For example, van Doesburg et al. (2012a) observed significantly greater distances between the MN and flexor digitorum superficialis tendon of the long finger during both index finger and thumb motions for patients with CTS.

More recently, researchers have studied the effects of forceful gripping on deformation of the MN in the transverse carpal tunnel (Loh et al., 2016; Woo et al., 2016; Woo et al., 2019). In one study, Cowley et al. (2017) found that MN circularity increased during gripping tasks when the wrist was flexed. While these changes suggest an injury mechanism of strain and/or stress on the MN, the underlying causes of deformation were not investigated. One plausible explanation may relate to the dynamic interaction between the MN and finger flexor tendons. During forceful tasks, the finger flexor tendons develop active tension and migrate palmarly (Nanno et al., 2015; Yoshii et al., 2009), which might displace the MN within the carpal tunnel and increase strain and/or stress depending on its new position. However, further research is needed to explore the relationship between MN displacement and deformation. More specifically, assessing both MN

deformation and displacement relative to other carpal tunnel structures throughout the entire time course of loading and unloading the fingertips during forceful gripping tasks may elucidate the underlying causes of deformational changes to the MN.

Chapter 2

Review of Literature

2.1 Wrist and Hand Musculoskeletal Disorders

Musculoskeletal disorders (MSDs) of the wrist and hand are prevalent in the workplace due to their frequent use in work tasks involving object manipulation and forceful grasp (Bernard & Putz-Anderson, 1997; Palmer et al., 2007). While carpal tunnel syndrome (CTS) is the most frequently reported neuropathy of the wrist/hand, common precursors include finger flexor tendinopathies, such as tendinitis, tendonosis and tenosynovitis (Barr et al., 2004). The latter disorders may develop due to repetitive tendon sliding in the carpal tunnel (Heilskov-Hansen et al., 2016).

CTS is the most frequently reported peripheral neuropathy due to, in part, well-established clinical diagnosis guidelines (Kaymak et al., 2008). Patients with CTS experience swelling from inflammation, pain, numbness, and paresthesia as well as loss of dexterity and weakness of the hand (Ugbolue et al., 2005). These symptoms not only affect worker performance, but also negatively influence quality of daily living considering hand use is essential in numerous quotidian tasks. Since symptoms are often exacerbated at night, patients commonly suffer from sleep deprivation, which not only affects physical performance but also has negative psychological impacts (Zamborsky et al., 2017).

CTS is commonly categorized as a work-related musculoskeletal disorder (WMSD), repetitive strain injury (RSI), or cumulative trauma disorder (CTD), implying injury results from the accumulation of loading over time. Although the underlying injury pathway is not well-understood and likely multifactorial (Roquelaure et al., 1997), CTS ultimately results from median nerve (MN) compression (Kubo et al., 2018). This compression may arise due to an increase in

the volume of carpal tunnel contents or a decrease in the size of the carpal tunnel, both of which increase hydrostatic pressure within the carpal tunnel and compress the median nerve (Keir et al., 1998; Keir et al., 2007).

Patients with finger flexor tendinitis experience similar symptoms. Although the criterion for clinical diagnosis varies in the literature (Bernard & Putz-Anderson, 1997), tendinitis may include swelling along the tendon, pain with resisted motion, and even tendon locking with a palpable node. Tenosynovitis is also an inflammatory disease; however, the injury is mainly to the synovial sheath around the tendon with similar symptoms occurring to that area (Giovagnorio, 1997). Unlike tendinitis and tenosynovitis, tendinosis involves the degeneration of tendon without inflammation but yields similar symptoms.

According to the Workplace Safety and Insurance Board (WSIB) of Ontario, annual lost time claims for the wrist, hand, and fingers averaged 7,865 between 2012 and 2016, accounting for 14.4% of all lost time claims (WSIB, 2016). Furthermore, these claims are also attributed with the longest absences from work due to the high percentage of cases that require surgery (Barr et al., 2004; Manketlow et al., 2004; Zakaria, 2004). The costs associated with these disorders cause social and economic burdens on employees and employers. While claims costing is scarce, Manketlow et al. (2004) reported that one worker with CTS costs the WSIB an average of \$13,200 (CAD), with the largest expense attributed to lost time from work. However, these estimates are associated with direct costs and do not account for the numerous indirect costs associated with injury, such as time to train a replacement employee and decreased workplace productivity.

2.2 Anatomy of the Carpal Tunnel

There are several structures within the carpal tunnel that function reciprocally to generate wrist and hand movements (Figure 2.1). Eight carpal bones in two rows are located on the dorsal border of the carpal tunnel, which include: the trapezium, trapezoid, capitate, and hamate (distal row); and the scaphoid, lunate, pisiform, and triquetrum (proximal row). The transverse carpal ligament (TCL) forms the palmar border, or the roof, of the carpal tunnel, attaching to the scaphoid and trapezium bones on the radial side, and the pisiform and hook of the hamate on the ulnar side (Saladin, 2007). The TCL is a thick and fibrous ligament that provides a mechanical advantage to the flexor tendons passing through the carpal tunnel, functioning as a pulley to reduce tendon displacements while preventing bowstringing during wrist flexion (Armstrong & Chaffin, 1979). However, the TCL may also cause contact stress (perpendicular force per unit area) with the median nerve and tendons as they move palmarly during wrist or finger flexion (Armstrong & Chaffin, 1979; Gabra et al., 2016). The tendons passing through the carpal tunnel primarily produce metacarpophalangeal joint, proximal interphalangeal joint, and distal interphalangeal joint flexion while also assisting with wrist flexion and include: four flexor digitorum superficialis (FDS) tendons (1 for each finger), four flexor digitorum profundus (FDP) tendons (1 for each finger), and 1 flexor pollicis longus (FPL) tendon of the thumb. The median nerve (MN) is located near the palmar and radial borders in the carpal tunnel and separates into two branches at the level of the hamate that innervates the thenar muscles, palmar surface of the hand, and three lateral fingertips (Saladin, 2007).

The subsynovial connective tissue (SSCT) is an important structure that surrounds the finger flexor tendons and the MN inside the carpal tunnel, thereby facilitating tendon and nerve gliding (Filius et al., 2017). It is composed of multiple layers of collagen bundles interconnected

by vertical fibrils that allow for sequential recruitment of adjacent layers during longitudinal tendon and nerve displacement (Guimberteau et al., 2010), with the deep layers (closer to tendon/nerve) moving first, followed by superficial layers (further from tendon/nerve). The collagen layers are surrounded by a gel-like interfibrillar matrix, which gives the structure viscoelastic properties (Guimberteau et al., 2010). Specifically, like other viscoelastic materials, the SSCT becomes deformed with applied force, and this deformation is dependent on the rate of loading thereby demonstrating time-dependent properties (Gould et al., 2019). Using ultrasound, Tat et al. (2013) demonstrated time-dependent changes in the relative displacement between the FDS tendon and SSCT. It was hypothesized that during proximal tendon displacements associated with wrist/finger flexion, SSCT layers were loaded sequentially through their inter-connecting fibrils (Figure 2.2). However, during distal tendon displacements associated with wrist/finger extension, the SSCT layers unloaded at a uniform rate. Furthermore, Filius et al. (2014) reported that SSCT strain (change in length relative to its resting length) during larger tendon displacements and velocities resulted in increased gliding resistance energy. For example, peak forces and resistance energy were 1.7-4.2 times greater in higher velocities versus lower velocities (60 mm/s versus 2 mm/s) owing to viscoelastic shear (energy loss due to friction). This finding suggests that while the SSCT is vital for tendon function, its threshold for injury may be lowered by greater tendon/nerve displacements and/or velocities due to viscoelastic strain and shear.

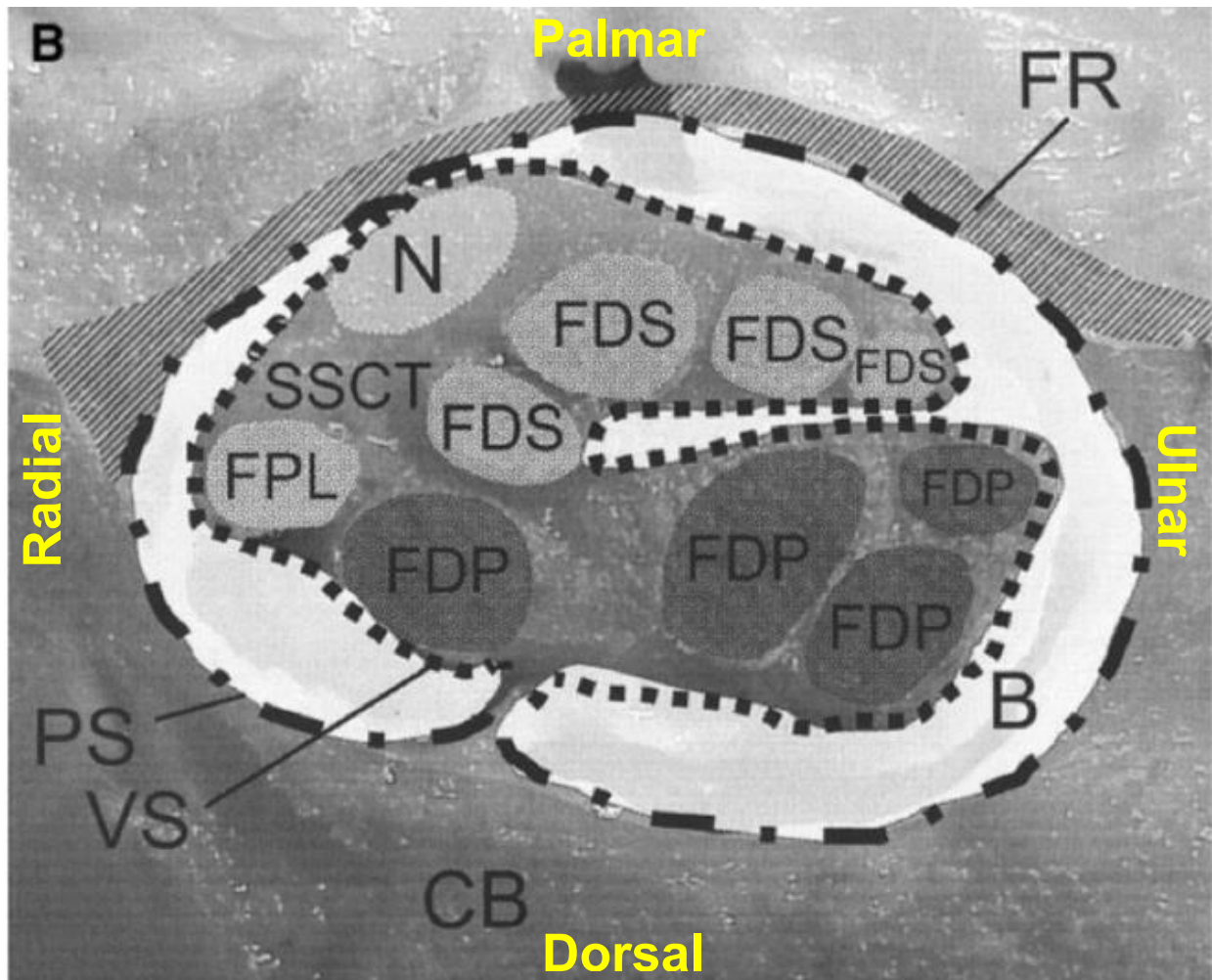


Figure 2.1. Transverse section of the carpal tunnel within the left wrist at the hamate level. Note: N – Median Nerve, FDS – Flexor digitorum superficialis, SSCT – subsynovial connective tissue, FPL – Flexor pollicis longus, FDP – Flexor digitorum profundus, FR – Flexor retinaculum, CB – Carpal bones, VS – Visceral synovium, PS – Parietal synovium. *Note: Image reproduced from Ettema et al., 2007 (page 293) with the permission of John Wiley and Sons.*

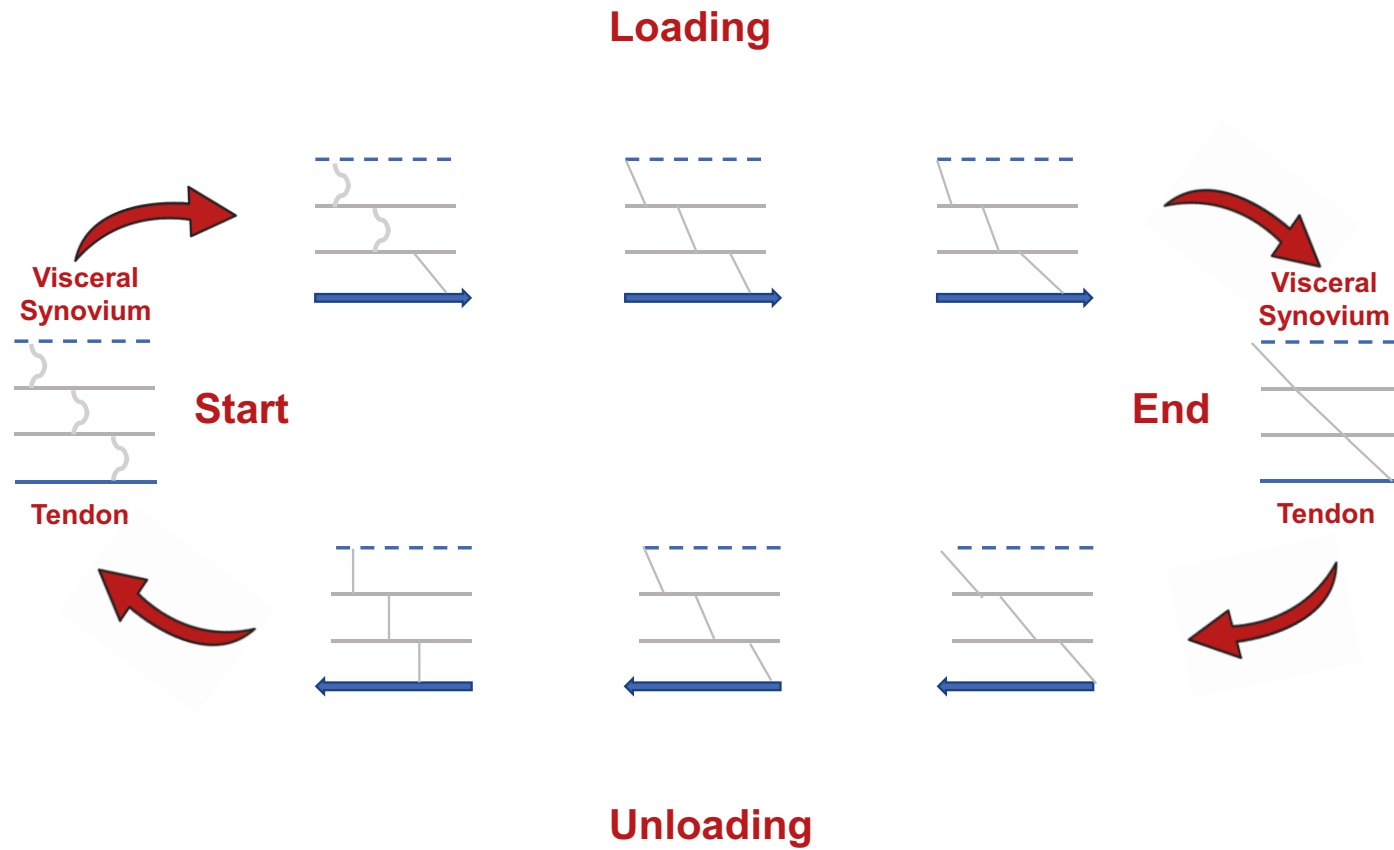


Figure 2.2. Theoretical model of gliding patterns between the flexor digitorum superficialis (FDS) tendon and surrounding subsynovial connective tissue (SSCT) inside the carpal tunnel during the loading phase with proximal tendon displacement (wrist/finger flexion) and the unloading phase with distal tendon displacement (wrist/finger extension). *Note: FDS tendon – Solid blue line, Visceral synovium – Dashed blue line, SSCT layers and interconnecting fibrils – Gray lines; Image belongs to the author.*

2.3 *Injury Mechanisms of Carpal Tunnel Syndrome*

Carpal tunnel syndrome (CTS) is considered an entrapment neuropathy; median nerve (MN) compression is caused by elevated hydrostatic pressure within the carpal tunnel and has numerous damaging effects, both physiologically and to sensorimotor function. Pressures above 30 mmHg may cause neurophysiological changes while pressures above 60 mmHg may cause complete sensory conduction block (Lundborg et al., 1982). It has been reported that CTS patients have a carpal tunnel pressure (CTP) above 30 mmHg in a neutral wrist posture, whereas healthy controls generally have pressures less than 10 mmHg (Keir et al., 2007).

While it is well-known that CTS patients have an elevated CTP, the underlying mechanical causes are complex and multi-factorial. Patients with CTS have noticeable changes to the subsynovial connective tissue (SSCT). CTS patients appear to undergo a process of non-inflammatory remodeling, which includes a re-organization of irregular collagen bundles, resulting in the thickening and fibrosis of the SSCT. These changes ultimately increase the volume within the carpal tunnel, which in turn increases CTP (Donato et al., 2009; Festen-Schrier & Amadio, 2018, Rempel et al., 1997). As the SSCT encompasses more space, the other structures within the carpal tunnel must accommodate, causing their deformation such as compression of the MN. Researchers have also observed additional changes to both longitudinal (Korstanje et al., 2012) and transverse (Cowley et al., 2017; Filius et al., 2013; Greening et al., 2001; Lopes et al., 2011; Nanno et al., 2015; van Doesburg et al., 2010) tendon and nerve displacement. For instance, the MN in healthy individuals moves dorsally in the carpal tunnel during wrist flexion while the MN in CTS patients is restricted, therefore minimizing translation during tendon loading and leading to compression (Festen-Schrier & Amadio, 2018). Additionally, fibrosis of the SSCT may increase strain and shear with adjacent structures (Tat et al., 2013), which may also cause further changes

to the SSCT and CTP. While both MN deformation and displacement have been investigated individually, there remains a need to study these metrics in concert to determine the inter-relationships within the development of work-related CTS.

2.4 Occupational Risk Factors

Forceful tasks, repetitive movements, fast work pace, and non-neutral postures as well as exposure to hand-transmitted vibration and extreme temperatures all increase the risk of developing wrist and hand MSDs (Punnett & Wegman, 2004; Bernard & Putz-Anderson, 1997). In a systematic review undertaken by the National Institute of Occupational Safety and Health (NIOSH), there was strong evidence that forceful and repetitive tasks were individually associated with the development of CTS (Bernard & Putz-Anderson, 1997). Silverstein et al. (1987) reported high force jobs with loads above 4 kg were 2.9 times more likely to develop CTS than low force jobs irrespective of repetition, whereas highly repetitive tasks performed in less than 30 seconds per cycle were 5.5 times more likely to develop CTS than low repetition tasks irrespective of force. Remarkably, a combination of high force and high repetition increased CTS risk by 15.5 times compared to low force and low repetition tasks, demonstrating that a combination of risks factors multiplicatively increased the prevalence of MSD. In another study by Chiang et al. (1990), 207 workers from frozen food industries exposed to highly repetitive tasks and cold temperatures had a CTS prevalence of 37%, further demonstrating an interaction between physical and environmental exposures.

Although NIOSH found insufficient evidence for wrist and hand posture as an independent risk factor, there was strong evidence of a relationship between posture combined with any other risk factor and CTS (Bernard & Putz-Anderson, 1997). Harris-Adamson et al. (2014) further

demonstrated that combining posture with other physical risk factors increased the risk of developing wrist MSDs. For example, forceful gripping and wrist flexion of only 7° in the “high exposure group” increased the risk of wrist tendinosis by 2.69 times compared to forceful gripping and wrist flexion of 2.8° in the “low exposure group”. Manes (2012) studied an American group of 50 motorcyclists, a hobby that exposes the wrist to non-neutral postural changes to control the brakes and throttle, in addition to the vibration from the engine. The researchers found that 30% of the bikers had evidence of carpal tunnel syndrome. Research exploring tendon gliding resistance in the carpal tunnel also demonstrates a multiplicative interaction between forceful exertions and non-neutral wrist postures, linking a plausible injury mechanism to physical risk factors in ergonomics (Kociolek et al., 2015).

2.5 Longitudinal Ultrasound Studies of the Carpal Tunnel

In order to observe tendon motion and strain potential within the carpal tunnel, numerous studies have used ultrasonography in the longitudinal plane to measure tendon displacement, velocity, and additional metrics associated with tenosynovial strain. Flexor digitorum superficialis (FDS) tendon has a striated pattern and the surrounding subsynovial connective tissue (SSCT) is hyperechoic, enabling researchers to easily identify these structures via ultrasound. Several studies have used colour Doppler imaging to measure FDS tendon and SSCT motion and FDS – SSCT relative motion (Kociolek et al., 2015; Korstanje et al., 2010b; 2012; Soeters et al., 2004; Tat et al., 2015) while other studies have applied a block-matching algorithm based on normalized cross-correlation to quantify tendon displacement (Korstanje et al., 2010b, van Doesburg et al., 2012b).

Tat et al. (2013) used colour Doppler ultrasound to investigate the shear strain index (SSI, $(\text{FDS tendon displacement} - \text{SSCT displacement}) / \text{FDS tendon displacement} \times 100\%$) and

maximum velocity ratio (MVR, $\text{maximum velocity}_{\text{ssct}}/\text{maximum velocity}_{\text{fds}}$) between the FDS tendon and SSCT during repetitive long finger flexion-extension cycles for 30 minutes. SSI increased 20.4% from the 1st to 30th minute, while the MVR decreased 8.9% in finger flexion and 8.7% in finger extension, all indicating greater relative motion. Kociolek & Keir (2016) also used colour Doppler imaging to evaluate relative motion, where it was found that FDS – SSCT relative displacement (calculated as a percentage) increased from 27.2% in 30° wrist extension to 39.9% in 30° wrist flexion. While the above studies demonstrated the effects of finger and wrist postures, Kociolek et al. (2016) showed that movement frequency and fingertip force further increased relative displacement between FDS tendon and SSCT. These studies demonstrate a relationship between occupational risk factors and longitudinal tendon function, and may increase the risk of developing wrist/hand MSDs including CTS.

2.6 Transverse Ultrasound Studies of the Carpal Tunnel

Carpal tunnel structures of healthy participants have also been observed in the transverse plane, investigating either deformation or displacement of the finger flexor tendons and median nerve (MN) within the carpal tunnel (Table 2.1). MN cross-sectional area, perimeter, various measures of circularity, radial-ulnar width, and palmar-dorsal height are all commonly used to evaluate its morphology and deformation (Cowley et al., 2017). MN and/or flexor tendon displacements are also measured by defining their centroid(s) and determining distances in relation to other carpal tunnel structures (Gabra et al., 2016; Yoshii et al., 2009).

A number of studies have investigated the transverse carpal tunnel during wrist and finger postures or motions without applied force, with particular relevance for clinical outcomes (van Doesburg et al., 2012a; Wang et al., 2014; Yoshii et al., 2009). Yoshii et al. (2009) evaluated MN

and long finger FDS tendon displacements in different finger motions by identifying their centroid coordinates and measuring the relative distances between the two structures. During isolated long finger flexions, the distance between the MN and FDS tendon decreased in the radial-ulnar direction and increased in the palmar-dorsal direction compared to concurrent four finger flexion. Additionally, MN circularity increased during long finger flexion. A number of studies also found differences between CTS patients in comparison to healthy controls (van Doesburg et al., 2012a; van Doesburg et al., 2012b; van Doesburg et al., 2012c; Wang et al., 2014). For example, van Doesburg et al. (2012a) reported greater MN deformation as well as greater absolute and relative MN and FDS tendon displacements in CTS patients than healthy controls. These findings demonstrate significant differences in carpal tunnel dynamics between healthy and injured wrists, which may be attributed to carpal tunnel structures occupying greater space, causing the structures to deviate from their pre-pathological positions and/or movement patterns.

While clinically relevant studies have investigated both passive (Greening et al., 2001) and active (Yoshii et al., 2009) wrist and finger motions, very few studies have evaluated forceful tasks typical of the workplace. There is evidence of changes in longitudinal tendon sliding due to forceful efforts (Kociolek et al., 2016; Korstanje et al., 2010a). However, there are several gaps in the literature with respect to transverse studies, with a few notable exceptions (Cowley et al., 2017; Gabra et al., 2016; Woo et al., 2016; Woo et al., 2019). One of these exceptions includes a study conducted by Cowley et al. (2017), which assessed the shape of the MN in a series of static ultrasound images of different grip types (chuck, key, and four-finger pinch grips), wrist postures (30° flexion, 0°, 30° extension), and force levels (0%, 25%, 50% of maximum voluntary effort). MN circularity increased when the wrist was flexed during forceful chuck and four-finger pinch grips. In contrast, the MN flattened in wrist extension. Gabra et al. (2016) considered a different

set of metrics, investigating transverse displacements during occupationally relevant test conditions by extracting a single ultrasound image at the beginning and at the end of forceful isometric finger pulls. When the wrist was flexed (versus non-flexed), the flexor tendons moved palmarly, transverse carpal ligament (TCL) arch height increased, and TCL-tendon distances decreased during the finger pulls. Despite these findings, there remains a need to explore the relationship between MN deformation and displacement. Simultaneously assessing both deformation and displacement relative to other carpal tunnel structures, and throughout the entire time course of loading and unloading the fingertips during forceful efforts, may elucidate the underlying causes of MN deformational changes and work-related injury pathways leading to CTS.

Table 2.1. Methodological considerations for ultrasound imaging studies of the carpal tunnel in the transverse plane.

Author	Title	Ultrasound System	Transducer / Acquisition Frequency	Scanning Location	Depth
Cowley et al., 2017	The influence of wrist posture, grip type, and grip force on median nerve shape and cross-sectional area	Aixplorer (Supersonic Imagine, Aix-en-Provence, France)	SL-15 linear transducer / Acquisition frequency not provided	Distal crease at the pisiform and scaphoid tubercle level; 90° to the forearm	Not provided
Gabra et al., 2016	In vivo tissue interaction between the transverse carpal ligament and finger flexor tendons	Acuson S2000 (Siemens Medical Solutions, Mountain View, CA)	9L4 linear transducer / 7MHz	Perpendicular to the palm	3 cm
Greening et al., 2001	The use of ultrasound imaging to demonstrate reduced movement of the median nerve during wrist flexion in patients with non-specific arm pain	Dynamic Imaging (Diasus, UK)	Linear array / 10–22 MHz	Placed at the distal wrist crease line against the palmar surface	Not provided
Lopes et al., 2011	Tendon and nerve excursion in the carpal tunnel in healthy and CTD wrists	HDI 5000 (Philips Medical Systems, Markham, ON)	Broad bandwidth linear array / 12–5 MHz	Placed at middle volar wrist crease; used carpal bony landmarks for reference points	2.4 cm
Turcotte & Kociolek, 2021	Median nerve travel and deformation in the transverse carpal tunnel increases with chuck grip force and deviated wrist position	L7 (Clarius Mobile Health, Burnaby, BC)	Linear array / 12 MHz	Placed parallel to the distal wrist crease, at the base of the thenar eminence	15 mm

van Doesburg et al., 2012a	Transverse plane tendon and median nerve motion in the carpal tunnel: ultrasound comparison of carpal tunnel syndrome patients and healthy volunteers	Acuson Sequoia C512 (Siemens Medical Solutions, Malvern, PA)	15L8 linear array / 15 MHz	Placed transverse to the wrist crease and perpendicular to the long axes of the forearm	20 mm
Wang et al., 2014	Transverse ultrasound assessment of median nerve deformation and displacement in the human carpal tunnel during wrist movements	Acuson Sequoia C512 (Siemens Medical Solutions, Malvern, PA)	15L8 linear array / 8–14 MHz	Placed at proximal carpal tunnel, perpendicular to the median nerve	Adjusted between 25-30 mm according to the thickness of the examined hand
Woo et al., 2016	Development of kinematic graphs of median nerve during active finger motion: implications of smartphone use	HD11 XE (Philips Medical Systems, Bothell, WA)	L12–5 linear array / 3–12 MHz	Placed transversely at the level of the wrist crease (corresponding to the proximal carpal tunnel)	Not provided
Woo et al., 2019	Morphological changes of the median nerve within the carpal tunnel during various finger and wrist positions: an analysis of intensive and nonintensive electronic device users	HD11 XE (Philips Medical Systems, Bothell, WA)	L12–5 linear array / 5–12 MHz	Placed transversely at the carpal tunnel inlet (relating to the level of pisiform-scaphoid)	Not provided
Yoshii et al., 2009	Ultrasound assessment of the displacement and deformation of the median nerve in the human carpal tunnel with active finger motion	Acuson Sequoia C512 (Siemens Medical Solutions, Malvern, PA)	15L8 linear array / 14MHz	Placed at the level of the wrist crease with the wrist in the neutral position	20 mm

2.7. Grip Types in Occupational Settings

Forceful gripping using both precision and power grip types are known to influence carpal tunnel dynamics, and many of these grips are commonly used in occupational settings, including pulp, chuck, and power grips (Figure 2.3). Occupational tasks ranging from light precision grips used by medical practitioners to forceful power grips used by industrial labourers are common, with several examples highlighted in the literature including hand-intensive tasks performed by nurses (MacDonald & Keir, 2018), dental practitioners (Bramson et al., 1998; Dong et al., 2008), endoscopists (Shergill et al., 2009), and meat cutters (McGorry et al., 2003). For example, MacDonald & Keir (2018) assessed pinch forces during syringe use in lab nurses, floor nurses, and pharmacy assistants. A chuck grip was predominately used for syringe tasks, with thumb forces up to 57% of maximum voluntary effort (MVE). Bramson et al. (1998) reported the pinch force for periodontal scaling and root planning required up to 20% MVE. Dong et al. (2008) reported pinch forces up to 18 N during dental scaling performed by dentists; however, dental students applied 46% more force for the same scaling task. Endoscopists performing colonoscopies reported pinch forces up to 46% of MVE during left colon insertions (Shergill et al., 2009). Industrial workers performing assembly line work also utilize several forceful grip types to complete various tasks, especially when a task demands the use of a hand-held tool. McGorry et al. (2003) studied the use a power grip while workers performed meat cutting operations (including lamb shoulder boning and beef rib trimming) at a meat packaging plant and found a mean power grip force of 28.3% MVE with a peak power grip force of 72.6% MVE. Clearly, there remains a need for workplace interventions aimed at reducing forceful pinch and grip tasks, especially within the medical field and meat processing industry.

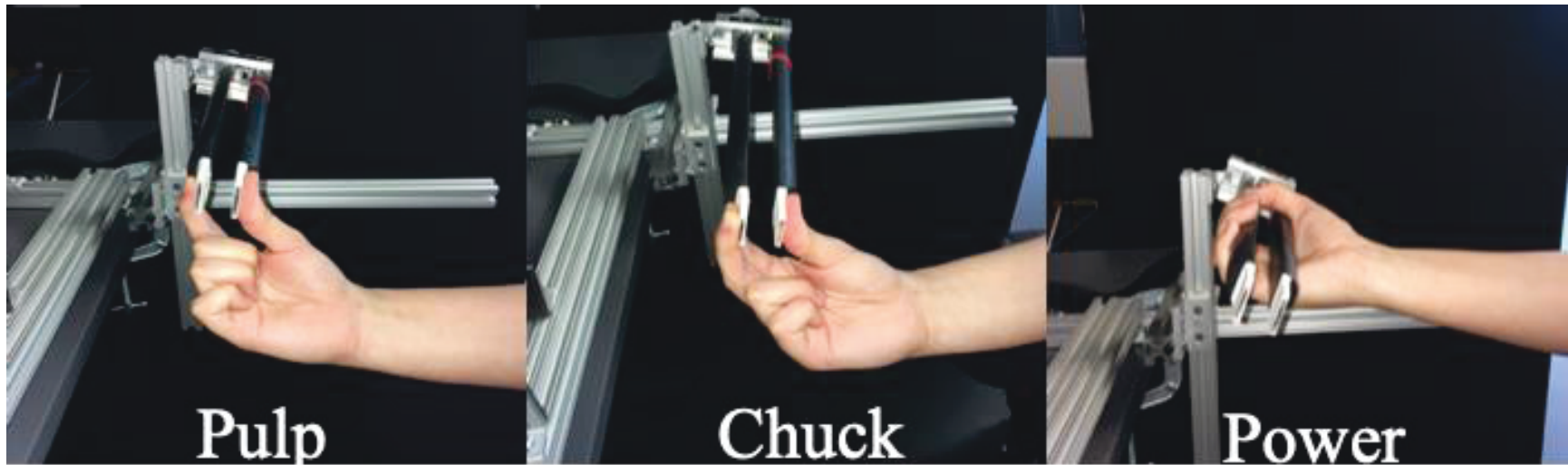


Figure 2.3. Common grip types used to complete various occupational tasks. The pulp pinch involves the index and opposing thumb. The chuck pinch involves the index, middle and opposing thumb. The power grip involves the use of all digits to form a fist. *Note: Images belong to the author.*

Chapter 3

Summary of Literature

Gripping tasks using both precision and power grips in occupational settings often result in high musculoskeletal loads to the finger flexors (Bramson et al., 1998; Dong et al., 2008; MacDonald & Keir, 2018; Shergill et al., 2009), which are known to result in wrist and hand MSDs (Armstrong & Chaffin, 1979; Bernard & Putz-Anderson, 1997; Silverstein et al., 1987). Wrist and hand MSDs have numerous negative impacts on both employees and employers due to the severity of symptoms and long return-to-work times following surgery and rehabilitation (Manktelow et al., 2004). While physical risk factors, such as forceful exertions, repetitive movements, and non-neutral postures are known to increase MSD risk (Harris-Adamson et al., 2014), underlying injury pathways are still not well understood for even well-defined disorders such as CTS. However, there is a growing area of research exploring the relation between occupational risk factors and carpal tunnel dynamics (Cowley et al., 2017; Gabra et al., 2016; Loh et al., 2018; Shergill et al., 2009; Vignais et al., 2016; Woo et al., 2016; Woo et al., 2019; Yoshii et al., 2009). Current studies often focus on a single carpal tunnel structure in isolation, such as the flexor tendon gliding system (Tat et al., 2015) or median nerve deformation (Cowley et al., 2017). Very few studies explore mechanical interactions of adjacent structures within the carpal tunnel, such as the median nerve, flexor digitorum superficialis tendons, and transverse carpal ligament (Gabra et al., 2016). Furthermore, to my knowledge all studies imaging in the transverse plane of the carpal tunnel have utilized a static imaging methodology, whereby a single static image is collected to represent a specific biomechanical condition. While these studies shed light on how different physical work factors influence median nerve deformation (Cowley et al., 2017; MacDonald & Keir, 2018; Vignais et al., 2016; Woo et al., 2016; Woo et al., 2019; Yoshii et al., 2009), there remains a need

to elucidate the underlying mechanisms of these deformational changes. Simultaneously assessing both deformation and displacement relative to other carpal tunnel structures, and throughout the entire time course of loading and unloading the fingertips during forceful exertions, may provide clarity on the underlying causes of median nerve deformation as well as work-related injury pathways leading to CTS.

Chapter 4

Purposes and Hypotheses

4.1 Purposes

The objective of this ultrasound study was to simultaneously evaluate transverse deformation and displacement of the median nerve (MN) relative to the flexor digitorum superficialis (FDS) tendons inside the carpal tunnel. Furthermore, a continuous imaging protocol was utilized throughout the entire time course of both loading and unloading the fingertips during different gripping types to better understand the underlying changes in carpal tunnel dynamics over the history of the tasks.

4.2 Hypotheses

It was hypothesized that:

- a) The MN would gradually be deformed (becoming more circular) and displaced (migrating ulnarly) in concert as fingertip forces progressively increased due to the active development of flexor tendon tension during the gripping tasks;
- b) Differences in MN deformation and displacement in the carpal tunnel would be observed in the fingertip loading versus unloading phases of the gripping tasks, thus providing clarity on the relationship between position and deformation changes of the MN as well as its potential influences on injury such as MN entrapment in work-related CTS.

Chapter 5

Methods

5.1 Participants

As this project involved research with human participants, it was approved by both the Nipissing University Research Ethics Board (File # 101506) and Brock University Research Ethics Board (File # 18-097) prior to data collection (Appendix A). Fourteen healthy participants (7 male, 7 female) were recruited from a convenient sample of students, staff, and faculty at Brock University in St Catharines, ON (Table 5.1). Upon providing informed consent (Appendix B), participants completed a brief questionnaire to screen for health conditions that may influence carpal tunnel dynamics; answering “yes” to any of the health-related screening questions disqualified the volunteer from participating in this study. Briefly, the exclusion criteria included a history of upper limb injury, peripheral nerve disease, wrist tendinopathy, radial malunion, colles fracture, wrist/hand surgery, degenerative joint disease, diabetes mellitus, arthritis, gout, thyroid conditions, amyloidosis, sarcoidosis, renal failure, or corticosteroid injections in addition to any symptoms of pain, tingling, or numbness to the hand (Kociolek & Keir, 2015; Loh & Muraki, 2015; Wang et al., 2014). The full screening questionnaire is provided in Appendix C. On completion of the study, participants were compensated 30 dollars.

Table 5.1. Mean (SD) participant characteristics.

	Age (yrs)	Height (cm)	Weight (kg)
Male (n=7)	23.9 (1.9)	182.0 (7.9)	85.1 (13.6)
Female (n=7)	24.0 (1.4)	167.3 (6.2)	62.3 (7.7)
Total (n=14)	23.9 (1.6)	174.6 (10.2)	73.7 (15.9)

5.2 Experimental Set-up

Participants were seated at a height adjustable table with their right shoulder in a neutral position ($\sim 0^\circ$ glenohumeral flexion and abduction) and elbow at approximately 135° of flexion. The right forearm was supported in supination using a custom designed thermoplastic splint, which included support for the dorsal hand. The support structure also included a hinge aligned with the radiocarpal joint to adjust static wrist position in the flexion-extension axis. A custom probe holder with an adjustable ball-and-socket joint fixed an ultrasound probe parallel to the distal wrist crease at the base of the thenar and hypothenar eminences (Figure 5.1). A generous amount of ultrasound gel was applied to the palmar wrist, thus ensuring good acoustic coupling for cineloop recordings while also minimizing external pressure applied to the wrist by the researcher. Participants interacted with a grip dynamometer (MIE Medical Research, Leeds, United Kingdom) with an adjustable grip span, which was set at 2.5 cm for pinching tasks (pulp and chuck pinches) and 4.0 cm for grip tasks (power grip). The dynamometer was attached directly to the testing apparatus using 80/20 aluminum extrusion and linear motion components (80/20 Incorporated, Columbia City, Indiana) to ensure correct wrist joint position while performing the different pinches/grips.

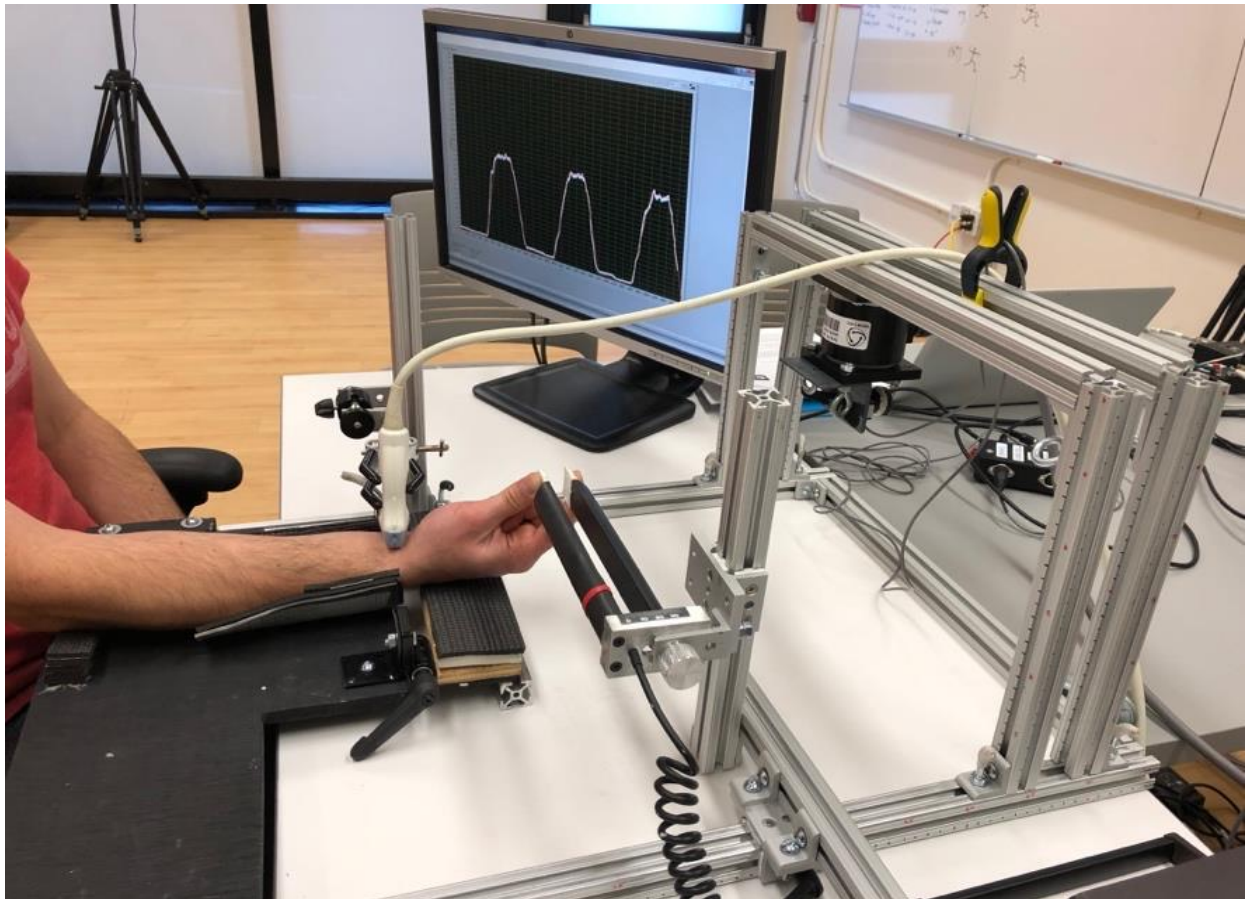


Figure 5.1. Custom built testing apparatus supporting the right distal upper limb of the participant. Adjustable features allowed the grip dynamometer to translate in 3 axes (superior-inferior, proximal-distal, medial-lateral) and rotate about 1 axis (medial-lateral) to enable interaction with the participant. The ultrasound probe was positioned at the base of the wrist using a three-prong clamp attached to a locking ball-and-socket joint. *Note: Image belongs to the author.*

5.3 Experimental Protocol

Participants performed 3 grip types while applying force in 2 static wrist positions for a total of 6 experimental conditions. Specifically, participants performed (i) pulp and (ii) chuck pinches as well as (iii) power grip with the wrist fixed passively in (i) 0° neutral and (ii) 30° flexion (Figure 5.2). The abovementioned grip types are common in occupational settings (DiDomenico & Nussbaum, 2003; Greig & Wells, 2004) and were previously investigated to quantify changes in median nerve morphology during forceful gripping tasks (Cowley et al., 2017).

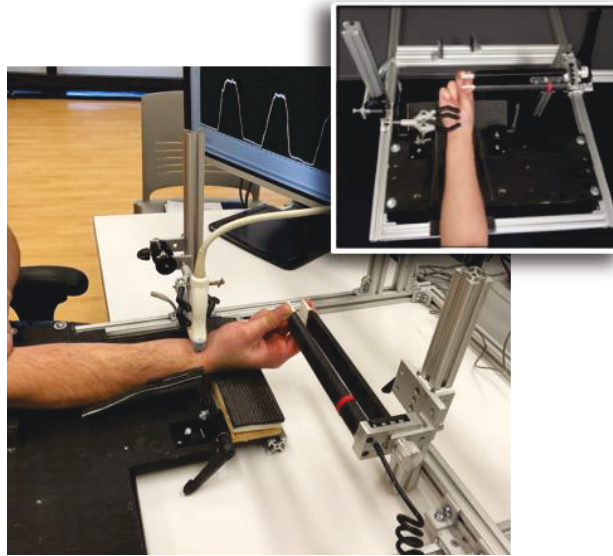


Figure 5.2. Experimental set-up with the wrist in the 0° neutral wrist position and 30° flexed wrist position (inset). *Note: Images belong to the author.*

5.3.1 *Maximum Voluntary Efforts*

Prior to beginning the aforementioned experimental trials, each participant was asked to perform 3 maximum voluntary efforts (MVEs) in all 3 grip types (9 MVEs in total). MVEs were block randomized, with grip types presented in random order and all 3 maximal efforts performed

consecutively for each grip type. Block randomization was selected to minimize setup time associated with the grip dynamometer. MVEs were performed in the experimental testing apparatus with the wrist in neutral position. Each MVE was held for approximately 3-5 seconds with a minimum of 60 seconds of rest between successive MVEs to mitigate neuromuscular fatigue. Participants were provided with real-time force feedback on a visual display and the researchers also gave verbal encouragement to elicit maximal efforts. For each MVE, the maximal effort was computed as the ± 50 ms window centered around the peak force. An average of all 3 MVEs was calculated for each grip type, which was then used to scale trapezoidal shaped force profiles in the experimental gripping trials.

5.3.2 *Grip Force Ramp Trials*

For each experimental gripping trial, participants performed 3 consecutive trapezoidal shaped force profiles while receiving online force feedback via visual display (Figure 5.3). During each force profile, participants traced a 2-second force ramp up from 0% to 50% MVE, followed by a 2-second plateau at 50% MVE, and then a 2-second ramp down from 50% to 0% MVE. Additionally, 4.0 seconds of rest was provided between successive force profiles, thus ensuring that grip force was near 0% MVE at the onset of each force profile. Participants were provided with at least 2 practice trials for each experimental condition with the opportunity for additional practice trials as required. Grip type was block randomized within each wrist position to limit setup time (i.e. all randomized grips were performed within each randomized wrist position – 0° neutral; 30° flexion).

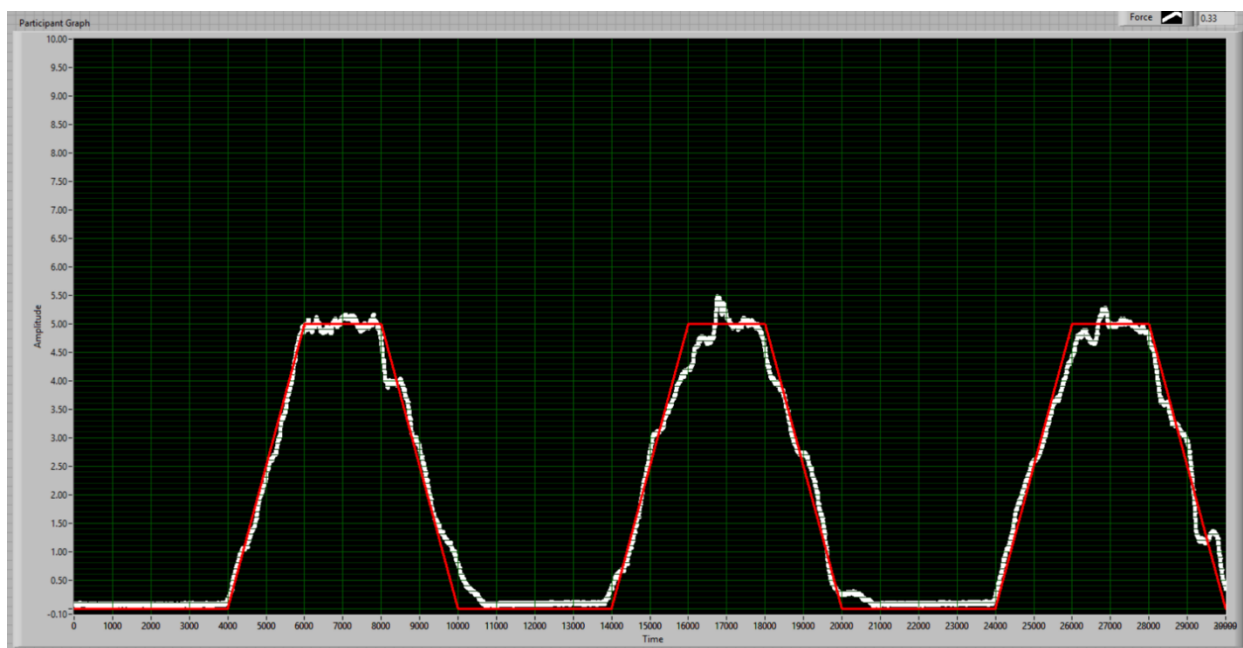


Figure 5.3. Online display of the force matching task. For each gripping trial, participants received real-time force feedback (white) while tracing trapezoidal force profiles (red). *Note: Image belongs to the author.*

5.4 Data Collection

30-second cineloops of the transverse carpal tunnel were captured using the Vivid I ultrasound system (GE Healthcare, Milwaukee, WI) with a high-frequency linear array transducer (12L, GE Healthcare). Cineloops were captured in B-mode at an acquisition frequency of 13MHz and a frame rate of 25 fps. Scans were set at a fixed depth of 30 mm with 1 focal point placed at the depth of the median nerve to ensure clear images of carpal tunnel borders, which included: hook of hamate, trapezium, and transverse carpal ligament (TCL); in addition to carpal tunnel structures: median nerve (MN), flexor digitorum superficialis tendons of the index finger (FDS_I), and middle finger (FDS_M). Each structure has distinct properties to distinguish and accurately identify them from the ultrasound images. The palmar borders of the bony landmarks are highly hyperechoic with distinct morphological features and are also attachment points for the TCL. The MN has low echogenicity, appearing darker in images with a surrounding layer of connective tissue at a higher echogenicity. The flexor tendons also have a higher echogenicity compared to nerve and are generally located dorsally and ulnarly of the MN. Active finger motions (e.g. wiggling the index finger and middle finger separately) were used to assist with identifying the tendons since their anatomical placement relative to each other can vary from person to person.

As per above, participants were instructed to force match trapezoidal shaped grip force profiles using a hand-held dynamometer in different grip types (Figure 5.3). The grip force tasks in each block were individually scaled to the participant's MVEs and displayed on a flat-screen monitor using a custom program written in LabView (version 14.0.1f11, National Instruments Corp, Austin, Texas). All grip force data were amplified and digitally sampled with a USB high speed analog-to-digital converter at 1000 Hz (USB-6255, National Instruments Corp, Austin, Texas). Additionally, grip force data and the ultrasound cineloop in each trial were synced using a

custom-built trigger, which was required to extract specific images within each cineloop at desired force levels for subsequent analyses (more detail below).

5.5 Data Analysis

Images were extracted from 0% to 50% in 10% increments of grip force MVE during both the ramp up and ramp down phases for all 3 trapezoidal grip force profiles, totaling 36 images per condition ([6 forces ramping up + 6 force ramping down per force profile] \times 3 force profiles per condition = 36 images per condition; Figure 5.4). Images were extracted from the cineloops using a custom MatLab program (9.2, The Mathworks Inc., Natick, MA, USA), and further analyzed with ImageJ (1.52a, National Institutes of Health, Bethesda, MD). Unfortunately, images in the 30° wrist flexion position did not reliably provide distinct borders for the MN, and therefore the decision was made by the research team to only analyze images for grip conditions collected in the 0° neutral wrist position (i.e. omit images collected in 30° wrist flexion). Therefore, for this thesis a total of 1,512 images were individually analyzed in Image J (14 participants \times 3 grip conditions / participant \times 36 images / grip condition = 1,512 images).

The boundaries of the MN and flexor digitorum superficialis tendons (FDS_I and FDS_M) were manually traced via Image J's polygon tool in all 36 images for each condition (0%-50% ramp up, 50%-0% ramp down, for all 3 force profiles). The cross-sectional area, diameters (D_x – radial-ulnar, D_y – palmar-dorsal), circularity ($4\pi[\text{area}/\text{perimeter}^2]$; values ranging from 0 to 1; 1 = perfect circle), and minimal enclosing rectangle of these structures were measured to assess deformation (Crowley et al., 2017, Mhanna et al., 2016). The transverse carpal ligament was also examined and digitized with Image J's multi-point tool. Seven points were selected to outline the palmar border and determine the coordinates to evaluate shape changes, including arch height.

Position of the carpal tunnel structures were assessed via calculation of the centroid, as the weighted average of all the pixels of the traced structure via the polygon tool (Gabra et al., 2016; Goh et al., 2015). Subsequently, MN position in the X- and Y- axes was determined relative to the FDS_M in all 36 images for each condition, thus enabling assessment of relative MN-FDS_M position throughout the 30-second duration to determine time/trial dependent effects.

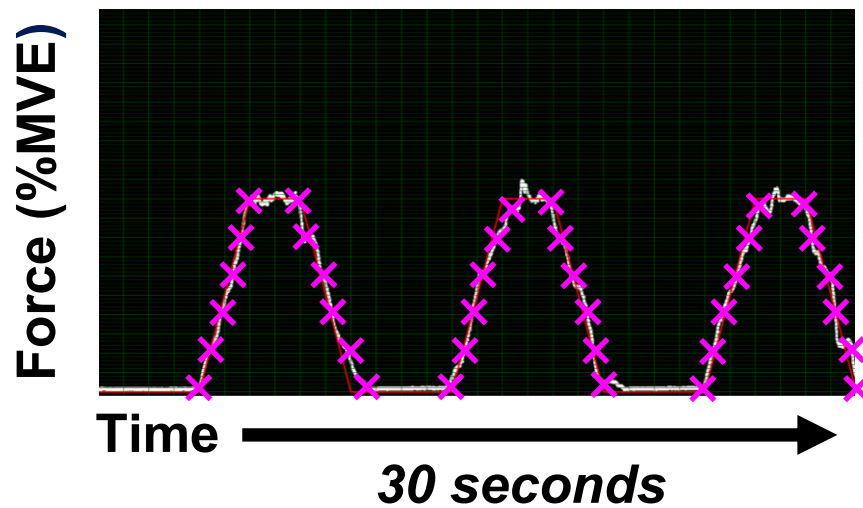


Figure 5.4. Online display of the force matching task. The X's represent where ultrasound images were extracted along the gripping trials. *Note: Image belongs to the author.*

5.6 Statistical Analysis

Three-way repeated measures analysis of variance (ANOVA) statistical models were used to test the effects of grip type (pulp, chuck, and power), ramp force direction (ramp up vs. ramp down), and force production level (0%-50% in 10% increments of MVE) on MN deformation metrics (cross-sectional area, perimeter, width, height, circularity) and relative position between the MN and FDS_M in the X- and Y- axes. A separate ANOVA was run for each metric ($\alpha = 0.05$). Variance of the differences between conditions were assessed for equality using Mauchly's Test of Sphericity. In cases where the assumption of sphericity was violated ($\alpha < 0.05$), a correction

was applied to the degrees of freedom (Greenhouse-Geisser applied when $\epsilon < 0.75$; Hyunh-Feldt applied when $\epsilon > 0.75$), thus yielding a more conservative outcome (Field, 2013). Significant main effects and interactions were further analyzed with either trend analysis or Bonferroni corrected pairwise tests. Trend analysis was used for significant main effects and interactions involving force production level, since each force level was spaced equidistantly (0%-50% in 10% increments of MVE). Pairwise tests were used to follow-up all other significant main effects and interactions; specifically, those that did not involve force production level ($\alpha = 0.05$).

Chapter 6

Results

6.1 Maximum Voluntary Efforts (MVEs) and Grip Forces

Maximum grip forces elicited over the MVE trials were (mean \pm standard error of the mean) 347.31 \pm 23.69 N in power grip, 91.3 \pm 7.23 N in chuck grip, and 66.33 \pm 6.27 N in pulp grip (Table 6.1). MVE trial-to-trial repeatability was good, with a coefficient of variation of 4.53 \pm 0.94%, 5.74 \pm 1.21%, and 7.02 \pm 1.61% for power, chuck, and pulp grips, respectively. Participants successfully followed the grip force template during the experimental trials; root-mean-squared error over all extracted grip force levels (0% to 50% MVE) was 2.84 \pm 0.30 N, with the largest errors occurring at 50% MVE due to participants undershooting the target by 4.22 \pm 0.33% (Appendix D).

Table 6.1. Mean (\pm standard error of the mean) of the MVEs for the 3 grip types (N).

Grip Type	MVE 1	MVE 2	MVE 3	Mean
Power	339.10 (23.56)	349.77 (24.00)	353.07 (24.42)	347.31 (23.69)
Chuck	89.41 (6.38)	92.76 (8.07)	91.75 (7.56)	91.3 (7.23)
Pulp	65.14 (6.50)	66.98 (6.34)	66.86 (6.19)	66.33 (6.27)

6.2 Median Nerve Deformation

6.2.1 Cross-Sectional Area (CSA)

There was a significant grip type by ramp force direction interaction on the median nerve (MN) CSA ($F_{2,22}=9.35$, $p=0.001$). For the chuck grip condition, MN CSA was lower while ramping force up from 0% to 50% MVE compared to ramping force down from 50% to 0% MVE

($p=0.021$). However, there were no changes between the ramp up versus down phases for both the pulp and power grip conditions (Figure 6.1). No other significant main effects or interactions were found for MN CSA (Appendix E).

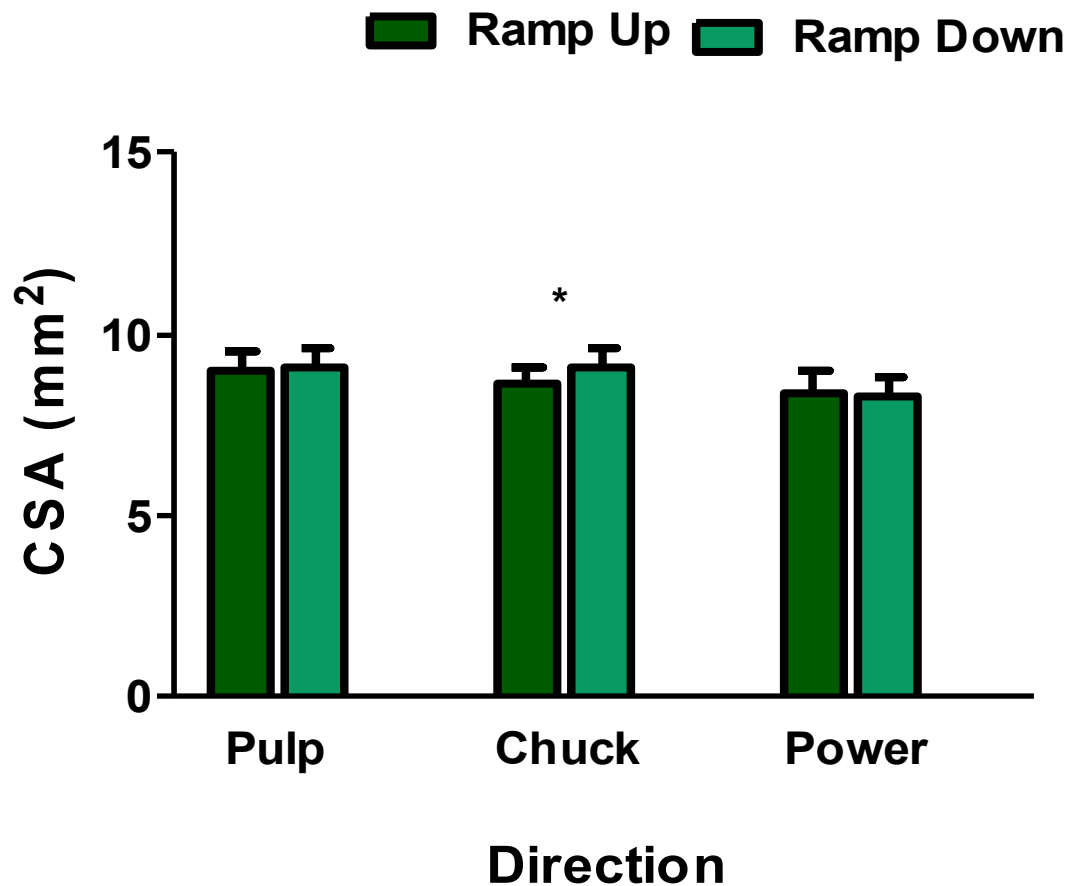


Figure 6.1. Mean (\pm standard error of the mean) MN CSA during the ramp up and ramp down phases of force for the three grip types. *Note: Asterisk indicates a significant difference.*

6.2.2 Perimeter

There was a main effect of grip type ($F_{2,22}=5.30$, $p=0.013$) and force production level ($F_{2,02,22,19}=6.108$, $p=0.008$) on the perimeter of the MN. Post-hoc testing revealed that the perimeter was significantly smaller for the chuck grip in comparison to the power grip ($p=0.011$; Figure 6.2). With respect to force production, MN perimeter decreased linearly from 0% to 50% MVE ($p=0.015$; Figure 6.3). Furthermore, there was a significant interaction between ramp force direction and force production level ($F_{5,55}=3.30$, $p=0.011$). During the ramp up, MN perimeter decreased curvilinearly, as indicated by a significant quadratic trend ($p=0.002$). Specifically, the perimeter decreased from 13.78 ± 0.48 mm to 12.85 ± 0.42 mm between 0% and 20% MVE, with no change from 20% to 50% MVE. During the ramp down, MN perimeter gradually increased as indicated by a significant linear trend ($p=0.035$). Interestingly, the perimeter at the end of the ramp down phase did not return to its original magnitude at the beginning of the trial (Figure. 6.4). The three-way interaction did not achieve significance ($F_{1,42,32,28}=0.48$, $p=0.887$).

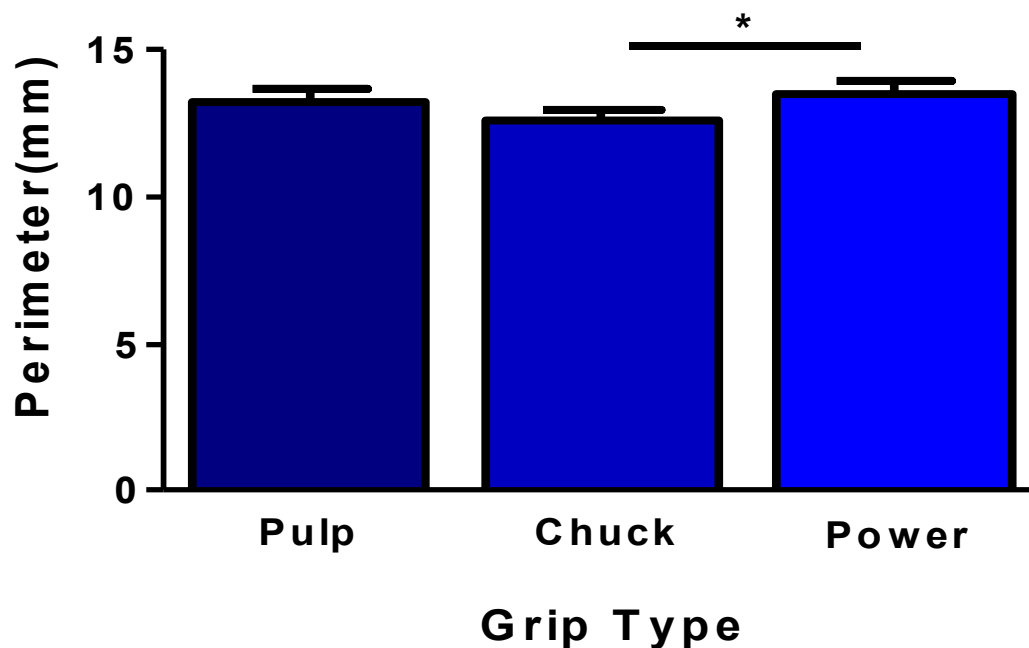


Figure 6.2. Mean (\pm standard error of the mean) MN perimeter during the three grip types.
Note: Asterisk indicates a significant difference.

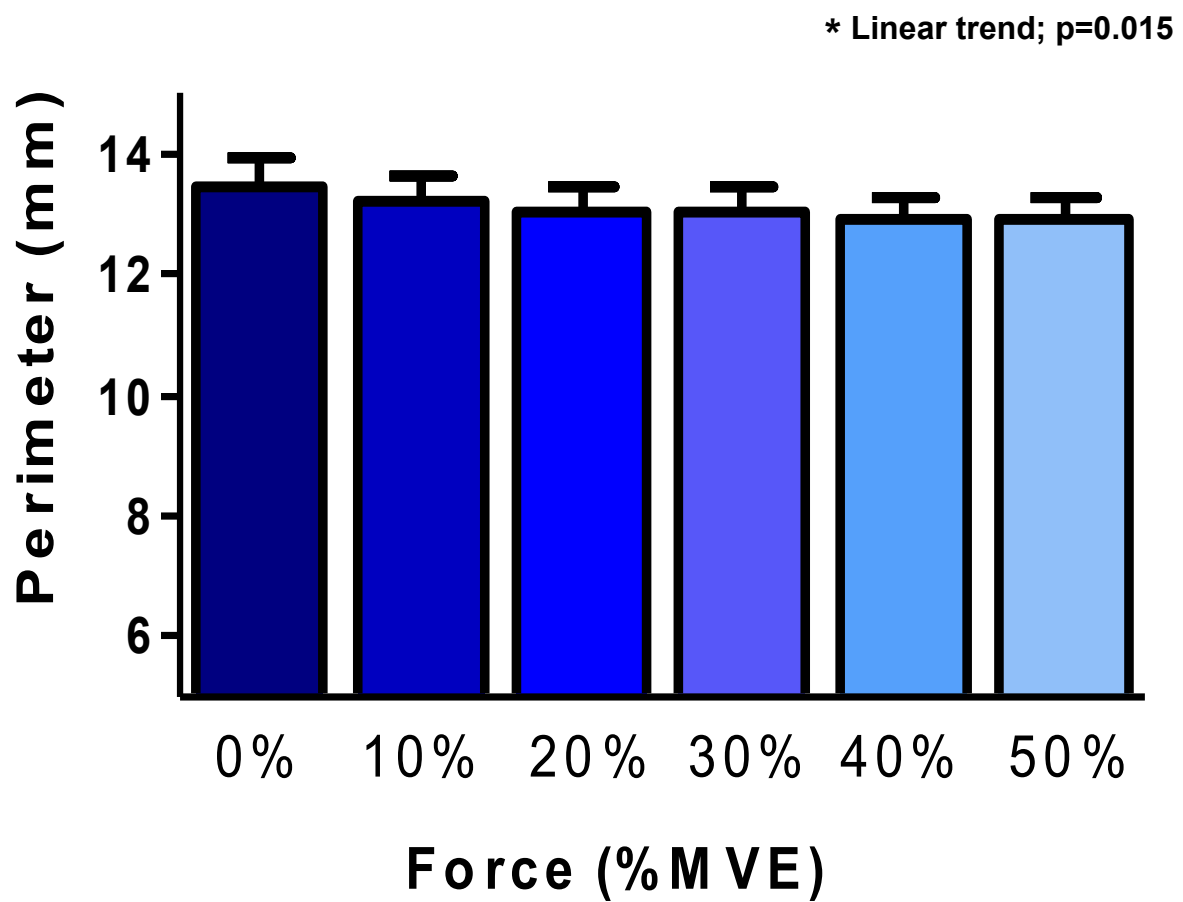


Figure 6.3. Mean (\pm standard error of the mean) MN perimeter with grip force production.

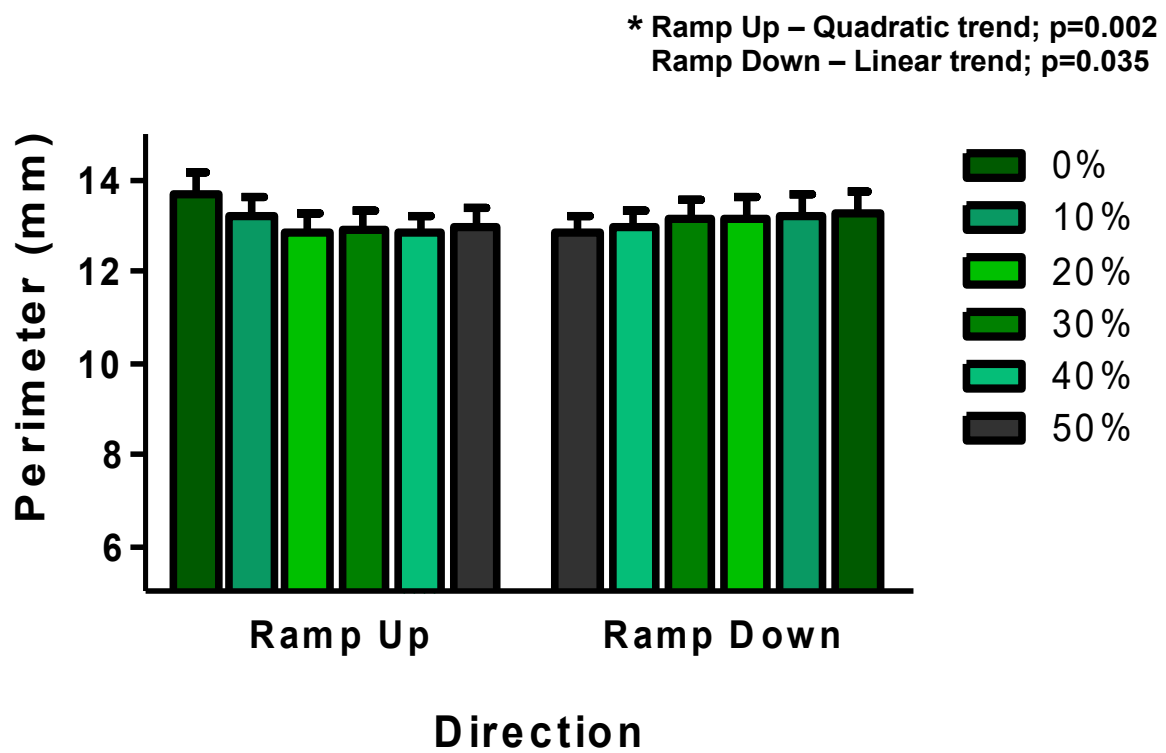


Figure 6.4. Mean (\pm standard error of the mean) MN perimeter during the ramp up and ramp down phases throughout grip force production.

6.2.3 Width

Similar to the results for MN perimeter, there was a significant main effect of grip type ($F_{2,22}=6.93$, $p=0.005$) and force production level ($F_{1,70,18.74}=9.83$, $p=0.002$) on the width of the MN. Once again, MN width was smaller in chuck versus power grip ($p=0.001$; Figure 6.5). Trend analysis revealed a quadratic relationship between MN width and force production level, with MN width decreasing from 0 to 20% MVE, followed by little change thereafter ($p=0.001$; Figure 6.6). A significant interaction between ramp force direction and force production level on MN width ($F_{5,55}= 3.78$, $p=0.005$) also mirrored perimeter results. Briefly, during the ramp up phase, MN width decreased over the force levels and fit a quadratic trend ($p<0.001$), while a linear trend was observed during the ramp down phase to describe an increase in width ($p=0.014$; Figure 6.7). Once again, the three-way interaction did not achieve significance ($F_{0.52,9.96}=0.57$, $p=0.800$).

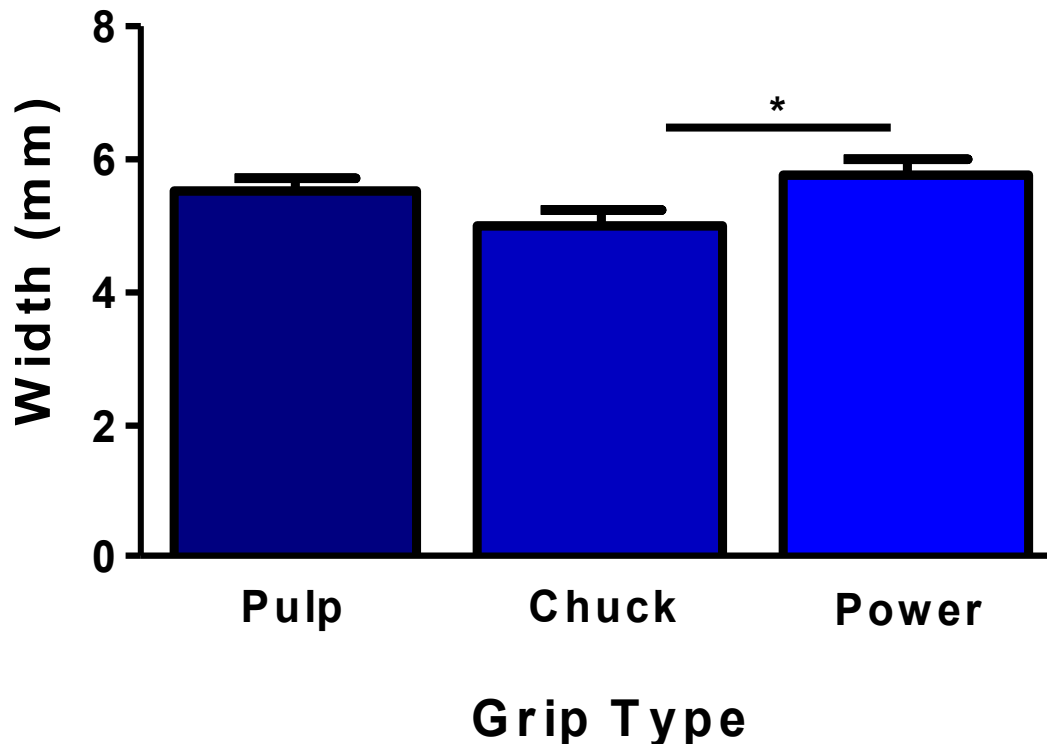


Figure 6.5. Mean (\pm standard error of the mean) MN width during the three grip types.
Note: Asterisk indicates a significant difference.

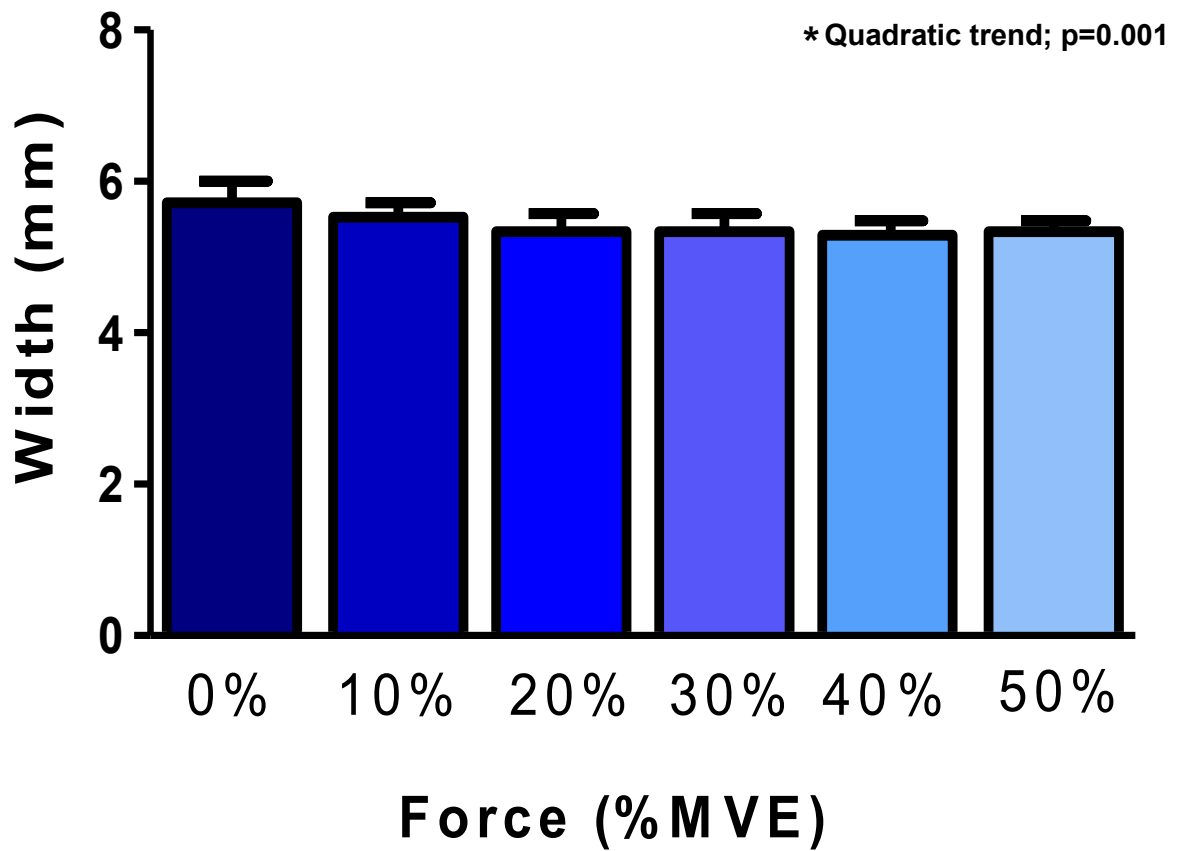


Figure 6.6. Mean (\pm standard error of the mean) MN width during grip force production.

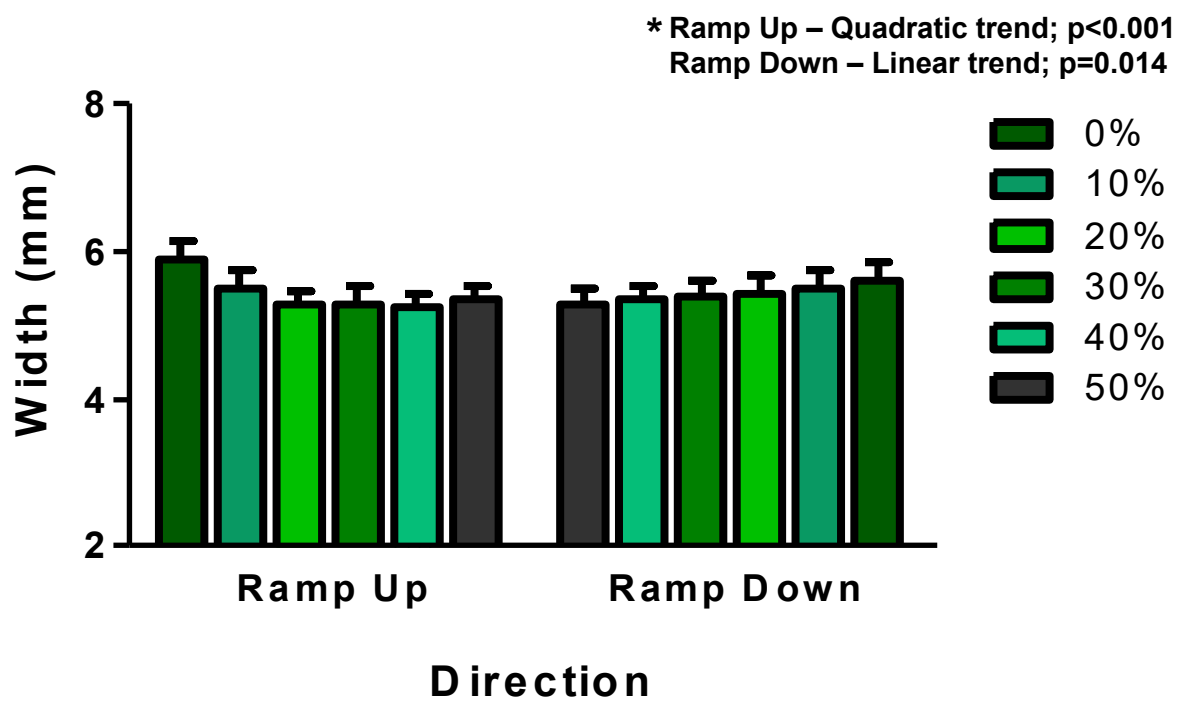


Figure 6.7. Mean (\pm standard error of the mean) MN width during the ramp up and ramp down phases throughout grip force production.

6.2.4 Height

While the ANOVA showed a main effect of grip type on MN height ($F_{2,22}=3.95, p=0.034$), post-hoc testing did not reveal any significant pairwise comparisons. However, there was a trend towards greater MN height in the chuck grip compared to the power grip ($p=0.086$; Figure 6.8). Although a main effect of force production level on MN height was also trending, it did not reach statistical significance after applying the Greenhouse-Geisser correction for violating sphericity ($F_{2.05,22.55}=3.33, p=0.053$; Figure 6.9). In contrast, there was a significant interaction between grip type and ramp force direction on the height of the MN ($F_{2,22}=3.53, p=0.047$). For the power grip, MN height was higher while force was being ramped up versus down ($p=0.039$). On the other hand, there were no significant differences between the ramp up and down phases for both the pulp and chuck grips (Figure 6.10).

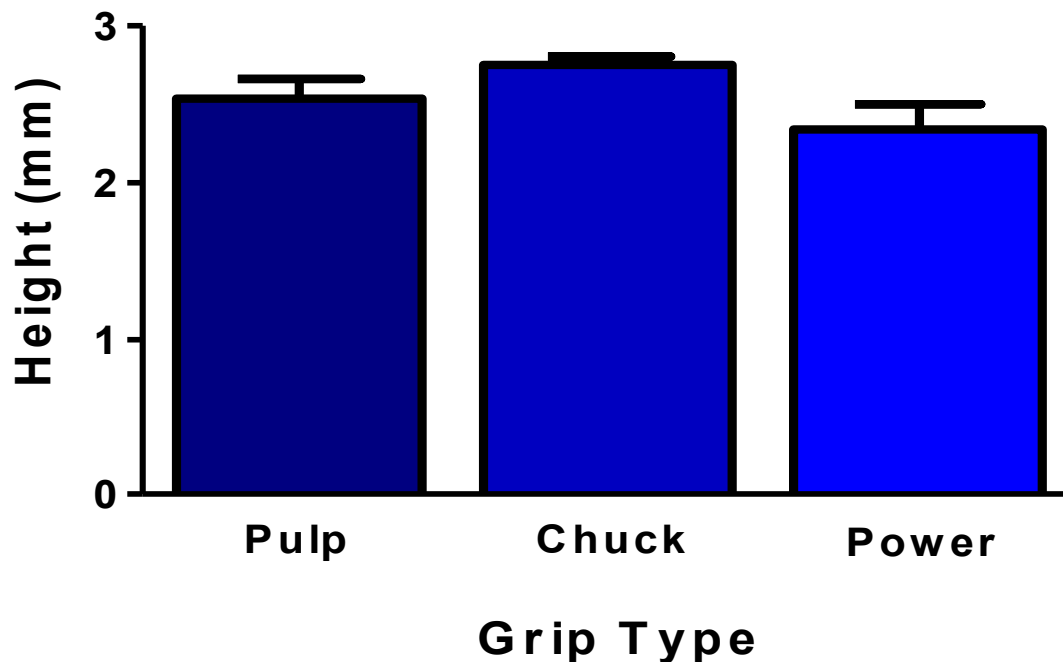


Figure 6.8. Mean (\pm standard error of the mean) MN height during the three grip types.
Note: Asterisk indicates a significant difference.

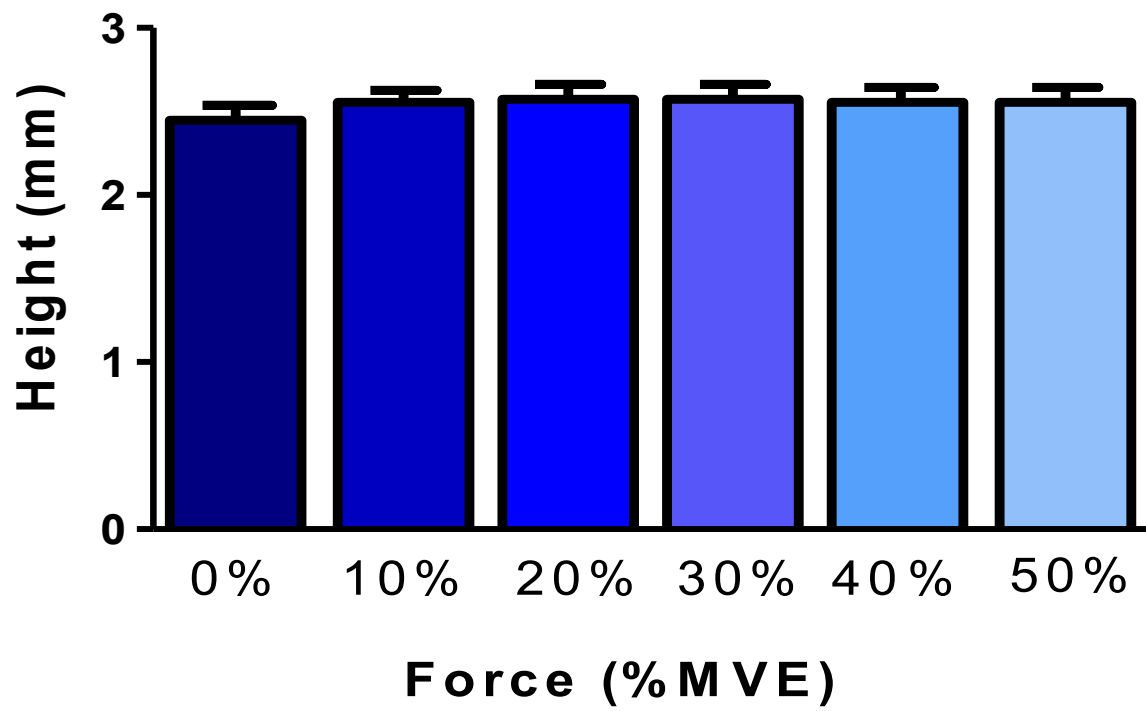


Figure 6.9. Mean (\pm standard error of the mean) MN height during grip force production.

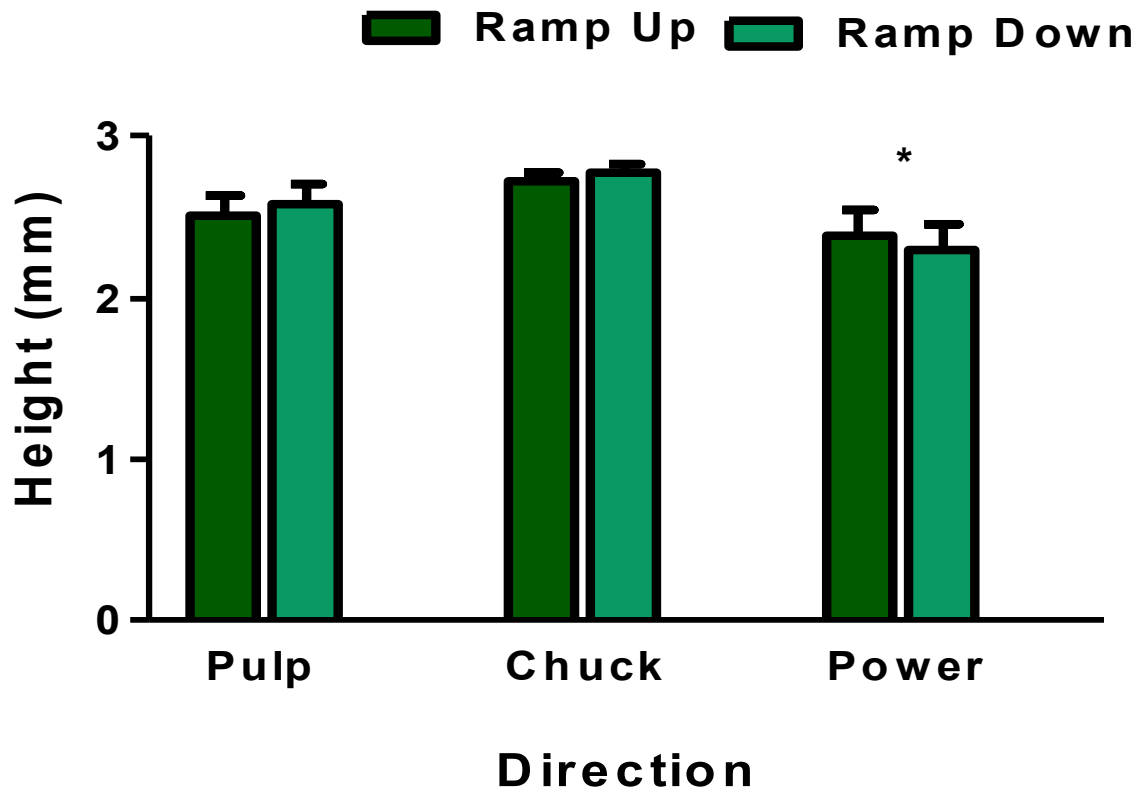


Figure 6.10. Mean (\pm standard error of the mean) MN height while ramping force up and ramping force down for the three grip types. *Note: Asterisk indicates a significant difference.*

6.2.5 Circularity

There was a main effect of grip type ($F_{2,22}=9.95$, $p=0.001$) and force production level ($F_{1.43,15.73}= 7.70$, $p=0.008$) on the circularity of the MN. The nerve was more circular during the chuck grip compared to the power grip ($p=0.001$; Figure 6.11). With respect to force production, MN circularity exhibited a quadratic trend from 0% to 50% MVE ($p=0.002$). Specifically, MN circularity increased by 8% from 0% - 20% MVE, with only a 1% increase from 20% - 50% MVE (Figure 6.12). After correcting for sphericity there were no significant two-way or three-way interactions involving circularity of the MN. However, a two-way interaction between ramp force direction (ramp up vs. down) and force production level was trending ($F_{1.60,17.61}= 3.18$, $p=0.075$). MN circularity appeared to increase curvilinearly while ramping force up from 0% to 50% MVE, and appeared to decrease linearly while ramping force down from 50% to 0% MVE (Figure 6.13). As with width, MN circularity at the end of the ramping down phase did not return to its initial shape from the beginning of the ramping up phase (MN circularity at 0% ramp up – 0.588; 0% ramp down – 0.634).

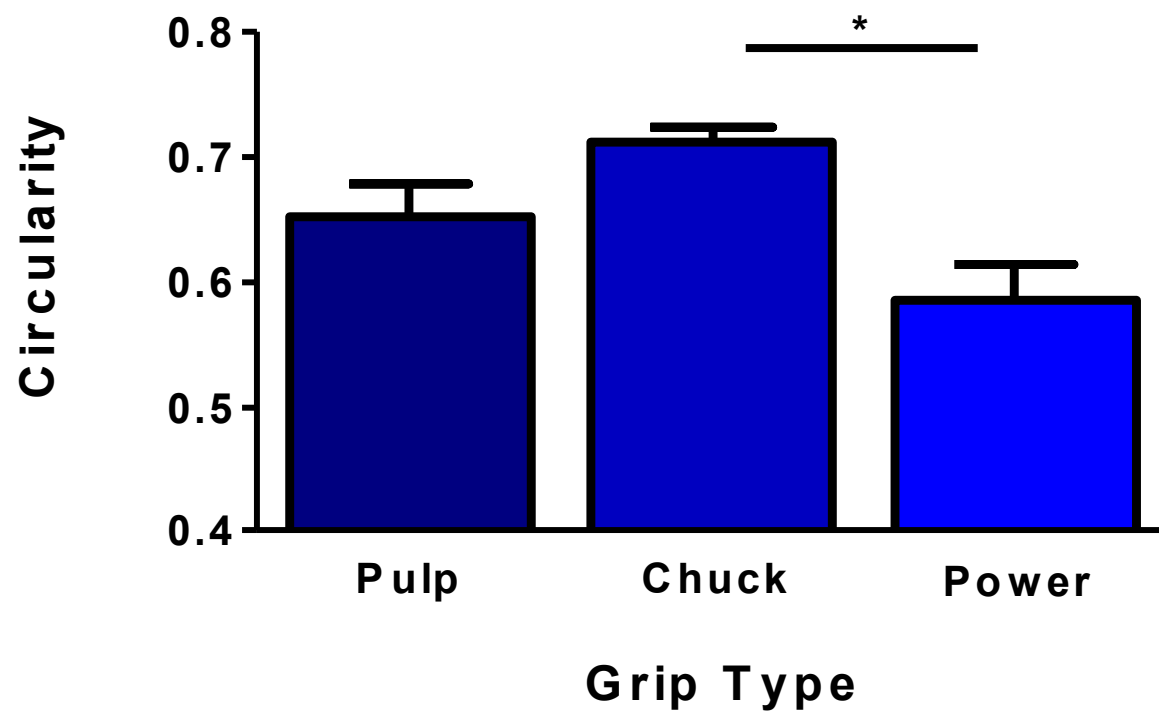


Figure 6.11. Mean (\pm standard error of the mean) MN circularity during the three grip types. *Note:* Asterisk indicates a significant difference.

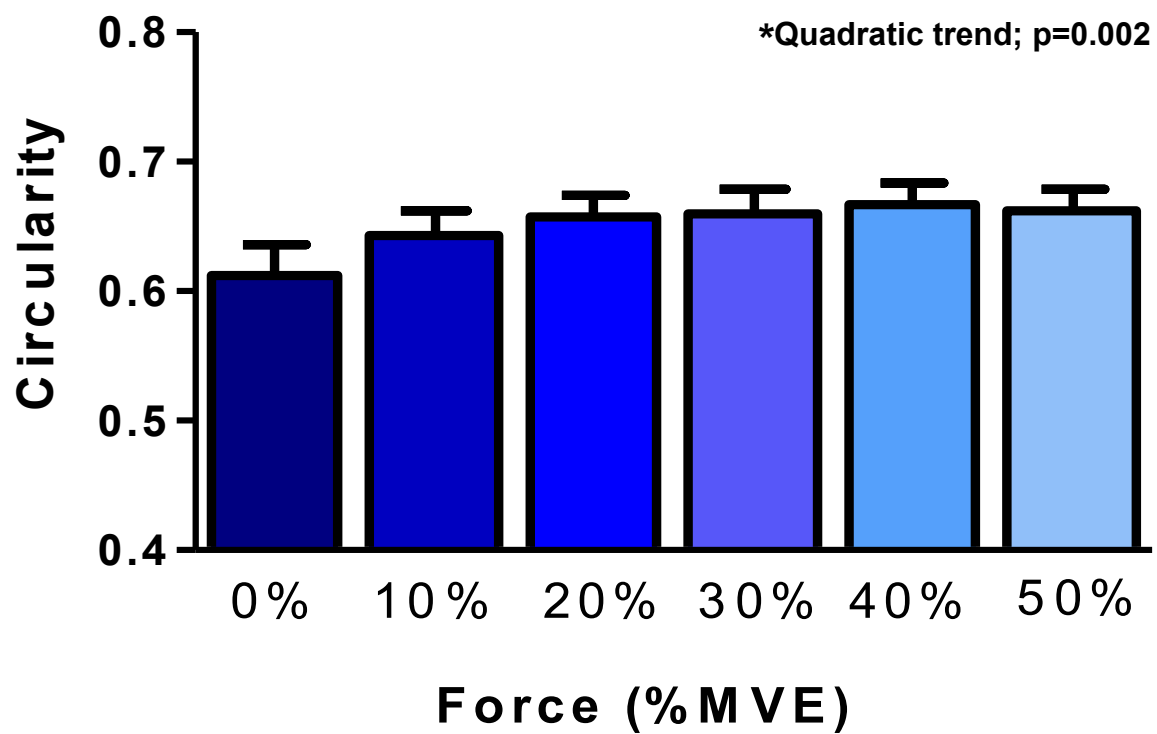


Figure 6.12. Mean (\pm standard error of the mean) MN circularity during grip force production.

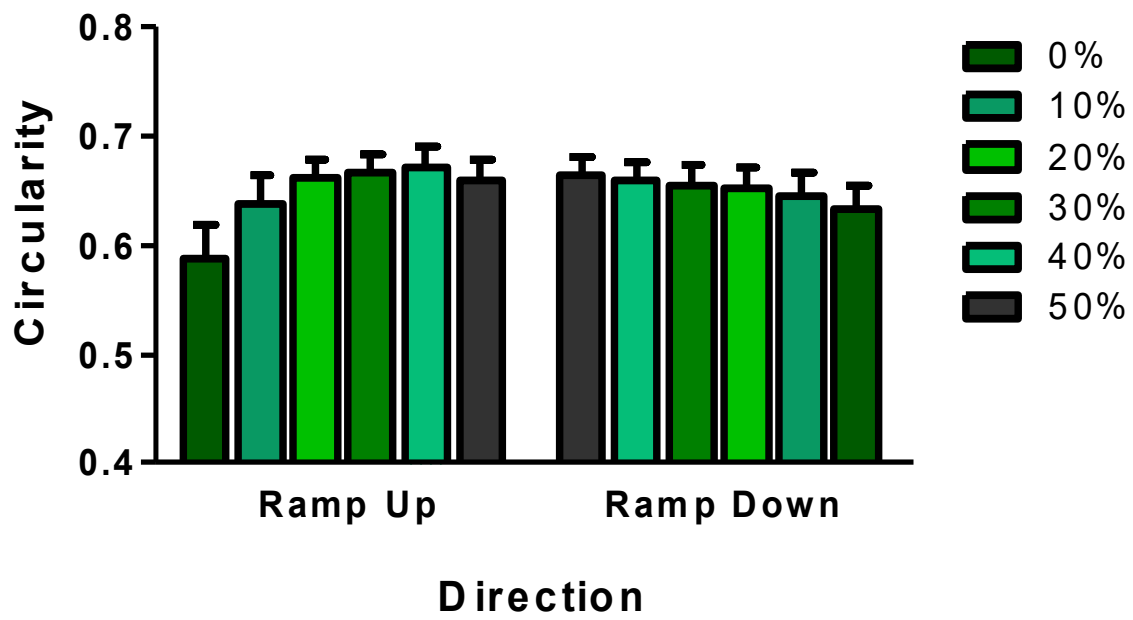


Figure 6.13. Mean (\pm standard error of the mean) MN circularity during the ramp up and ramp down phases throughout grip force production.

6.3 Median Nerve Relative Displacement

6.3.1 Radial-Ulnar (X-) Axis

In the radial-ulnar axis, there was a main effect of force production level ($F_{1.09,12.01}=16.68$, $p=0.001$) and ramp force direction ($F_{1,11}=19.93$, $p=0.001$) on relative position between the median nerve (MN) and flexor digitorum superficialis of the middle finger (FDS_M). Specifically, the MN displaced ulnarly relative to the FDS_M, with a gradual (i.e. linear) change in its relative position of 45.8% from 0% to 50% MVE ($p=0.001$; Figure 6.14). With respect to ramp force direction, the MN displaced ulnarly during the ramp down compared to the ramp up phase (Figure 6.15).

There was also a significant interaction between ramp force direction and force production level on MN-FDS_M relative displacement ($F_{1.18,12.97}=11.09$, $p=0.004$). During the ramp up phase, the MN displaced ulnarly relative to the FDS_M, with an initial MN position of 1.87 ± 0.70 mm ulnar to the FDS_M at 0% MVE, and a final MN position of 3.85 ± 0.40 mm ulnar to the FDS_M at 50% MVE. This gradual change corresponded to a 106% change in position and fit a linear trend ($p=0.001$; Figure 6.16). During the ramp down phase, the MN displaced radially relative to the FDS_M, and this change was also best described by a linear trend ($p=0.01$); however, the percent change was smaller (13%), indicating less displacement in ramp down vs. ramp up (Appendix F). No other 2-way or 3-way interactions achieved statistical significance.

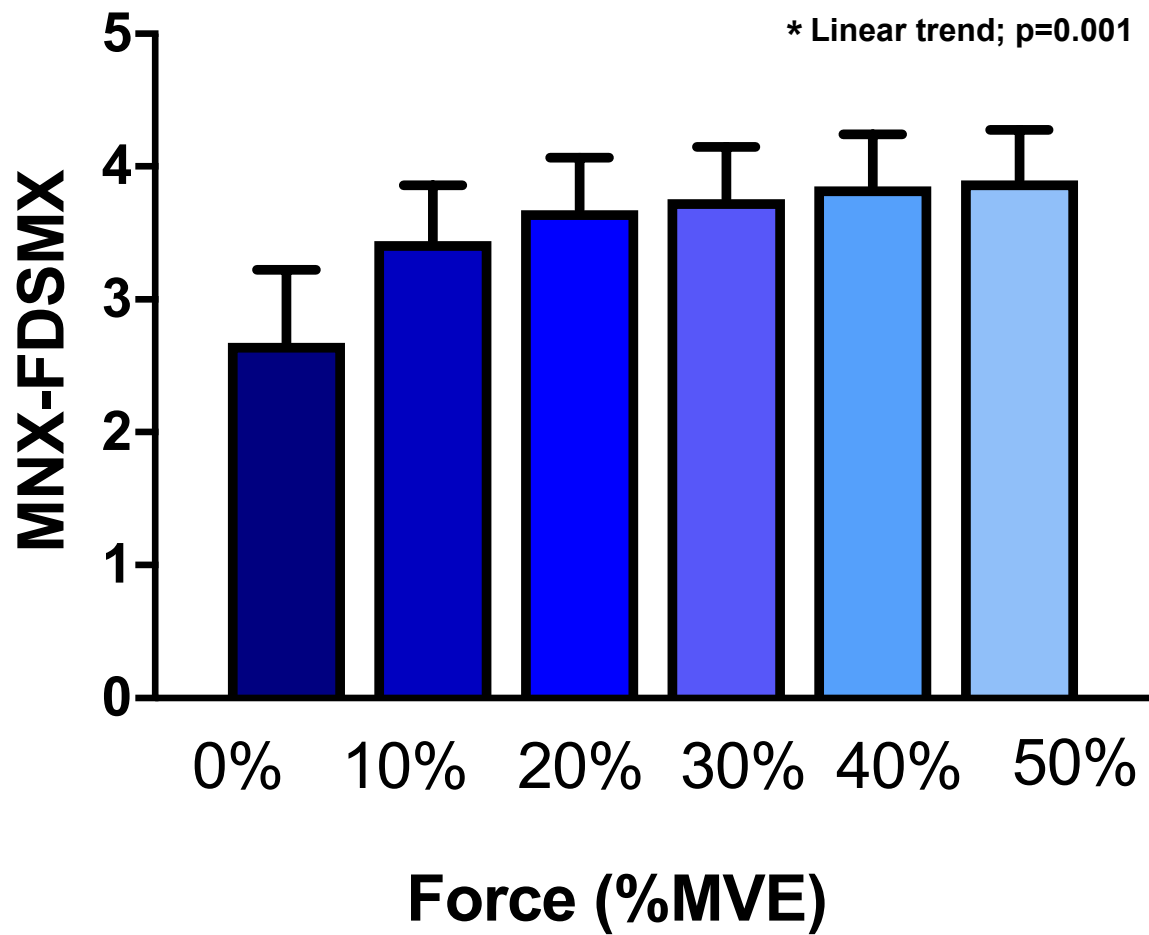


Figure 6.14. Mean (\pm standard error of the mean) median nerve (MN) position relative to the flexor digitorum superficialis tendon of the middle finger (FDS_M) in the X-axis during grip force production. *Note: + indicates ulnar position; – indicates radial position.*

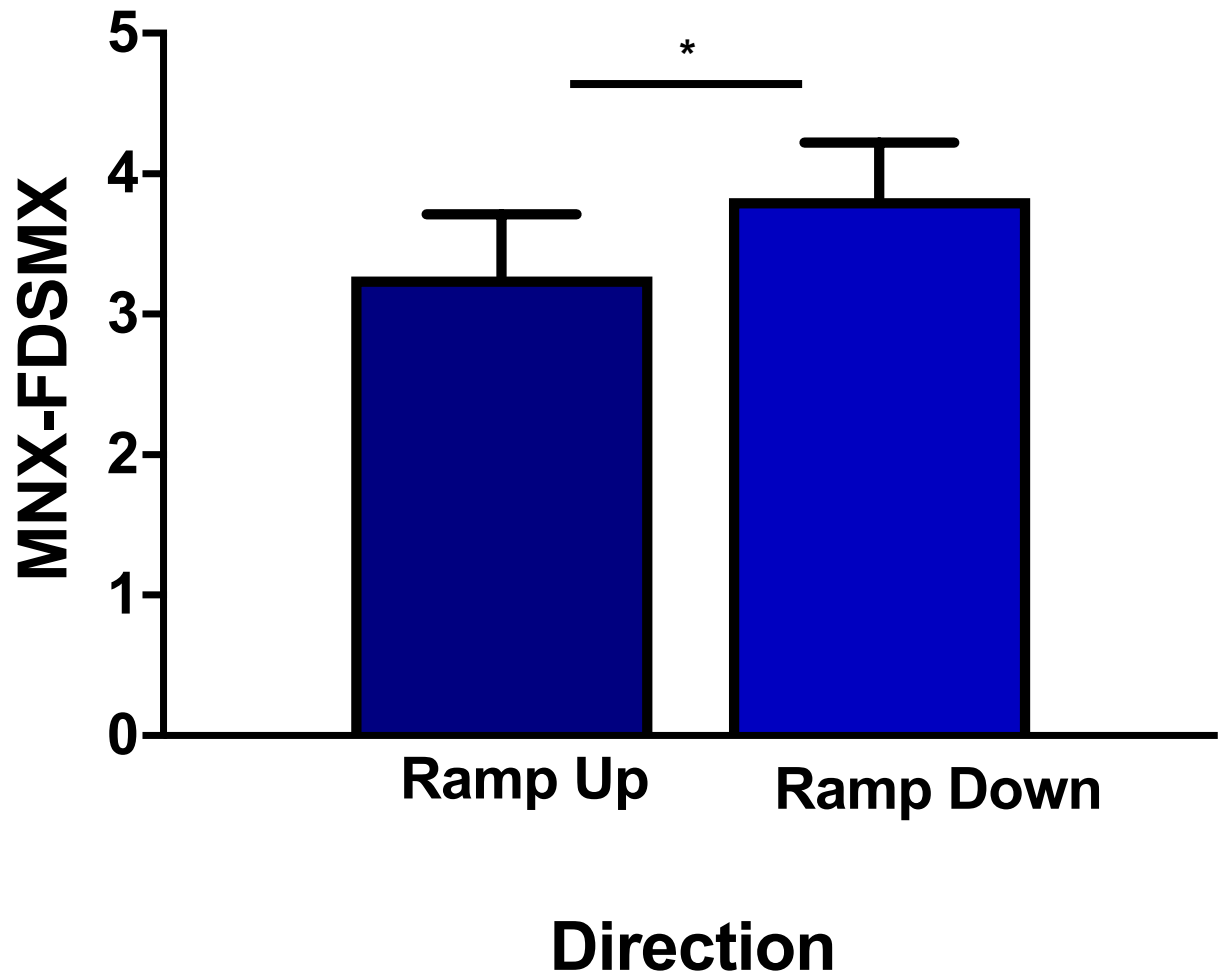


Figure 6.15. Mean (\pm standard error of the mean) median nerve (MN) position relative to the flexor digitorum superficialis tendon of the middle finger (FDS_M) in the X-axis during ramp up versus ramp down. *Note: Asterisk indicates a significant difference; + indicates ulnar position; – indicates radial position.*

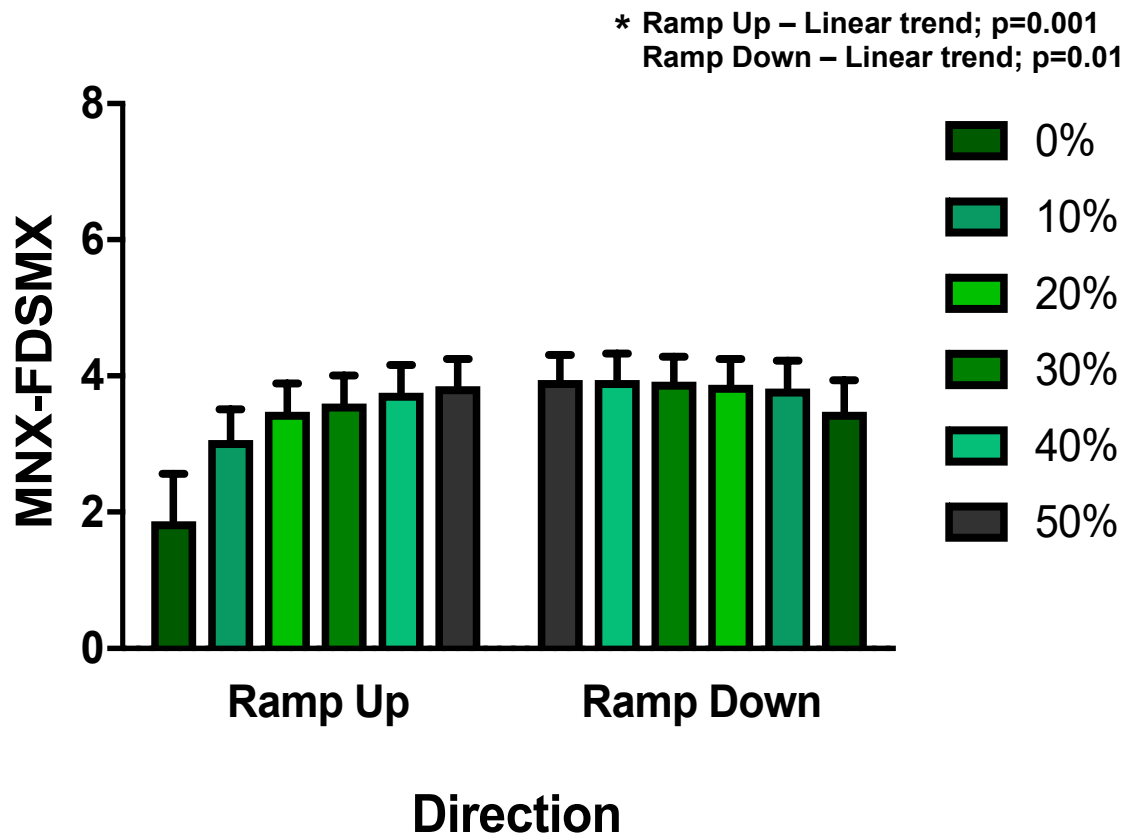


Figure 6.16. Mean (\pm standard error of the mean) median nerve (MN) position relative to the flexor digitorum superficialis tendon of the middle finger (FDS_M) in the X-axis during the ramp up and ramp down phases throughout grip force production. *Note: + indicates ulnar position; – indicates radial position.*

6.3.2 Palmar-Dorsal (Y-) Axis

In the palmar-dorsal axis, there was also a main effect of grip type ($F_{2,22}=8.01$, $p=0.002$) and force production level ($F_{1,19,13.07}=10.460$, $p=0.005$) on relative position between the MN and FDS_M. MN position was located palmarly relative to the FDS_M in all 3 grip types; however, MN position in the chuck grip was dorsal compared to the power grip and pulp grip (Figure 6.17). Following statistical trend analysis, force production level presented as a quadratic relationship, with the MN migrating dorsally relative to the FDS_M from 0% to 20% MVE, representing a 59% change in MN-FDS_M relative position; however, very little change occurred between 20% to 50% MVE ($p<0.001$; Figure 6.18).

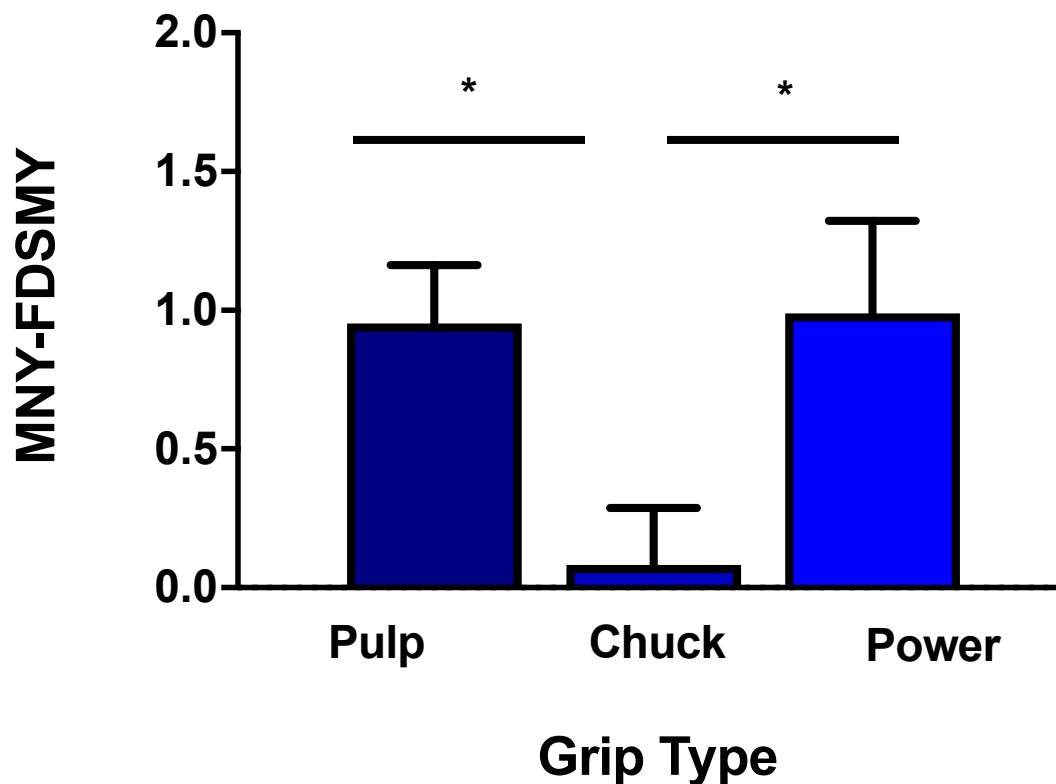


Figure 6.17. Mean (\pm standard error of the mean) median nerve (MN) position relative to the flexor digitorum superficialis tendon of the middle finger (FDS_M) in the Y-axis with different grip types. Note: Asterisk indicates a significant difference; + indicates palmar position; - indicates dorsal position.

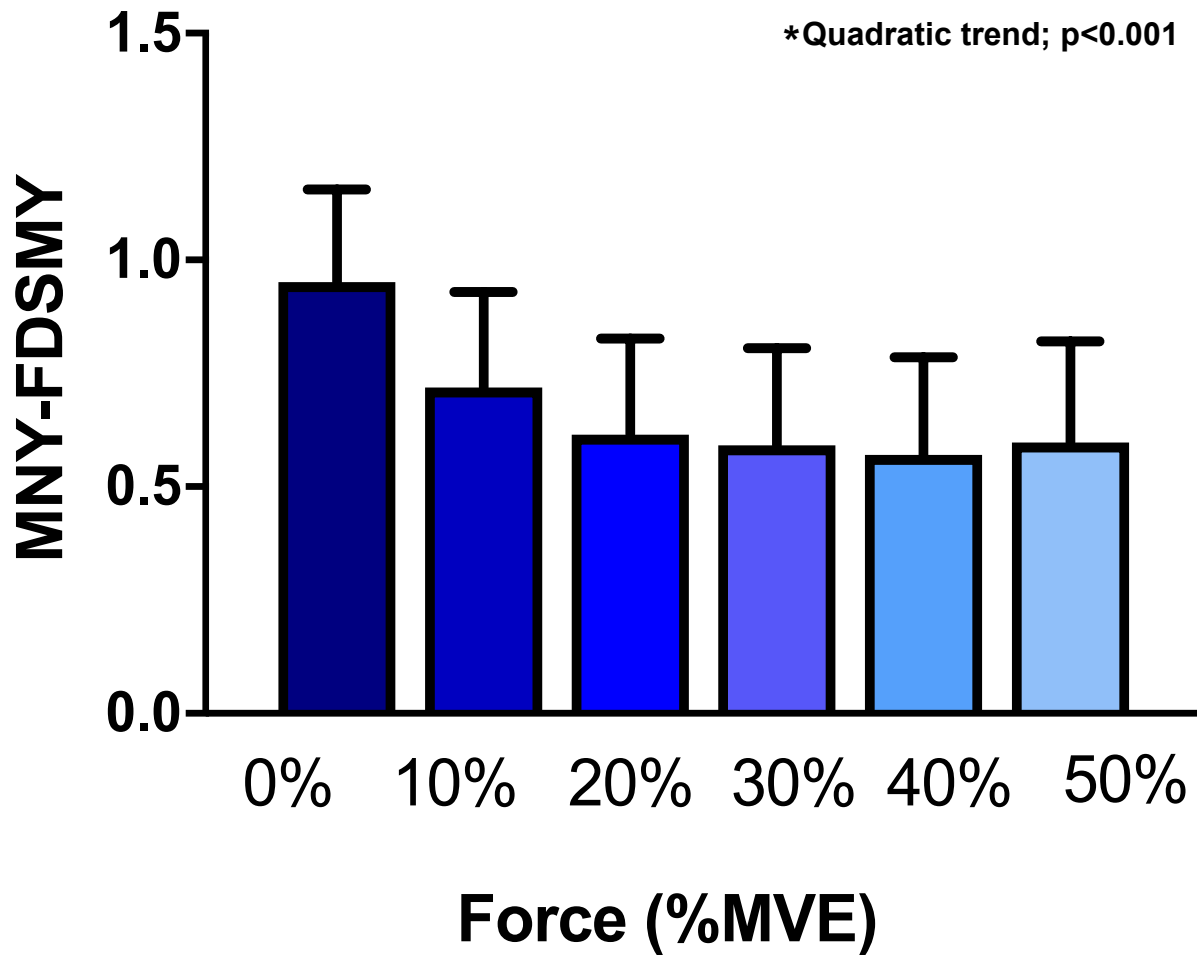


Figure 6.18. Mean (\pm standard error of the mean) median nerve (MN) position relative to the flexor digitorum superficialis tendon of the middle finger (FDS_M) in the Y-axis during grip force production. *Note: + indicates palmar position; – indicates dorsal position.*

Furthermore, there was a significant interaction between grip type and force production level on relative position between the MN and FDS_M in the Y-axis ($F_{2.51,27.59}=4.19, p=0.019$). Post-hoc testing in the chuck grip showed a quadratic trend throughout force production level ($p<0.001$). Specifically, the MN migrated dorsally relative to the FDS_M between 0-20% MVE, with very little change thereafter (20%-50% MVE). While no significant changes were seen in power and pulp grips, a linear relationship between MN-FDS_M relative position and force production level was trending for pulp grip ($p=0.066$; Figure 6.19).

Finally, there was a significant interaction between ramp force direction and force production level on MN-FDS_M relative position ($F_{2.08,22.88}=4.15, p=0.028$). During ramp up, MN position was 1.07 ± 0.21 mm palmar to the FDS_M at 0% MVE, and subsequently migrated dorsally with a MN position of 0.60 ± 0.22 mm palmar to the FDS_M at 20% MVE corresponding to a positional change of 80%. However, there was no further change from 20% to 50% MVE, representative of a quadratic trend throughout force production level ($p<0.001$; Figure 6.20). During ramp down, a quadratic trend also provided the best fit ($p=0.001$), with little change from 50% to 20% MVE followed by the MN migrating palmarly between 20% and 0% MVE. However, the percent change between 20% and 0% MVE was smaller in ramp down (39%) such that the MN did not return to its original position (i.e. 0% MVE for ramp up \neq 0% MVE for ramp down). As with all other deformation and relative displacement metrics, the three-way interaction for MN-FDS_M in the Y-axis did not achieve statistical significance ($F_{3.70,40.74}=2.41, p=0.069$).

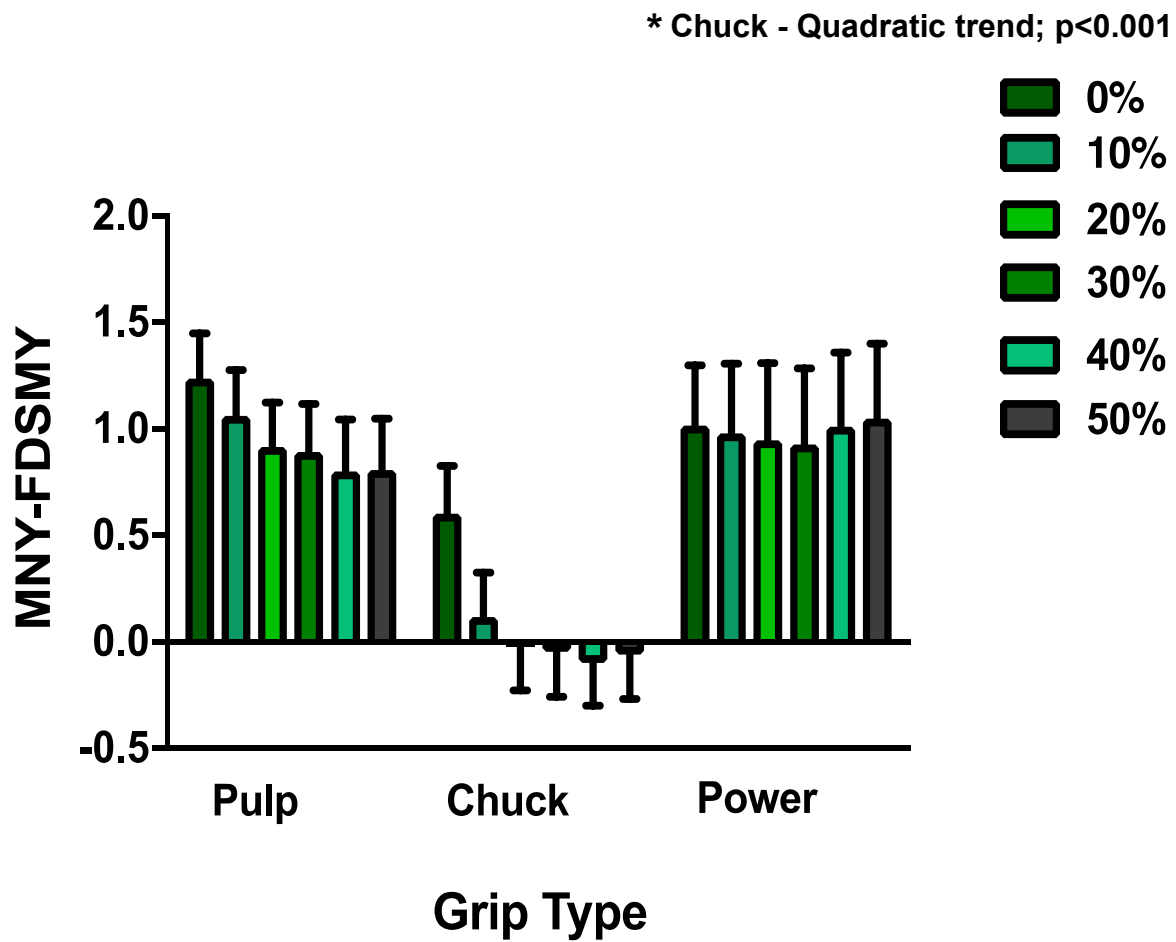


Figure 6.19. Mean (\pm standard error of the mean) median nerve (MN) position relative to the flexor digitorum superficialis tendon of the middle finger (FDS_M) in the Y-axis during three different grip types throughout grip force production. *Note: + indicates palmar position; - indicates dorsal position.*

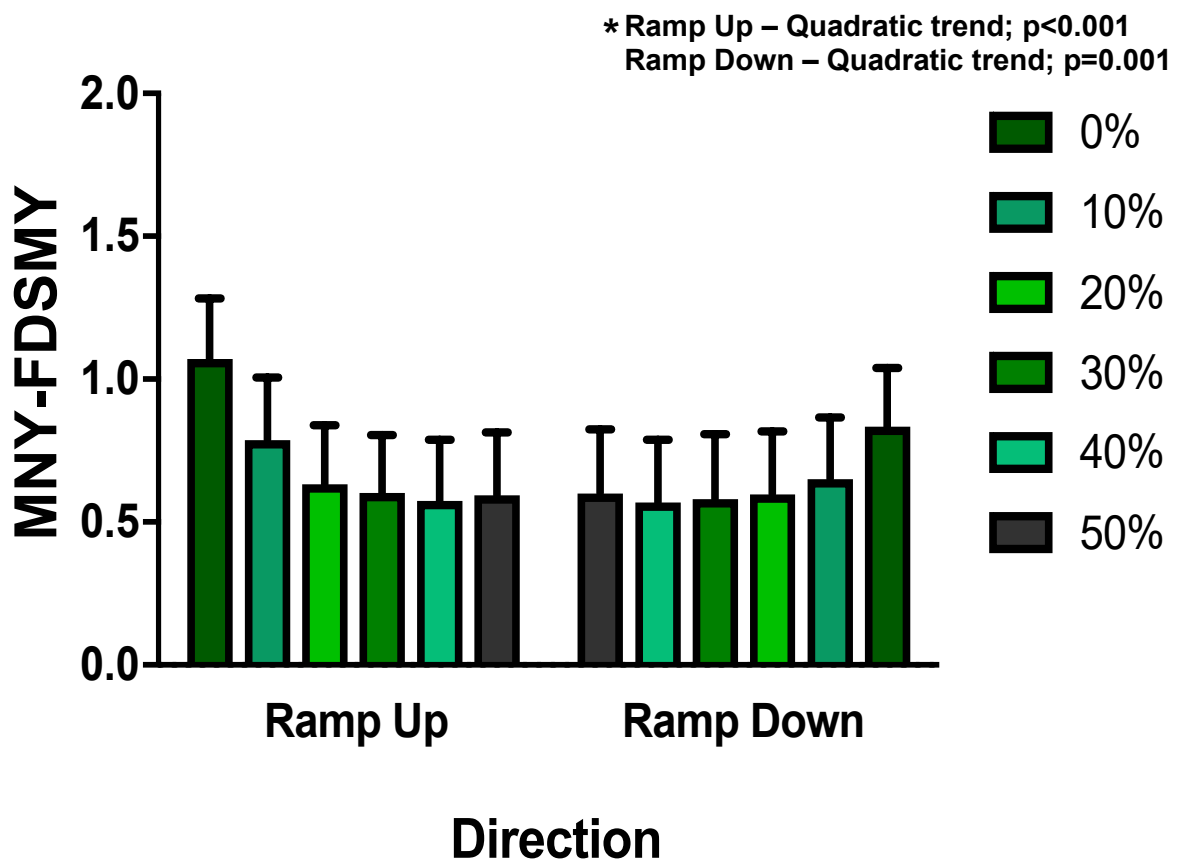


Figure 6.20. Mean (\pm standard error of the mean) median nerve (MN) position relative to the flexor digitorum superficialis tendon of the middle finger (FDS_M) in the Y-axis during the ramp up and ramp down phases throughout grip force production. *Note: + indicates palmar position; – indicates dorsal position.*

Chapter 7

Discussion

Median nerve (MN) deformation and displacement relative to the flexor digitorum superficialis tendon of the middle finger (FDS_M) were both assessed in concert during three occupational grip types while ramping grip force up from 0% to 50% of maximal voluntary effort (MVE) followed by ramping grip force down from 50% to 0% MVE. To my knowledge, this is the first study to assess MN deformation and displacement throughout the entire time course of loading and unloading the fingertips. Previous studies used a single image of the carpal tunnel to represent each static loading condition within the experimental protocol, such as maintaining a grip with next to no grip force (~0% MVE), a medium grip force (~25% MVE), and a high grip force level (~50% MVE), all performed in separate experimental trials (Cowley et al., 2017; Gabra et al., 2016; Loh et al., 2018; Woo et al., 2016; Yoshii et al., 2009). In contrast, the use of trapezoidal force ramping profiles in my study enabled me to extract images of the MN from 0% to 50% MVE in 10% increments of MVE. Furthermore, images were extracted while loading (i.e. ramp up) and unloading (i.e. ramp down) the fingertips, thus resulting in 12 images per trapezoidal ramp, and 3 consecutive trapezoidal ramps per experimental condition, for a total of 36 images per experimental condition. This allowed me to analyze time-dependent changes throughout the entire trials, which to my knowledge is a novel contribution to the literature.

In this study, I documented deformational changes to the MN, including time-dependent changes in MN width, height, perimeter, and circularity. During the ramp up phase, the MN generally became more circular from 0% to 20% MVE due to decreased width in the radial-ulnar axis and increased height in the palmar-dorsal axis; however, there was very little change from 20% to 50% MVE. In contrast, the MN flattened (i.e. became less circular) during the ramp down

phase, which occurred more gradually (i.e. linearly) throughout 50% to 0% MVE. Relative changes in deformation were also particularly interesting, since the deformational changes associated with ramping force up were not completely reversed by ramping force back down. Interestingly, MN displacement also changed in a time-dependent manner, and these results generally mirrored those observed for deformation metrics. For example, in the palmar-dorsal axis, the MN migrated dorsally relative to the FDS_M while ramping force up from 0% to 20% MVE. As observed previously for the deformation metrics, there were no further changes in MN position in the palmar-dorsal axis from 20% to 50% MVE. Conversely, the MN migrated palmarly during the ramp down. However, the percent change was considerably smaller (% change for ramp up – 80%; ramp down – 39%), such that the nerve did not return to its original position at the beginning of the trial. The results were similar for MN displacement relative to the FDS_M in the radial-ulnar axis, showing differences in ramping force up versus down. Since both deformation and displacement metrics changed in a similar time-dependent manner, this may suggest that MN deformation changes are linked to its displacement relative to other anatomical structures within the carpal tunnel. Interestingly, the time-dependent trends observed in the transverse plane of the carpal tunnel mirror previous research demonstrating viscoelastic characteristics of flexor tendon and surrounding subsynovial connective tissue (Kociolek & Keir, 2015; Kociolek et al., 2015; Kociolek et al., 2016; Tat et al., 2016). Thickening and fibrosis of the connective tissue that loosely binds the anatomical structures within the carpal tunnel may ultimately result in increased local strain, and eventually cause entrapment of the MN (van Doesburg et al., 2012a; van Doesburg et al., 2012b).

While the exact injury pathway(s) of carpal tunnel syndrome (CTS) remain elusive, the progression of this repetitive strain disorder ultimately results in entrapment of the MN. Several

mechanisms are likely involved in the development of CTS, including localized contact stress (Armstrong & Chaffin, 1979), elevated carpal tunnel pressure (Vignais et al., 2016), and increased strain and shear between the anatomical structures and surrounding connective tissue within the carpal tunnel (Tat et al., 2013; Tat et al., 2015; Tat et al., 2016). Although ultrasound imaging cannot directly measure strain or shear, studies in the longitudinal plane of the carpal tunnel have shown the relative motion between the MN, flexor tendons, and surrounding subsynovial connective tissue (SSCT) is reduced in CTS patients versus healthy controls (van Doesburg et al., 2012a), and when the wrist/hand is subjected to physical exposures, such as frequent movements (Korstanje et al., 2012; Tat et al., 2013), forceful exertions (Kociolek et al., 2015) and non-neutral postures (Kociolek et al., 2015). While previous ultrasound studies of the transverse carpal tunnel have documented MN deformational changes in response to physical exposures, very few have demonstrated changes in MN cross-sectional area (Cowley et al., 2017; Yao et al., 2020). Therefore, these previous results are not consistent with an injury pathway caused by nerve compression (even if that is the ultimate outcome in CTS). However, my current results may shed further light on a likely injury pathway involved in hand-intensive work. More specifically, simultaneous measurement of MN deformation and position throughout the entire time history of loading and unloading the fingertips suggests these two factors are intimately related. Therefore, one plausible explanation of injury development may be that the MN (a passive structure) is displaced by the tendons (an active structure) within the transverse carpal tunnel, which increases strain between the MN and surrounding SSCT, thereby resulting in deformation of the MN. The current results support the implication of the SSCT, since the time-dependent effects observed during loading and unloading in my study mirror the hysteretic effects previously quantified for the highly viscoelastic SSCT (Kociolek et al., 2016).

A significant interaction between ramp force direction and force production level was observed for both MN deformation (width and perimeter) and MN position relative to the FDS_M (X- and Y- axes), with a curvilinear relationship observed from 0% to 50% MVE during ramp up (i.e. loading) and a linear trend from 50% to 0% MVE during ramp down (i.e. unloading). It is hypothesized that these time-dependent trends are indicative of a hysteretic effect owing to the highly viscoelastic SSCT, which tethers all anatomical structures to each other within the carpal tunnel (Guimberteau et al., 2010). Viscoelastic properties of the SSCT are well documented in the literature, including time-dependent differences in tenosynovial sliding during proximal tendon displacement associated with wrist/finger flexion versus distal tendon displacement associated with wrist/finger extension (Kociolek et al., 2016; Tat et al., 2013). Furthermore, energy loss due to viscoelastic shear from SSCT strain during large tendon displacements and velocities has also been quantified in the longitudinal direction (Filius et al., 2014; Filius et al., 2017; Kociolek et al., 2015; Tat et al., 2016). Since my current study captured similar time-dependent mechanical phenomena in the transverse plane of the carpal tunnel, my results suggest that SSCT strain in the radial-ulnar and palmar-dorsal axes may also contribute to its non-inflammatory remodelling (fibrosis and thickening), in turn increasing the volume of carpal tunnel contents, and increasing hydrostatic pressure. While this finding has important implications for injury, more work is needed to characterize viscoelastic properties of the SSCT in the radial-ulnar and palmar-dorsal axes since it is unlikely that the SSCT will demonstrate isotropic effects in all axes (Osamura et al., 2007).

A number of ultrasound studies have investigated whether physical risk factors influence MN cross-sectional area (CSA) since CTS ultimately results in the compression of the MN (Cowley et al., 2017; Greening et al., 2001; van Doesburg et al., 2012a; Wang et al., 2014; Yoshii et al., 2009). In this study, no significant main effects were found for MN CSA over the 3 grip

types (pulp, chuck, power), 2 ramp force directions (ramp up vs. ramp down), and 6 force production levels (0%-50% MVE in 10% increments of MVE). However, there was a significant interaction between grip type and ramp force direction on MN CSA, where the CSA was smaller during the ramp up (vs. ramp down) phase in the chuck grip condition; however, there were no significant differences in pulp or power grips. It is worth highlighting that of all the statistical tests performed (i.e. 3 main effects, 3 two-way interactions, 1 three-way interaction), the interaction between grip type and ramp force direction was the only significant finding with respect to MN CSA. Furthermore, post-hoc testing revealed that this significant interaction was the result of only 1 significant pairwise comparison (in chuck grip). Furthermore, this significant finding occurred from a difference between loading and unloading the fingers (i.e. ramp force direction), which to my knowledge was not previously tested since other assessments used a static loading protocol. Generally, my findings coincide with previous research that also found no significant main effects of grip type and grip force on the MN CSA (Cowley et al., 2017; Turcotte & Kociolek, 2021; van Doesburg et al., 2010; van Doesburg et al., 2012b; Wang et al., 2014). Overall, these previous results on MN CSA, combined with the dearth of significant findings in my study, suggest that the MN is relatively resistant to compressive changes with the addition of external load.

MN width, height, perimeter, and circularity were assessed to test for deformation during the experimental conditions, and significant effects involving grip type, ramp force direction, and force production level were all observed. Across all the grip types, the greatest deformational changes to the MN occurred while ramping force up from 0% to 20% MVE, which resulted in increased circularity of the MN. Generally, this resulted in a quadratic trend, with the greatest deformational changes occurring from 0% to 20% MVE, with very little change thereafter (20% - 50% MVE). However, deformational changes while ramping force down from 50% to 0% MVE

were more consistent, often resulting in a linear trend. Both MN width and perimeter provide good examples of the differing trend analyses while ramping force up and down. These results are consistent with previous studies that tested different wrist and finger positions (such as grip types) and/or manipulated finger loads (Loh et al., 2018; MacDonald & Keir, 2018; van Doesburg et al., 2010; Wang et al., 2014; Yoshii et al., 2009). While considering that I observed deformational changes (i.e. changes in width, height, perimeter, and circularity) but with little to no coincident change in the MN CSA, these results together may suggest that the MN is changing shape as a function of strain from surrounding tissues as opposed to being compressed against the transverse carpal ligament (this is also supported by nerve movement patterns in the palmar-dorsal axis as discussed below). Similar results were found by Cowley et al. (2017) during a chuck grip, which showed that MN circularity increased by 12.5% from 0% MVE grip force with 0° wrist flexion (MN circularity = 0.56 ± 0.11) to 50% MVE grip force with 30° flexion (MN circularity = 0.63 ± 0.11). Meanwhile the percent change in MN CSA over the same conditions was only 1.8%. Since the present study assessed the MN dynamically throughout force production, it appears that the deformational changes are at least related to (if not caused by) changes in the position of the MN relative to the other structures within the carpal tunnel, further resulting in strain of the SSCT.

Interestingly, MN displacement also changed in a time-dependent manner, mirroring results observed for the deformation metrics. More specifically, the largest MN position changes occurred during the ramp up from 0%-20% MVE, where the MN moved ulnarly and dorsally relative to the FDS_M. While the position of the MN was reversed during ramping force down, moving radially and palmarly, overall there was less displacement in the ramp down such that the MN did not return to its original position within the carpal tunnel. This may have consequences for occupational grip tasks that are performed repetitively, since SSCT strain would be sustained

if the wrist/hand is not moved to a neutral position between gripping efforts to enable the carpal tunnel structures to return to their ‘resting’ position. Generally, my results of MN displacement match with previous research (van Doesburg et al. 2012a; Wang et al., 2014; Yoshii et al., 2009). For example, Yoshii et al. (2009) found that the FDS_M was dorsal to the MN following isolated middle finger movement, and further displaced either radially or ulnarly during full fist motion. Turcotte & Kociolek (2021) also documented several movement patterns of the MN, with 64% of chuck grip trials in an ulnar deviated wrist posture migrating toward the radial border of the carpal tunnel, and 75% of chuck grip trials in a radial deviated wrist posture migrating toward the ulnar border.

In my study, I also documented a significant grip type by force production level interaction on position of the MN in the palmar-dorsal axis (i.e. Y-axis). Specifically, I found greater dorsal displacement in the chuck grip (compared to the pulp grip and power grip), which was represented by a quadratic trend from 0% to 50% MVE (Figure 6.19). When assessing both displacement and deformation in conjunction, it appears that the active carpal tunnel structures (i.e. the flexor tendons) determined both the position and shape of the passive structures. More specifically, when comparing the three grip types, the middle finger is the most activated during the chuck grip with both the FDS_M and the FDS_I developing active tension and therefore causing the nerve to migrate dorsally and ulnarly while becoming more circular. In contrast, the four active tendons in the power grip span almost the entire radial-ulnar axis of the carpal tunnel, resulting in the MN remaining palmar to the FDS_M . Yoshii et al. (2009) also found that the MN deformed more with a single-digit versus four-digit (i.e. full fist) movement, highlighting the importance of considering the configuration of the active tendons inside the carpal tunnel to fully understand movement and deformation patterns of the MN. In my study, significant differences involving grip type were also

observed with deformation metrics, including smaller width and perimeter as well as greater circularity of the MN in the chuck grip compared to the power grip. This further highlights the importance of considering the configuration of carpal tunnel structures associated with various grip types in addition to the effects of force production level.

Altogether, I observed the greatest changes in both MN deformation and displacement relative to the FDS_M tendon between 0 and 20% MVE. Further increases in force throughout the trials (from 20% to 50% MVE) resulted in little to no change for all outcome variables. As mentioned above, these time-dependent changes appear to match previous hysteretic effects documented for the flexor tendons and adjacent SSCT (Festen-Schrier & Amadio, 2018). The flexor tendons and MN are both surrounded by the SSCT in the carpal tunnel, which is crucially important for both tendon and nerve gliding to reduce friction (Tat et al., 2013). The SSCT is comprised of multiple thin layers of collagen, which are connected by perpendicular fibrils. Mechanically, deep layers of the SSCT closest to the flexor tendons and MN move first followed by the more superficial layers during longitudinal tendon/nerve displacements (Zhao et al., 2007). Longitudinal ultrasound assessment has also demonstrated that repetitive finger motion increases strain of the SSCT (Kociolek et al., 2015), which likely explains damage to the deepest collagen layers of the SSCT in patients with CTS (Donato et al., 2009). My results suggest that MN and FDS tendon displacement in the radial-ulnar and palmar-dorsal axes of the carpal tunnel may also contribute to strain of the SSCT, furthering complicating the plausible pathomechanisms of work-related CTS. When the SSCT becomes damaged due to excessive strain and/or shear in the longitudinal axis as well as the radial-ulnar and palmar-dorsal axes, its collagen layers become fibrotic and thicken, which in turn increases the volume of the carpal tunnel contents, elevates hydrostatic pressure, and compromises blood-flow to carpal tunnel structures including intra-

neural blood flow (Tat et al., 2015). These changes to the MN and the subsynovial gliding apparatus within the carpal tunnel may ultimately lead to different movement patterns between the active tendons and passive MN, ultimately leading to entrapment of the MN (van Doesburg et al., 2012c).

In addition to better understanding injury development of the wrist/hand, my results also have important implications for the workplace including ergonomic thresholds to prevent injury. More specifically, MN deformation and displacement occurred at relatively low grip force intensities, with the greatest changes between 0% and 20% MVE. These results suggest that prolonged repetitive efforts at even low forces are sufficient to displace the MN and flexor tendons within the carpal tunnel in all three axes, which may damage the SSCT owing to the accumulation of strain and/or shear over time. Several ergonomic assessment methods are available to predict injury risk of the wrist/hand, including the Threshold Limit Value for Hand Activity Level (ACGIH, 2001) as well as the Strain Index (Moore & Garg, 1995). Notably, both methods were recently updated, which altered the relationship between repetitive and forceful efforts and injury risk scores (ACGIH, 2018; Garg et al., 2017). For example, Garg et al. (2017) recently released the Revised Strain Index, which increased the injury risk weightings for movement frequency and duration per exertion, thereby placing a greater emphasis on repetition regardless of the intensity of force. Similarly, the updated Threshold Limit Value for Hand Activity Level (ACGIH, 2018) lowered the peak forces associated with the Threshold Limit. Altogether, these changes appear to acknowledge that wrist/hand injury may occur at relatively low force, which aligns with the findings in my study.

However, this study is not without limitations. To obtain transverse images of the carpal tunnel, participants were instructed to complete the trials in a supinated forearm position. This may

have increased length and strain of the flexor digitorum superficialis and profundus musculotendon units, which could influence maximal voluntary efforts (De Smet et al., 1998; Fan et al., 2019; Marley & Wehrman, 1992) as well as carpal tunnel dynamics (Rempel et al., 1998). While maximal grip forces differ as a function of forearm position (Mogk & Keir, 2003), all MVEs were performed in a supinated position for consistency with the experimental trials. Still, further research is needed to test the effects of MN deformation and strain in different forearm positions.

While great care was taken to correctly position the probe at the distal wrist crease, it is possible the angle of the probe was not always exactly 90° relative to the MN, even for gripping trials performed in a neutral wrist position. This could result in image parallax, and therefore influence the metrics (Mullin & Taylor, 2002). However, parallax error would be unlikely to influence the time-dependant trends observed in this study, especially given that the probe was locked in position throughout the entire trial and that any image parallax is expected to be reasonably small.

Furthermore, images were collected in a 30° flexed wrist position; however, the hyperechoic border of the MN was not distinct throughout the entire trapezoidal force ramps in a large subset of these trials. This likely resulted from additional challenges with ensuring the probe was directly perpendicular to the MN when the wrist was flexed to 30°. Capturing images throughout the entire time series of the ramp profiles was far more challenging than previous protocols that focused on static test conditions (i.e. sustaining a grip force at a constant level for each experimental condition). Limiting the analyses to the neutral wrist position ensured that carpal tunnel structures were correctly identified, including their borders throughout the gripping trials. Despite these challenges, the dynamic nature of the imaging protocol in my study allowed

me to document time-dependent effects, offering further insight into carpal tunnel dynamics in the transverse plane.

Finally, we only tested the right hand of healthy participants, and therefore we were unable to determine whether there were differences between each participant's dominant and non-dominant hand. However, since the extensive list of exclusion criteria in my study prevented the assessment of pathological wrist/hands, from a mechanical perspective both right and left examinations are expected to present similarly. In the case of testing patients with CTS, mechanical differences between the right and left wrist/hand would be far more likely (Ettema et al., 2007). Future studies would benefit from testing both dominant and non-dominant hands in CTS patients and healthy controls as well as accounting for anthropometrics and/or sex.

Chapter 8

Conclusion

We observed changes to median nerve (MN) dynamics during gripping tasks in the transverse plane of the carpal tunnel, including coincident changes in both MN deformation (i.e. width, height, perimeter, and circularity) as well as displacement in the radial-ulnar and palmar-dorsal axes. Furthermore, we observed time-dependent effects throughout the trials, which were characterized by differences in the ramp up versus ramp down phases of the gripping tasks. Specifically, the MN became more circular and migrated ulnarly and dorsally while ramping force up from 0% to 20% MVE. However, very little to no change was documented from 20% to 50% MVE. On the other hand, the MN flattened (i.e. became less circular) during the ramp down phase, which occurred more gradually (i.e. linearly) throughout 50% to 0% MVE. Furthermore, the deformation and displacement that occurred when ramping force up was not completely reversed when ramping force down, such that the MN did not return to its initial shape or position in the carpal tunnel (when comparing the beginning and end of the trials). This is suggestive that MN deformation is linked to (if not caused by) its displacement in the carpal tunnel, which may infer an injury mechanism based on strain between the carpal tunnel structures and the subsynovial connective tissue that loosely binds these structures together (as opposed to an injury mechanism directly related to compressive force). Future studies might benefit from further manipulating the loading rates, or the slopes, of the trapezoidal force profiles to further study viscoelastic effects. Outcomes measures that focus on dynamics such as velocity and acceleration of the MN may also assist in elucidating potential injury pathways.

Chapter 9

References

- ACGIH. (2001). *2001 Threshold Limit Values for Chemical Substances and Physical Agents and Biological Exposure Indices*. Cincinnati, OH: American Conference of Governmental Industrial Hygienists (ACGIH).
- ACGIH. (2018). *2018 Threshold Limit Values for Chemical Substances and Physical Agents and Biological Exposure Indices*. Cincinnati, OH: American Conference of Governmental Industrial Hygienists (ACGIH).
- Armstrong, T. J., & Chaffin, D. B. (1979). Some biomechanical aspects of the carpal tunnel. *Journal of Biomechanics*, 12(7), 567-570.
- Barr, A. E., Barbe, M. F., & Clark, B. D. (2004). Work-related musculoskeletal disorders of the hand and wrist: epidemiology, pathophysiology, and sensorimotor changes. *Journal of Orthopaedic & Sports Physical Therapy*, 34(10), 610-627.
- Bernard, B. P., & Putz-Anderson, V. (1997). *Musculoskeletal Disorders and Workplace Factors: A Critical Review of Epidemiologic Evidence for Work-Related Musculoskeletal Disorders of the Neck, Upper Extremity, and Low Back*. Cincinnati, OH: US Department of Health and Human Services.
- Bramson, J. B., Smith, S., & Romagnoli, G. (1998). Evaluating dental office ergonomic risk factors and hazards. *The Journal of the American Dental Association*, 129(2), 174-183.
- Chiang, H. C., Chen, S. S., Yu, H. S., & Ko, Y. C. (1990). The occurrence of carpal tunnel syndrome in frozen food factory employees. *The Kaohsiung Journal of Medical Sciences*, 6(2), 73-80.
- Cowley, J. C., Leonardis, J., Lipps, D. B., & Gates, D. H. (2017). The influence of wrist posture, grip type, and grip force on median nerve shape and cross-sectional area. *Clinical Anatomy*, 30(4), 470-478.
- De Smet, L., Tirez, B., & Stappaerts, K. (1998). Effect of forearm rotation on grip strength. *Acta Orthopaedica Belgica*, 64(4), 360-362.
- DiDomenico, A., & Nussbaum, M. A. (2003). Measurement and prediction of single and multi-digit finger strength. *Ergonomics*, 46(15), 1531-1548.
- Donato, G., Galasso, O., Valentino, P., Conforti, F., Zuccalà, V., Russo, E., & Amorosi, A. (2009). Pathological findings in subsynovial connective tissue in idiopathic carpal tunnel syndrome. *Clinical Neuropathology*, 28(2), 129-135.

- Dong, H., Loomer, P., Barr, A., LaRoche, C., Young, E., & Rempel, D. (2008). The effect of tool handle shape on hand muscle load and pinch force in a simulated dental scaling task. *Applied Ergonomics*, 38(5), 525-531.
- Ettema, A. M., Zhao, C., Amadio, P. C., O'Byrne, M. M., & An, K. N. (2007). Gliding characteristics of flexor tendon and tenosynovium in carpal tunnel syndrome: a pilot study. *Clinical Anatomy*, 20(3), 292-299.
- Ettema, A. M., An, K. N., Zhao, C., O'Byrne, M. M., & Amadio, P. C. (2008). Flexor tendon and synovial gliding during simultaneous and single digit flexion in idiopathic carpal tunnel syndrome. *Journal of Biomechanics* 41, 292-298.
- Fan, S., Cepek, J., Symonette, C., Ross, D., Chinchalkar, S., & Grant, A. (2019). Variation of grip strength and wrist range of motion with forearm rotation in healthy young volunteers aged 23 to 30. *Journal of Hand and Microsurgery*, 11(2), 88-93.
- Festen-Schrier, V. J. M. M., & Amadio, P. C. (2018). The biomechanics of subsynovial connective tissue in health and its role in carpal tunnel syndrome. *Journal of Electromyography and Kinesiology*, 38, 232-239.
- Field, A. (2013). *Discovering Statistics Using IBM SPSS Statistics*. 4th Ed. Los Angeles, CA: SAGE Publications Ltd.
- Filius, A., Korstanje, J. W., Selles, R. W., Hovius, S. E., & Slijper, H. P. (2013). Dynamic sonographic measurements at the carpal tunnel inlet: reliability and reference values in healthy wrists. *Muscle & Nerve*, 48, 525-531.
- Filius, A., Thoreson, A. R., Yang, T. H., Vanhees, M., An, K. N., Zhao, C., & Amadio, P. C. (2014). The effect of low-and high-velocity tendon excursion on the mechanical properties of human cadaver subsynovial connective tissue. *Journal of Orthopaedic Research*, 32(1), 123-128.
- Filius, A., Thoreson, A. R., Ozasa, Y., An, K. N., Zhao, C., & Amadio, P. C. (2017). Delineation of the mechanisms of tendon gliding resistance within the carpal tunnel. *Clinical Biomechanics*, 41, 48-53.
- Gabra, J. N., Gordon, J. L., Marquardt, T. L., & Li, Z. M. (2016). In vivo tissue interaction between the transverse carpal ligament and finger flexor tendons. *Medical Engineering & Physics*, 38(10), 1055-1062.
- Garg, A., Moore, J. S., & Kapellusch, J. (2017). The Revised Strain Index: an improved upper extremity exposure assessment model. *Ergonomics*, 60, 912-922.
- Ghasemi-rad, M., Nosair, E., Vegh, A., Mohammadi, A., Akkad, A., Lesha, E., & Hasan, A. (2014). A handy review of carpal tunnel syndrome: from anatomy to diagnosis and treatment. *World Journal of Radiology*, 6(6), 284-300.

- Giovagnorio, F., Andreoli, C., & De Cicco, M. L. (1997). Ultrasonographic evaluation of de Quervain disease. *Journal of Ultrasound in Medicine*, 16(10), 685-689.
- Goh, C. H., Lee, B. H., & Lahiri, A. (2015). Biphasic motion of the median nerve in the normal Asian population. *Hand Surgery*, 20(1), 73-80.
- Gould, T. E., Jesunathadas, M., Nazarenko, S., & Piland, S. G. (2019). Mouth protection in sports. *Materials in Sports Equipment*, 199-231.
- Greening, J., Lynn, B., Leary, R., Warren, L., O'Higgins, P., & Hall-Craggs, M. (2001). The use of ultrasound imaging to demonstrate reduced movement of the median nerve during wrist flexion in patients with non-specific arm pain. *Journal of Hand Surgery*, 26(5), 401-406.
- Greig, M., & Wells, R. (2004). Measurement of prehensile grasp capabilities by a force and moment wrench: methodological development and assessment of manual workers. *Ergonomics*, 47(1), 41-58.
- Guimberteau, J. C., Delage, J. P., McGrouther, D. A., & Wong, J. K. F. (2010). The microvacuolar system: how connective tissue sliding works. *Journal of Hand Surgery (European Volume)*, 35(8), 614-622.
- Harris-Adamson, C., You, D., Eisen, E., Goldberg, R., & Rempel, D. (2014). The impact of posture on wrist tendinosis among blue-collar workers: the San Francisco study. *Human Factors*, 56(1), 143-150.
- Heilskov-Hansen, T., Mikkelsen, S., Svendsen, S. W., Thygesen, L. C., Hansson, G., & Thomsen, J. F. (2016). Exposure-response relationships between movements and postures of the wrist and carpal tunnel syndrome among male and female house painters: a retrospective cohort study. *Occupational and Environmental Medicine*, 73(6), 401-408.
- Kaymak, B., Özçakar, L., Çetin, A., Çetin, M. C., Akıncı, A., & Haşçelik, Z. (2008). A comparison of the benefits of sonography and electrophysiologic measurements as predictors of symptom severity and functional status in patients with carpal tunnel syndrome. *Archives of Physical Medicine and Rehabilitation*, 89(4), 743-748.
- Keir, P. J., Bach, J. M., & Rempel, D. M. (1998). Effects of finger posture on carpal tunnel pressure during wrist motion. *Journal of Hand Surgery*, 23(6), 1004-1009.
- Keir, P. J., Bach, J. M., Hudes, M., & Rempel, D. M. (2007). Guidelines for wrist posture based on carpal tunnel pressure thresholds. *Human Factors*, 49(1), 88-99.
- Kociolek, A. M., & Keir, P. J. (2015). Development of a kinematic model to predict finger flexor tendon and subsynovial connective tissue displacement in the carpal tunnel. *Ergonomics*, 58(8), 1398-1409.
- Kociolek, A. M., Tat, J., & Keir, P. J. (2015). Biomechanical risk factors and flexor tendon frictional work in the cadaveric carpal tunnel. *Journal of Biomechanics*, 48(3), 449-455.

- Kociolek, A. M., Tat, J., & Keir, P. J. (2016). Viscoelastic characteristics of the subsynovial connective tissue during flexor tendon gliding in the carpal tunnel. 19th Biennial Meeting of the Canadian Society for Biomechanics. Hamilton ON, July 19-22.
- Kociolek, A. M., & Keir, P. J. (2016). Relative motion between the flexor digitorum superficialis tendon and paratenon in zone V increases with wrist flexion angle. *Journal of Orthopaedic Research*, 34(7), 1248-1255.
- Korstanje, J. H., Selles, R. W., Stam, H. J., Hovius, S. R., & Bosch, J. G. (2010a). Development and validation of ultrasound speckle tracking to quantify tendon displacement. *Journal of Biomechanics*, 43(7), 1373-1379.
- Korstanje, J. H., Schreuders, T. R., van der Sijde, J., Hovius, S. R., Bosch, J. G., & Selles, R. W. (2010b). Ultrasonographic assessment of long finger tendon excursion in zone v during passive and active tendon gliding exercises. *Journal of Hand Surgery*, 35(4), 559-565.
- Korstanje, J. H., Scheltens-De Boer, M., Blok, J. H., Amadio, P. C., Hovius, S. R., Stam, H. J., & Selles, R. W. (2012). Ultrasonographic assessment of longitudinal median nerve and hand flexor tendon dynamics in carpal tunnel syndrome. *Muscle & Nerve*, 45(5), 721-729.
- Kubo, K., Zhou, B., Cheng, Y., Yang, T., Qiang, B., An, K. N., & Zhao, C. (2018). Ultrasound elastography for carpal tunnel pressure measurement: a cadaveric validation study. *Journal of Orthopaedic Research*, 36(1), 477-483.
- Kutluhan, S., Akhan, G., Demirci, S., Duru, S., Koyuncuoglu, H. R., Ozturk, M., & Cirak, B. (2001). Carpal tunnel syndrome in carpet workers. *International Archives of Occupational and Environmental Health*, 74(6), 454-457.
- Loh, P. Y., & Muraki, S. (2015). Effect of wrist angle on median nerve appearance at the proximal carpal tunnel. *PLoS ONE*, 10(2), e0117930.
- Loh, P. Y., Nakashima, H., & Muraki, S. (2016). Effects of grip force on median nerve deformation at different wrist angles. *PeerJ*, 4, e2510.
- Loh, P. Y., Yeoh, W. L., Nakashima, H., & Muraki, S. (2018). Deformation of the median nerve at different finger postures and wrist angles. *PeerJ*, 6, e5406.
- Lopes, M. M., Lawson, W., Scott, T., & Keir, P. J. (2011). Tendon and nerve excursion in the carpal tunnel in healthy and CTD wrists. *Clinical Biomechanics*, 26(9), 930-936.
- Lundborg, G., Gelberman, R. H., Minteer-Convery, M., Lee, Y. F., & Hargens, A. R. (1982). Median nerve compression in the carpal tunnel—functional response to experimentally induced controlled pressure. *Journal of Hand Surgery*, 7(3), 252-259.

- MacDonald, V., & Keir, P. J. (2018). Assessment of musculoskeletal disorder risk with hand and syringe use in chemotherapy nurses and pharmacy assistants. *IIE Transactions on Occupational Ergonomics and Human Factors*, 6(3-4), 128-142.
- Manes, H. R. (2012). Prevalence of carpal tunnel syndrome in motorcyclists. *Orthopedics*, 35(5), 399-400.
- Manktelow, R. T., Binhammer, P., Tomat, L. R., Bril, V., & Szalai, J. P. (2004). Carpal tunnel syndrome: cross-sectional and outcome study in Ontario workers. *Journal of Hand Surgery*, 29(2), 307-317.
- Marley, R. J., & Wehrman, R. R. (1992). Grip strength as a function of forearm rotation and elbow posture. *Proceedings of the Human Factors Society Annual Meeting*, 36(10), 791-795.
- McGorry, R. W., Dowd, P. C., & Dempsey, P. G. (2003). Cutting moments and grip forces in meat cutting operations and the effect of knife sharpness. *Applied Ergonomics*, 34(4), 375-382.
- Mhanna, C., Marquardt, T. L., & Li, Z. (2016). Adaptation of the transverse carpal ligament associated with repetitive hand use in pianists. *PLoS ONE*, 11(3), e0150174.
- Mogk, J., & Keir, P. (2003). The effects of posture on forearm muscle loading during gripping. *Ergonomics*, 46(9), 956-975.
- Moore, J. S., & Garg, A. (1995). The strain index: a proposed method to analyze jobs for risk of distal upper extremity disorders. *American Industrial Hygiene Association Journal*, 56(5), 443-458.
- Mullin, S. K., & Taylor, P. J. (2002). The effects of parallax on geometric morphometric data. *Computers in Biology and Medicine*, 32(6), 455-464.
- Nanno, M., Sawaizumi, T., Kodera, N., Tomori, Y., & Takai, S. (2015). Transverse ultrasound assessment of the displacement of the median nerve in the carpal tunnel during wrist and finger motion in healthy volunteers. *Journal of Nippon Medical School*, 82(4), 170-179.
- Osamura, N., Zhao, C., Zobitz, M. E., An, K. N., & Amadio, P. C. (2007). Evaluation of the material properties of the subsynovial connective tissue in carpal tunnel syndrome. *Clinical Biomechanics*, 22(9), 999-1003.
- Palmer, K. T., Harris, E. C., & Coggon, D. (2007). Carpal tunnel syndrome and its relation to occupation: a systematic literature review. *Occupational Medicine*, 57(1), 57-66.
- Punnett, L., & Wegman, D. (2004). Work-related musculoskeletal disorders: the epidemiologic evidence and the debate. *Journal of Electromyography and Kinesiology*, 14(1), 13-23.
- Rempel, D., Keir, P. J., Smutz, W. P., & Hargens, A. (1997). Effects of static fingertip loading on carpal tunnel pressure. *Journal of Orthopaedic Research*, 15(3), 422-426.

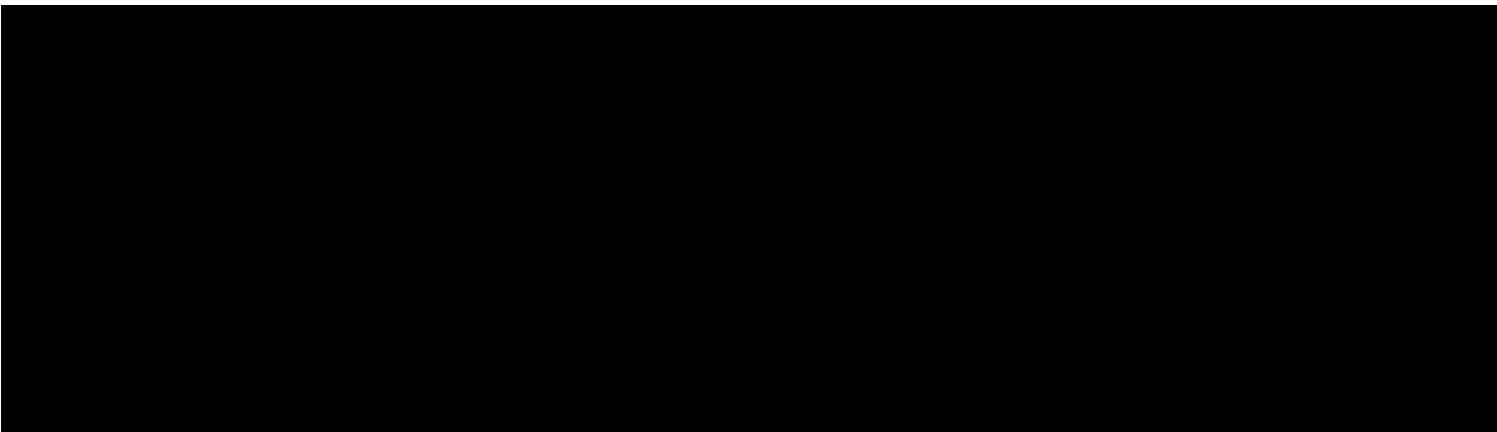
- Rempel, D., Bach, J. M., Gordon, L., & So, Y. (1998). Effects of forearm pronation/supination on carpal tunnel pressure. *Journal of Hand Surgery*, 23(1), 38-42.
- Roquelaure, Y., Mechali, S., Dano, C., Fanello, S., Benetti, F., Bureau, D., & Penneau-Fontbonne, D. (1997). Occupational and personal risk factors for carpal tunnel syndrome in industrial workers. *Scandinavian Journal of Work, Environment & Health*, 364-369.
- Saladin, K. S. (2007). *Anatomy & Physiology: The Unity of Form and Function*. 7th Ed. New York, NY: McGraw-Hill Education.
- Shergill, A. K., Asundi, K. R., Barr, A., Shah, J. N., Ryan, J. C., McQuaid, K. R., & Rempel, D. (2009). Pinch force and forearm-muscle load during routine colonoscopy: a pilot study. *Gastrointestinal Endoscopy*, 69(1), 142-146.
- Silverstein, B. A., Fine, L. J., & Armstrong, T. J. (1987). Occupational factors and carpal tunnel syndrome. *American Journal of Industrial Medicine*, 11(3), 343-358.
- Silverstein, B., Welp, E., Nelson, N., & Kalat, J. (1998). Claims incidence of work-related disorders of the upper extremities: Washington state, 1987 through 1995. *American Journal of Public Health*, 88(12), 1827-1833.
- Soeters, J. M., Roebroek, M. E., Holland, W. J., Hovius, S. R., & Stam, H. J. (2004). Reliability of tendon excursion measurements in patients using a color Doppler imaging system. *Journal of Hand Surgery*, 29(4), 581-586.
- Tat, J., Kociolek, A. M., & Keir, P. J. (2013). Repetitive differential finger motion increases shear strain between the flexor tendon and subsynovial connective tissue. *Journal of Orthopaedic Research*, 31(10), 1533-1539.
- Tat, J., Kociolek, A. M., & Keir, P. J. (2015). Validation of color Doppler sonography for evaluating relative displacement between the flexor tendon and subsynovial connective tissue. *Journal of Ultrasound in Medicine*, 34(4), 679-687.
- Tat, J., Kociolek, A. M., & Keir, P. J. (2016). Relative displacement of the tendon and subsynovial connective tissue using ultrasound captures different phenomena than mechanical tendon shear. *Journal of Biomechanics*, 49(15), 3682-3687.
- Turcotte, K. E., & Kociolek, A. M. (2021). Median nerve travel and deformation in the transverse carpal tunnel increases with chuck grip force and deviated wrist position. *PeerJ*, 9, e11038.
- Ugbohue, U. C., Hsu, W. H., Goitz, R. J., & Li, Z. M. (2005). Tendon and nerve displacement at the wrist during finger movements. *Clinical Biomechanics*, 20(1), 50-56.
- van Doesburg, M. H. M., Yoshii, Y., Villarraga, H. R., Henderson, J., Cha, S. S., An, K. N., & Amadio, P. C. (2010). Median nerve deformation and displacement in the carpal tunnel during index finger and thumb motion. *Journal of Orthopaedic Research*, 28(10), 1387-1390.

- van Doesburg, M. H. M., Henderson, J., van der Molen, A. B. M., An, K. N., & Amadio, P. C. (2012a). Transverse plane tendon and median nerve motion in the carpal tunnel: ultrasound comparison of carpal tunnel syndrome patients and healthy volunteers. *PLoS ONE*, 7(5), e37081.
- van Doesburg, M. H. M., Henderson, J., Yoshii, Y., van der Molen, A. B. M., Cha, S. S., An, K. N., & Amadio, P. C. (2012b). Median nerve deformation in differential finger motions: ultrasonographic comparison of carpal tunnel syndrome patients and healthy controls. *Journal of Orthopaedic Research*, 30(4), 643-648.
- van Doesburg, M. H. M., Yoshii, Y., Henderson, J., Villarraga, H. R., Moran, S. L., & Amadio, P. C. (2012c). Speckle-tracking sonographic assessment of longitudinal motion of the flexor tendon and subsynovial tissue in carpal tunnel syndrome. *Journal of Ultrasound in Medicine*, 31(7), 1091-1098.
- Vignais, N., Weresch, J., & Keir, P. J. (2016). Posture and loading in the pathomechanics of carpal tunnel syndrome: a review. *Critical Reviews in Biomedical Engineering*, 44(5), 397-410.
- Wang, Y., Zhao, C., Passe, S. M., Filius, A., Thoreson, A. R., An, K. N., & Amadio, P. C. (2014). Transverse ultrasound assessment of median nerve deformation and displacement in the human carpal tunnel during wrist movements. *Ultrasound in Medicine & Biology*, 40(1), 53-61.
- Woo, E. H. C., White, P., Ng, H. K., & Lai, C. W. K. (2016). Development of kinematic graphs of median nerve during active finger motion: implications of smartphone use. *PloS ONE*, 11(7), e0158455.
- Woo, E. H. C., White, P., & Lai, C. W. K. (2019). Morphological changes of the median nerve within the carpal tunnel during various finger and wrist positions: an analysis of intensive and nonintensive electronic device users. *Journal of Hand Surgery*, 44(7), 610-611.
- WSIB. (2016). Statistical Supplement of the 2014 Annual Report. Toronto, ON: Workplace Safety and Insurance Board (WSIB) of Ontario Communications Division.
- Yao, B., Gan, K., Lee, A., & Roll, S. C. (2020). Comparing shape categorization to circularity measurement in the evaluation of median nerve compression using sonography. *Journal of Diagnostic Medical Sonography*, 36(3), 224-232.
- Yoshii, Y., Villarraga, H. R., Henderson, J., Zhao, C., An, K. N., & Amadio, P. C. (2009). Ultrasound assessment of the displacement and deformation of the median nerve in the human carpal tunnel with active finger motion. *Journal of Bone and Joint Surgery*, 91(12), 2922-2930.
- Zakaria, D. (2004). Rates of carpal tunnel syndrome, epicondylitis, and rotator cuff claims in Ontario workers during 1997. *Age*, 46(54.86), 74-52.

- Zamborsky, R., Kokavec, M., Simko, L., & Bohac, M. (2017). Carpal tunnel syndrome: symptoms, causes and treatment options. *Ortop Traumatol Rehabil*, 19(1), 1-8.
- Zhao, C., Ettema, A. M., Osamura, N., Berglund, L. J., An, K. N., & Amadio, P. C. (2007). Gliding characteristics between flexor tendons and surrounding tissues in the carpal tunnel: a biomechanical cadaver study. *Journal of Orthopaedic Research*, 25(2), 185-190.

Appendix A

Nipissing University and Brock University Research Ethics Certificates



July 20, 2017

Dr. Aaron Kociolek
Schulich School of Education\Physical Health and Education
Nipissing University



Dear Aaron,

It is our pleasure to advise you that the Research Ethics Board (REB) has reviewed your protocol titled 'The role of musculoskeletal interactions on wrist and hand biomechanics' and has granted ethical approval. Your protocol has been approved for a period of one year.

Modifications: Any changes to the approved protocol or corresponding materials must be reviewed and approved through the amendment process prior to its implementation.


Adverse/Unanticipated Event: Any adverse or unanticipated events must be reported immediately via the Research Portal.

Renewal/Final Report: Please ensure you submit an Annual Renewal or Final Report 30 days prior to the expiry date of your ethics approval. You will receive an email prompt 30 days prior to the expiry date.

Wishing you great success on the completion of your research.

Sincerely,


Dana R. Murphy, PhD
Chair, Research Ethics Board





June 18, 2018

Dr. Aaron Kociolek
Schulich School of Education\Physical Health and Education
Nipissing University



Expiry Date: July 20, 2018

Dear Aaron,

It is our pleasure to advise you that Research Ethics Board has reviewed your Request for Modification to protocol titled 'The role of musculoskeletal interactions on wrist and hand biomechanics' and has granted ethical approval.

Modifications: Any changes to the approved protocol or corresponding materials must be reviewed and approved through the amendment process prior to its implementation.

Adverse/Unanticipated Event: Any adverse or unanticipated events must be reported immediately via the Research Portal.

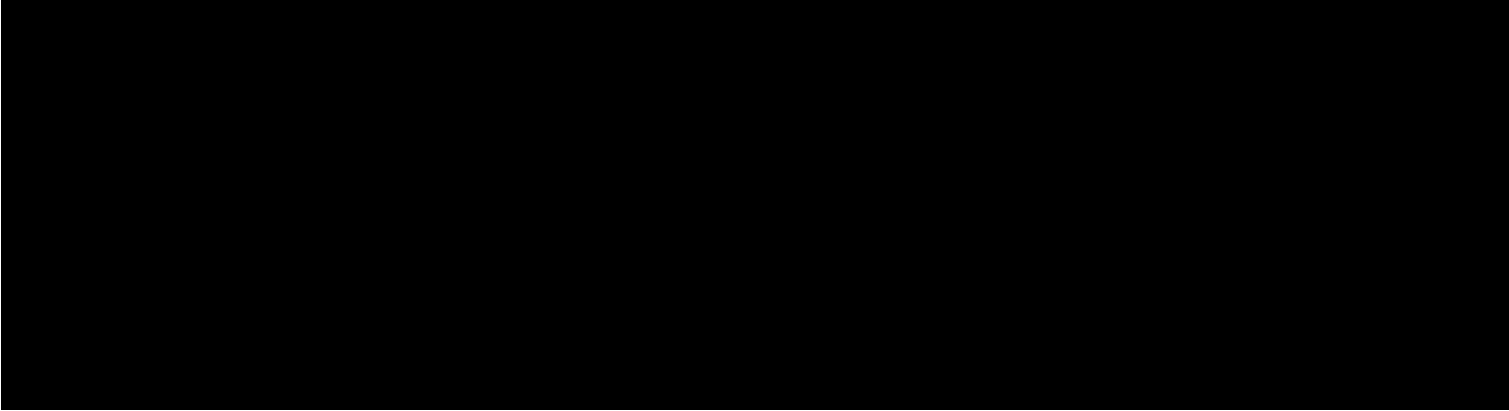
Renewal/Final Report: Please ensure you submit an Annual Renewal or Final Report 30 days prior to the expiry date of your ethics approval. You will receive an email prompt 30 days prior to the expiry date.

Wishing you great success on the completion of your research.

Sincerely,


Dana R. Murphy, PhD





July 09, 2018

Dr. Aaron Kociolek
Schulich School of Education\Physical Health and Education
Nipissing University



Expiry Date: July 9, 2019

Dear Aaron,

It is our pleasure to advise you that Research Ethics Board has reviewed your Request for Renewal to protocol titled 'The role of musculoskeletal interactions on wrist and hand biomechanics' and has granted ethical approval. This renewal is valid for one year. Prior to the next renewal date you will be sent a reminder and the link to ROMEO to renew for another year. You are reminded of your obligation to submit an Annual Renewal/Final Report prior to the renewal due date. When your research project is completed, you are required to submit a Final Report and the file will be closed. Please note that all protocols involving ongoing data collection or interaction with human participants are subject to re-evaluation after 5 years.

Modifications: Any changes to the approved protocol or corresponding materials must be reviewed and approved through the amendment process prior to its implementation.


Adverse/Unanticipated Event: Any adverse or unanticipated events must be reported immediately via the Research Portal.

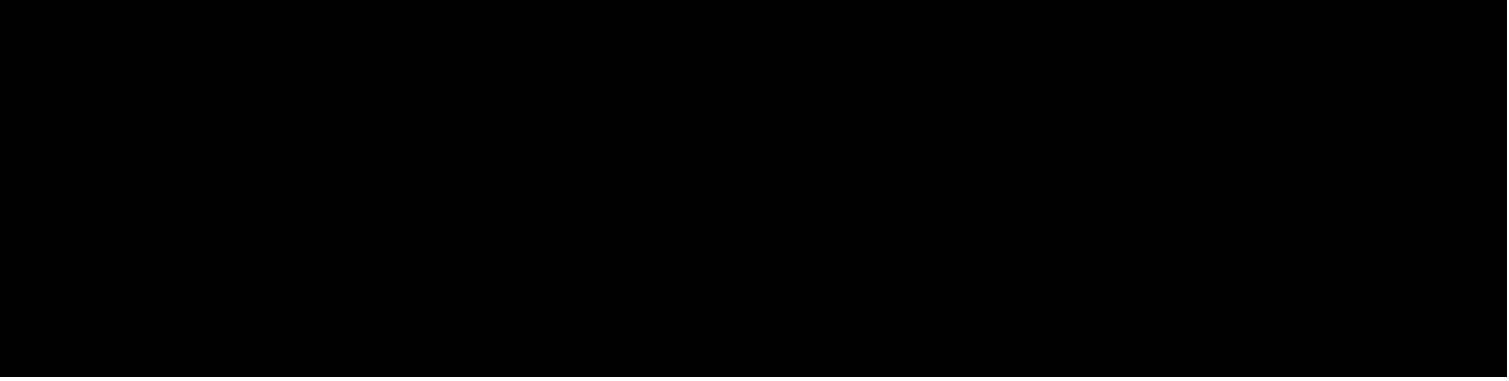
Renewal/Final Report: Please ensure you submit an Annual Renewal or Final Report 30 days prior to the expiry date of your ethics approval. You will receive an email prompt 30 days prior to the expiry date.

Wishing you great success on the completion of your research.

Sincerely,


Dana R. Murphy, PhD
Chair, Research Ethics Board





July 16, 2019

Dr. Aaron Kociolek
Faculty of Education and Professional Studies\Physical Health and Education
Nipissing University



Expiry Date: July 13, 2020

Dear Aaron,

It is our pleasure to advise you that Research Ethics Board has reviewed your Request for Renewal to protocol titled 'The role of musculoskeletal interactions on wrist and hand biomechanics' and has granted ethical approval. This renewal is valid for one year. Prior to the next renewal date you will be sent a reminder and the link to ROMEQ to renew for another year. You are reminded of your obligation to submit an Annual Renewal/Final Report prior to the renewal due date. When your research project is completed, you are required to submit a Final Report and the file will be closed.

Research protocols may be renewed a maximum of three times. If additional time is required, a new protocol must be submitted.

Modifications: Any changes to the approved protocol or corresponding materials must be reviewed and approved through the amendment process prior to its implementation.

Adverse/Unanticipated Event: Any adverse or unanticipated events must be reported immediately via the Research Portal.

Renewal/Final Report: Please ensure you submit an Annual Renewal or Final Report 30 days prior to the expiry date of your ethics approval. You will receive an email prompt 30 days prior to the expiry date.

Wishing you great success on the completion of your research.


Sincerely,

Steve Hansen, PhD
Chair, Research Ethics Board



July 31, 2020

Dr. Aaron Kociolek
Faculty of Education and Professional Studies\Physical Health and Education
Nipissing University



Expiry Date: July 30, 2021

Dear Aaron,

It is our pleasure to advise you that Research Ethics Board has reviewed your Request for Renewal to protocol titled 'The role of musculoskeletal interactions on wrist and hand biomechanics' and has granted ethical approval. This renewal is valid for one year. Prior to the next renewal date you will be sent a reminder and the link to ROMEO to renew for another year. You are reminded of your obligation to submit an Annual Renewal/Final Report prior to the renewal due date. When your research project is completed, you are required to submit a Final Report and the file will be closed.

Research protocols may be renewed a maximum of three times. If additional time is required, a new protocol must be submitted.

Modifications: Any changes to the approved protocol or corresponding materials must be reviewed and approved through the amendment process prior to its implementation.

Adverse/Unanticipated Event: Any adverse or unanticipated events must be reported immediately via the Research Portal.

Renewal/Final Report: Please ensure you submit an Annual Renewal or Final Report 30 days prior to the expiry date of your ethics approval. You will receive an email prompt 30 days prior to the expiry date.

Wishing you great success on the completion of your research.

Sincerely,

Steve Hansen, PhD
Chair, Research Ethics Board



Bioscience Research Ethics Board

Certificate of Ethics Clearance for Human Participant Research

DATE: 10/10/2018

PRINCIPAL INVESTIGATOR: KOCIOLEK, Aaron - Schulich School of Education\Physical Health and Education (Nipissing)

CO-INVESTIGATOR(S): Gabrielle Racine (XXXXXXX); Dean Hay (XXXXXXX); Alison Schinkel-Ivy (XXXXXXX)

FILE:



TYPE: Faculty Research

TITLE: The role of musculoskeletal interactions on wrist and hand biomechanics

ETHICS CLEARANCE GRANTED

Type of Clearance: NEW

Expiry Date: 10/1/2019

The Brock University Bioscience Research Ethics Board has reviewed the above named research proposal and considers the procedures, as described by the applicant, to conform to the University's ethical standards and the Tri-Council Policy Statement. Clearance granted from **10/10/2018** to **10/1/2019**.

The Tri-Council Policy Statement requires that ongoing research be monitored by, at a minimum, an annual report. Should your project extend beyond the expiry date, you are required to submit a Renewal form before 10/1/2019. Continued clearance is contingent on timely submission of reports.

To comply with the Tri-Council Policy Statement, you must also submit a final report upon completion of your project. All report forms can be found on the Research Ethics web page at <http://www.brocku.ca/research/policies-and-forms/research-forms>.

In addition, throughout your research, you must report promptly to the REB:

- a) Changes increasing the risk to the participant(s) and/or affecting significantly the conduct of the study;
- b) All adverse and/or unanticipated experiences or events that may have real or potential unfavourable implications for participants;
- c) New information that may adversely affect the safety of the participants or the conduct of the study;
- d) Any changes in your source of funding or new funding to a previously unfunded project.



Note: Brock University is accountable for the research carried out in its own jurisdiction or under its auspices and may refuse certain research even though the REB has found it ethically acceptable. If research participants are in the care of a health facility, at a school, or other institution or community organization, it is the responsibility of the Principal Investigator to ensure that the ethical guidelines and clearance of those facilities or institutions are obtained and filed with the REB prior to the initiation of research at that site.




Bioscience Research Ethics Board

Certificate of Ethics Clearance for Human Participant Research

DATE: 10/1/2019

PRINCIPAL INVESTIGATOR: KOCIOLEK, Aaron - Schulich School of Education\Physical Health and Education (Nipissing)

FILE: 

TYPE: Faculty Research

TITLE: The role of musculoskeletal interactions on wrist and hand biomechanics

ETHICS CLEARANCE GRANTED

Type of Clearance: RENEWAL	Initial Clearance Date: 10/10/2018 Expiry Date: 10/1/2020
----------------------------	--

The Brock University Bioscience Research Ethics Board has reviewed the above named research proposal and considers the procedures, as described by the applicant, to conform to the University's ethical standards and the Tri-Council Policy Statement.

Renewed certificate valid from **10/1/2019 to 10/1/2020**.

The Tri-Council Policy Statement requires that ongoing research be monitored by, at a minimum, an annual report. Should your project extend beyond the expiry date, you are required to submit a Renewal form before **10/1/2020**. Continued clearance is contingent on timely submission of reports.

To comply with the Tri-Council Policy Statement, you must also submit a final report upon completion of your project. All report forms can be found on the Office of Research Ethics web page at <http://www.brocku.ca/research/policies-and-forms/research-forms>.

In addition, throughout your research, you must report promptly to the REB:

- a) Changes increasing the risk to the participant(s) and/or affecting significantly the conduct of the study;
- b) All adverse and/or unanticipated experiences or events that may have real or potential unfavourable implications for participants;
- c) New information that may adversely affect the safety of the participants or the conduct of the study;
- d) Any changes in your source of funding or new funding to a previously unfunded project.



Note: Brock University is accountable for the research carried out in its own jurisdiction or under its auspices and may refuse certain research even though the REB has found it ethically acceptable. If research participants are in the care of a health facility, at a school, or other institution or community organization, it is the responsibility of the Principal Investigator to ensure that the ethical guidelines and clearance of those facilities or institutions are obtained and filed with the REB prior to the initiation of research at that site.

Certificate of Ethics Clearance for Human Participant Research

DATE: 9/18/2020

PRINCIPAL INVESTIGATOR: KOCIOLEK, Aaron - Schulich School of Education\Physical Health and Education (Nipissing)

FILE: [REDACTED]

TYPE: Faculty Research

TITLE: The role of musculoskeletal interactions on wrist and hand biomechanics

ETHICS CLEARANCE GRANTED

Type of Clearance: RENEWAL	Initial Clearance Date: 10/10/2018 Expiry Date: 10/1/2021
----------------------------	--

The Brock University Health Science Research Ethics Board has reviewed the above named research proposal and considers the procedures, as described by the applicant, to conform to the University's ethical standards and the Tri-Council Policy Statement.

Renewed certificate valid from **9/18/2020 to 10/1/2021**.

The Tri-Council Policy Statement requires that ongoing research be monitored by, at a minimum, an annual report. Should your project extend beyond the expiry date, you are required to submit a Renewal form before **10/1/2021**. Continued clearance is contingent on timely submission of reports.

To comply with the Tri-Council Policy Statement, you must also submit a final report upon completion of your project. All report forms can be found on the Office of Research Ethics web page at <http://www.brocku.ca/research/policies-and-forms/research-forms>.

In addition, throughout your research, you must report promptly to the REB:

- a) Changes increasing the risk to the participant(s) and/or affecting significantly the conduct of the study;
- b) All adverse and/or unanticipated experiences or events that may have real or potential unfavourable implications for participants;
- c) New information that may adversely affect the safety of the participants or the conduct of the study;
- d) Any changes in your source of funding or new funding to a previously unfunded project.

We wish you success with your research.

Approved: [REDACTED]

Craig Tokuno, Chair
Health Science Research Ethics Board

Note: Brock University is accountable for the research carried out in its own jurisdiction or under its auspices and may refuse certain research even though the REB has found it ethically acceptable. If research participants are in the care of a health facility, at a school, or other institution or community organization, it is the responsibility of the Principal Investigator to ensure that the ethical guidelines and clearance of those facilities or institutions are obtained and filed with the REB prior to the initiation of research at that site.

Appendix B

Participant Information Letter and Informed Consent



Participant Information Letter and Informed Consent for Identified Participants

You are being invited to participate in a research study called “*The role of musculoskeletal interactions on wrist and hand biomechanics*” lead by Dr Aaron Kociolek from the School of Physical and Health Education. The results of this study will contribute to both student and faculty research. If you have questions or concerns, please feel free to contact the lead researcher:

Dr Aaron M Kociolek

Assistant Professor

School of Physical & Health Education



Study Introduction and Purpose

Your hands are important for performing many daily activities and work tasks, from getting dressed, to preparing a meal, to using hand-held tools or technology. While using your hands takes very little thought, their biomechanics are complex. It is especially important to understand how different anatomical structures, including nerves, muscles, tendons, and ligaments, interact to provide steady hand function. The purpose of this study is to explore the inter-relationships between these anatomical structures during voluntary gripping tasks with your hands.

Participation Procedures

If you decide to volunteer, we will ask you to participate in an experiment conducted in the Biomechanics Laboratory (RSAC # 148). The study will last no more than 3 hours. Your participation will involve the following procedures:

- (1) You will be asked to complete a questionnaire about previous injuries, disorders, or conditions that may affect your hands. The survey will also ask about any related treatments or medications, your work experience, and musical instrument experience (if any) since both may influence your dexterity. The questionnaire will take about 15 minutes to complete.
- (2) We will attach up to 8 sensors on your dominant forearm and hand to measure your muscle activity. In order to provide useful data, the sensors need to be calibrated. This will involve Maximal Voluntary Efforts, or MVEs. You will be asked to squeeze a handle that has a built-in force sensor to measure your maximal gripping force. You will perform up to 8 MVEs (1 for each sensor). MVEs will take about 10 seconds each, and there will be rest periods to prevent fatigue. Altogether, setting up and calibrating the muscle sensors may take up to 30 minutes.
- (3) Next, we will attach small, reflective markers on your hand, which will allow motion capture cameras to measure your wrist and finger motions. The markers will be attached to your skin

using medical (hypoallergenic) double-sided tape. Taping the small markers on your skin may take up to 15 minutes.

- (4) We will also use an ultrasound system to scan your wrist, which will provide images of the nerves, muscles, tendons, and ligaments. In order to make sure all the anatomical structures of the wrist are in clear view, positioning the ultrasound scanner on the skin's surface may take up to 15 minutes.
- (5) Once the measurement equipment is setup and calibrated, you will be asked to perform 2 blocks of gripping tasks against a small object that has a small force sensor in it. The 1st block will involve different hand grips, and include different gripping forces and wrist postures. The 2nd block will involve gripping a small versus large object to change your grip span while also pulling forward or pushing backward with your hand. In total, you will be asked to perform 58 gripping tasks, each lasting no more than 30 seconds. While the gripping tasks will involve sub-maximal efforts that are unlikely to cause muscle fatigue, you will be provided with rest between each. Performing the gripping tasks with rest will take up to 80 minutes.
- (6) Once you have completed the gripping tasks, we will remove the measurement equipment from the surface of your skin, including the sensors over your muscles, motion capture markers, and ultrasound scanner. We can remove the electrodes and tape, or if you prefer, you can remove them yourself. It may take up to 5 minutes to remove the electrodes and tape and clean any adhesive residue on your skin with alcohol swabs.

Study Risks

This study does pose minimal risks to you, which you should be aware of before deciding if you would like to participate. The questionnaire will ask about your personal health. To ensure your responses remain confidential, you will be assigned a study number, and you will only be identified by this number, including on your health questionnaire. This will ensure your personal health responses remain confidential. Also, only the researchers will have access to your questionnaire, and it will be stored in a locked cabinet in Dr Kociolek's locked office.

It is possible you may experience discomfort or even anxiety during some segments of the study. In particular, performing Maximal Voluntary Efforts, or MVEs, with your hand may cause muscle fatigue, similar to what you might experience during vigorous exercise. In order to minimize your discomfort and fatigue, we will provide a break between each different finger task. During the breaks, we will ask how you are feeling. If at any time, you experience extreme discomfort or pain, please let us know immediately. Just like exercise, performing these finger tasks should never cause you any pain. If they do, we will stop the study immediately.

There is a remote chance that you could have an allergic reaction to the adhesive from the electrodes or medical tape. If you experience any itchiness or discomfort from wearing the measurement equipment, please let us know immediately, and we will remove all of the equipment from your skin.

Study Benefits

While this study will not benefit you directly, your participation will lead to a better understanding of wrist and hand function, which will improve clinical knowledge, including a better understanding of injury development. This research will also lead to better ergonomics in the workplace. Ultimately, our goal is to prevent musculoskeletal disorders of the wrist and hand.

Payment and Reimbursement

You will receive \$30.00 for your participation. If you withdraw from this study, you will still receive compensation.

In signing this consent form, you should understand that:

- You may ask questions at any given time during participation;
- Your participation is voluntary and that refusal to participate will involve no penalty, or loss of benefits to which you are otherwise entitled;
- You can refuse participation at any time during the experiment, and any data collected will not be included in the results of the experiment (unless otherwise stated);
- The researcher might be known to you; however, your identity will be protected by a participant coding system and a secure filing system;
- You will be assigned a code number, and your name will not be associated with the questionnaire or computer collected data.

Results will be available upon request. If you are interested in the results of the study, please contact Dr Aaron Kociolek. It is expected that the results will be presented at academic conferences and will be submitted for publication in peer-reviewed journals. The data will only be accessed by the investigators and will be on file in a secure location for a period of five years. Following that time, Dr Kociolek will destroy the data and any other materials.

This study has been reviewed and received ethics clearance through Nipissing University's Research Ethics Board. If you have questions regarding your rights as a research participant, contact: Ethics Administrator, Nipissing University, 100 College Drive – F307, North Bay, ON P1B 8L7 [REDACTED]

Confidentiality Process

Any information obtained in connection with this study that can be identified with you will remain confidential and will be disclosed only with your permission. Participation in this study is voluntary and you are free to withdrawal at any time. You have the right to refuse any question(s) that you find objectionable or that make you feel uncomfortable. You may withdrawal your consent at any time and discontinue participation without penalty.

Informed Consent to Participate

As a participant in this research project, I clearly understand that what I am agreeing to do, that I am free to decline involvement or withdrawal from this project at any time, and that steps are being taken to protect my safety and anonymity. I have read this participant information letter and the accompanying consent form. I have had any questions, concerns, or complaints answered to my satisfaction. I have been provided with a copy of this letter.

Name

Date

Signature

Witness Name

Date

Witness Signature

Appendix C
Screening Questionnaire



Participant Questionnaire:

The Role of Musculoskeletal Interactions on Wrist and Hand Biomechanics

A. PARTICIPANT IDENTIFICATION (to be completed by the researcher)

Participant #: _____ **Date:** _____

B. DEMOGRAPHICS / ANTHROPOMETRICS

Gender: _____

Age: _____

Height: _____

Weight: _____

C. HANDEDNESS

1) Are you right-handed, left-handed or ambidextrous?

right-handed ☐ **left-handed** ☐ **ambidextrous** ☐

D. HEALTH HISTORY

1) Have you ever had any of the following health conditions and/or treatment protocols performed on you currently and/or in the past? [*please check all that apply*]

- | | |
|--|--|
| <input type="checkbox"/> Diabetes mellitus | <input type="checkbox"/> Radial malunion |
| <input type="checkbox"/> Thyroid condition (e.g. Hypothyroidism) | <input type="checkbox"/> Colles fracture |
| <input type="checkbox"/> Gout | <input type="checkbox"/> Peripheral neuropathy |
| <input type="checkbox"/> Amyloidosis or Sarcoidosis | <input type="checkbox"/> Carpal tunnel syndrome |
| <input type="checkbox"/> Renal failure or Hemodialysis | <input type="checkbox"/> Flexor tendinopathy |
| <input type="checkbox"/> Degenerative joint disease | <input type="checkbox"/> Wrist/hand surgery |
| <input type="checkbox"/> Arthritis of the wrist/hand | <input type="checkbox"/> Hand pain/tingling/numbness |
| <input type="checkbox"/> Corticosteroid injection | <input type="checkbox"/> Other wrist/hand injury or disorder (not listed above): |
- _____
-
-

2) Are you currently on any medications? **Yes** ☐ **No** ☐

**** If *yes*, please list:**

E. WORK HISTORY

1) Occupation:

2) Location of work:

3) Hours at work per week:

4) Years at current job:

5) Typical tasks performed at work:

6) Have you ever-experienced a work-related wrist or hand injury? **Yes** ☐ **No** ☐

**** If *yes*, please elaborate (type of injury, onset, symptoms, and treatment):**

F. MUSIC HISTORY

1) Do you play musical instrument(s)? Yes ☐ No ☐

*** If yes, please answer the following questions:

a) Type of instrument(s):

b) Hour per week spent playing instrument(s):

c) Self-reported skill level (e.g. hobby, amateur, professional):

*** End ***

Appendix D

Grip Forces During the Experimental Trials

Table D.1 Mean (\pm standard error of the mean) grip forces extracted in both absolute (N) and relative (%) terms while ramping force up from 0%-50% MVE and ramping force down from 50%-0% MVE during the 6-second trapezoidal force profiles (2-second ramp up, 2-second plateau, 2-second ramp down).

	Up 0	Up 10	Up 20	Up 30	Up 40	Up 50	Down 50	Down 40	Down 30	Down 20	Down 10	Down 0
<i>Power</i>												
<i>Time (sec)</i>	0.00 (0.00)	0.42 (0.02)	0.83 (0.03)	1.31 (0.07)	1.80 (0.05)	2.26 (0.07)	4.09 (0.04)	4.36 (0.05)	4.76 (0.04)	5.24 (0.05)	5.74 (0.06)	6.35 (0.11)
<i>Force (%)</i>	0.00 (0.00)	10.02 (0.01)	20.01 (0.01)	30.02 (0.01)	40.01 (0.01)	47.80 (0.54)	46.35 (0.31)	40.02 (0.01)	30.01 (0.01)	20.01 (0.01)	10.19 (0.13)	0.00 (0.00)
<i>Force (N)</i>	0.00 (0.00)	34.99 (2.63)	69.89 (5.25)	104.83 (7.88)	139.75 (10.49)	167.44 (13.42)	161.82 (12.16)	139.77 (10.50)	104.82 (7.87)	69.89 (5.25)	35.42 (2.50)	0.00 (0.00)
<i>Chuck</i>												
<i>Time (sec)</i>	0.00 (0.00)	0.49 (0.02)	0.90 (0.03)	1.37 (0.06)	1.90 (0.09)	2.22 (0.08)	3.91(0.03)	4.23 (0.02)	4.56 (0.04)	4.96 (0.06)	5.38 (0.06)	6.11 (0.08)
<i>Force (%)</i>	0.00 (0.00)	10.02 (0.01)	20.02 (0.01)	30.02 (0.01)	40.02 (0.01)	45.78 (0.56)	45.33 (0.43)	40.03 (0.01)	30.02 (0.01)	20.02 (0.01)	10.02 (0.01)	0.00 (0.00)
<i>Force (N)</i>	0.00 (0.00)	9.07 (0.85)	18.11 (1.69)	27.16 (2.54)	34.68 (3.02)	39.71 (3.57)	39.41 (3.61)	34.69 (3.02)	27.16 (2.54)	18.11 (1.69)	9.06 (0.85)	0.00 (0.00)
<i>Pulp</i>												
<i>Time (sec)</i>	0.00 (0.00)	0.46 (0.03)	0.85 (0.05)	1.33 (0.06)	1.82 (0.07)	2.21 (0.07)	3.92 (0.06)	4.18 (0.04)	4.56 (0.05)	4.95 (0.04)	5.40 (0.03)	6.15 (0.08)
<i>Force (%)</i>	0.00 (0.00)	10.02 (0.01)	20.02 (0.01)	30.02 (0.01)	40.02 (0.01)	44.84 (0.64)	44.56 (0.44)	40.03 (0.01)	30.02 (0.01)	20.02 (0.01)	10.07 (0.05)	0.00 (0.00)
<i>Force (N)</i>	0.00 (0.00)	6.48 (0.71)	12.94 (1.41)	19.40 (2.12)	25.86 (2.83)	29.02 (3.16)	28.92 (3.22)	25.87 (2.83)	19.40 (2.12)	12.94 (1.41)	6.52 (0.72)	0.00 (0.00)

Appendix E

Within Subject Effects from Repeated Measures ANOVA

Table E.1. Tests of within-subject effects for median nerve cross-sectional area.

Factor(s)	DoF_{Factor}	DoF_{Error}	F Statistic	p-value
Grip Type	2.00	22.00	3.15	0.063
Ramp Force Direction	1.00	11.00	2.28	0.159
Force Production Level	2.11	23.18	0.36	0.714
Grip Type*Ramp Force Direction	2.00	22.00	9.34	0.001 *
Grip Type*Force Production Level	1.59	17.51	0.43	0.611
Ramp Force Direction*Force Production Level	5.00	55.00	1.49	0.208
Grip Type*Ramp Force Direction*Force Production Level	4.25	46.80	1.05	0.394

Note: DoF = Degrees of Freedom; Asterisk indicates statistical significance.

Table E.2. Tests of within-subject effects for median nerve perimeter.

Factor(s)	DoF_{Factor}	DoF_{Error}	F Statistic	p-value
Grip Type	2.00	22.00	5.30	0.013 *
Ramp Force Direction	1.00	11.00	0.04	0.838
Force Production Level	2.02	22.19	6.11	0.008 *
Grip Type*Ramp Force Direction	2.00	22.00	1.74	0.199
Grip Type*Force Production Level	2.34	25.71	0.45	0.672
Ramp Force Direction*Force Production Level	5.00	55.00	3.30	0.011 *
Grip Type*Ramp Force Direction*Force Production Level	4.88	53.70	0.48	0.483

Note: DoF = Degrees of Freedom; Asterisk indicates statistical significance.

Table E.3. Tests of within-subject effects for median nerve width.

Factor(s)	DoF_{Factor}	DoF_{Error}	F Statistic	p-value	
Grip Type	2.00	22.00	6.93	0.005	*
Ramp Force Direction	1.00	11.00	0.03	0.875	
Force Production Level	1.70	18.74	9.83	0.002	*
Grip Type*Ramp Force Direction	2.00	22.00	1.22	0.315	
Grip Type*Force Production Level	2.70	29.68	0.68	0.559	
Ramp Force Direction*Force Production Level	5.00	55.00	3.78	0.005	*
Grip Type*Ramp Force Direction*Force Production Level	4.50	49.53	0.57	0.706	

Note: DoF = Degrees of Freedom; Asterisk indicates statistical significance.

Table E.4. Tests of within-subject effects for median nerve height.

Factor(s)	DoF_{Factor}	DoF_{Error}	F Statistic	p-value	
Grip Type	2.00	22.00	3.95	0.034	*
Ramp Force Direction	1.00	11.00	0.83	0.381	
Force Production Level	2.05	22.55	3.33	0.053	
Grip Type*Ramp Force Direction	2.00	22.00	3.53	0.047	*
Grip Type*Force Production Level	4.19	46.10	1.29	0.289	
Ramp Force Direction*Force Production Level	2.76	30.35	0.83	0.478	
Grip Type*Ramp Force Direction*Force Production Level	10.00	110.00	1.70	0.090	

Note: DoF = Degrees of Freedom; Asterisk indicates statistical significance.

Table E.5. Tests of within-subject effects for median nerve circularity.

Factor(s)	DoF_{Factor}	DoF_{Error}	F Statistic	p-value
Grip Type	2.00	22.00	9.95	0.001 *
Ramp Force Direction	1.00	11.00	0.11	0.746
Force Production Level	1.43	15.73	7.70	0.008 *
Grip Type*Ramp Force Direction	2.00	22.00	1.31	0.290
Grip Type*Force Production Level	2.22	24.38	1.25	0.307
Ramp Force Direction*Force Production Level	1.60	17.61	3.18	0.075
Grip Type*Ramp Force Direction*Force Production Level	10.00	110.00	0.61	0.806

Note: DoF = Degrees of Freedom; Asterisk indicates statistical significance.

Table E.6. Tests of within-subject effects for median nerve position relative to the flexor digitorum superficialis tendon of the middle finger in the radial-ulnar (X-) axis.

Factor(s)	DoF_{Factor}	DoF_{Error}	F Statistic	p-value
Grip Type	2.00	22.00	2.40	0.115
Ramp Force Direction	1.00	11.00	19.93	0.001 *
Force Production Level	1.09	12.01	16.68	0.001 *
Grip Type*Ramp Force Direction	1.25	13.76	2.80	0.112
Grip Type*Force Production Level	3.38	37.16	2.00	0.125
Ramp Force Direction*Force Production Level	1.18	12.97	11.09	0.004 *
Grip Type*Ramp Force Direction*Force Production Level	3.16	34.81	2.41	0.081

Note: DoF = Degrees of Freedom; Asterisk indicates statistical significance.

Table E.7. Tests of within-subject effects for median nerve position relative to the flexor digitorum superficialis tendon of the middle finger in the palmar-dorsal (Y-) axis.

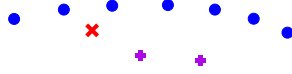
Factor(s)	DoF_{Factor}	DoF_{Error}	F Statistic	p-value	
Grip Type	2.00	22.00	8.01	0.002	*
Ramp Force Direction	1.00	11.00	2.46	0.145	
Force Production Level	1.19	13.07	10.46	0.005	*
Grip Type*Ramp Force Direction	2.00	22.00	6.13	0.008	*
Grip Type*Force Production Level	2.51	27.59	4.19	0.019	*
Ramp Force Direction*Force Production Level	2.08	22.88	4.15	0.028	*
Grip Type*Ramp Force Direction*Force Production Level	3.70	40.74	2.41	0.069	

Note: DoF = Degrees of Freedom; Asterisk indicates statistical significance.

Appendix F

Median Nerve and Flexor Tendon Position in the Carpal Tunnel

a)



b)



c)



d)



e)



f)



Figure F.1. Mean position of the median nerve (red x) located ulnarly to the flexor digitorum superficialis tendons of the index and middle fingers (purple +) and dorsally to the transverse carpal ligament (blue •) while ramping force up to (a) 0% MVE, (b) 10% MVE, (c) 20% MVE, (d) 30% MVE, (e) 40% MVE, and (f) 50% MVE during the pulp pinch gripping condition.

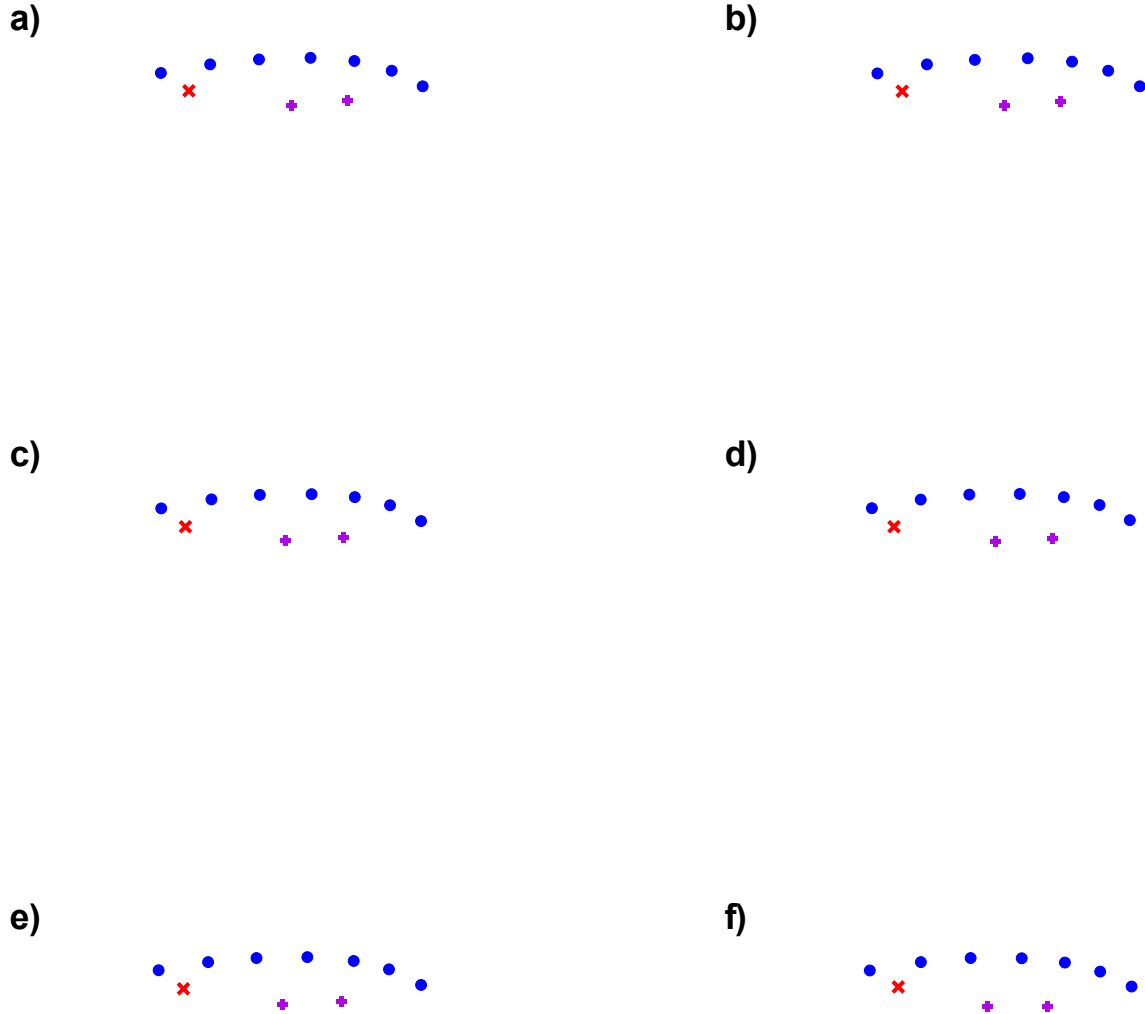


Figure F.2. Mean position of the median nerve (red x) located ulnarly to the flexor digitorum superficialis tendons of the index and middle fingers (purple +) and dorsally to the transverse carpal ligament (blue •) while ramping force down to (a) 50% MVE, (b) 40% MVE, (c) 30% MVE, (d) 20% MVE, (e) 10% MVE, and (f) 0% MVE during the pulp pinch gripping condition.

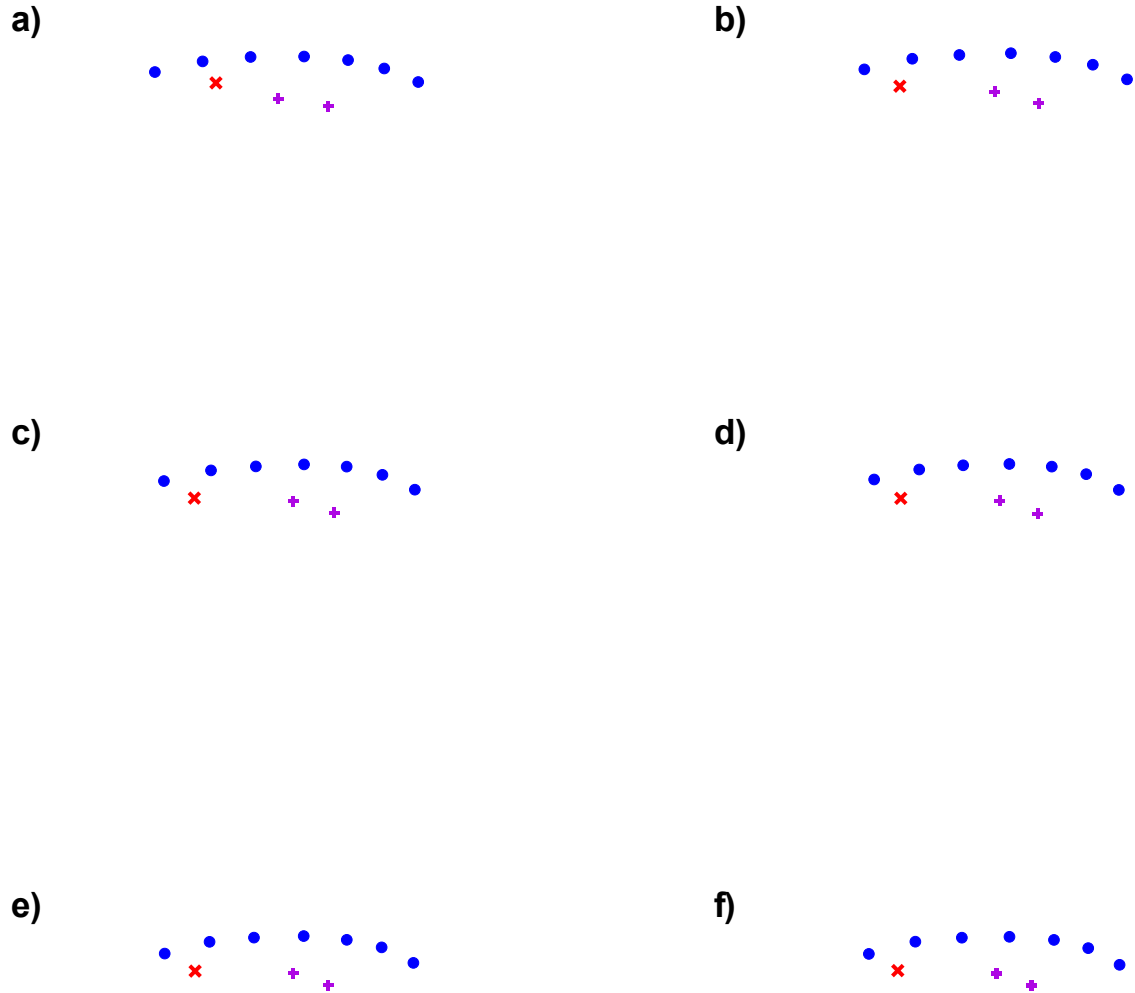


Figure F.3. Mean position of the median nerve (red x) located ulnarly to the flexor digitorum superficialis tendons of the index and middle fingers (purple +) and dorsally to the transverse carpal ligament (blue •) while ramping force up to (a) 0% MVE, (b) 10% MVE, (c) 20% MVE, (d) 30% MVE, (e) 40% MVE, and (f) 50% MVE during the chuck pinch gripping condition.

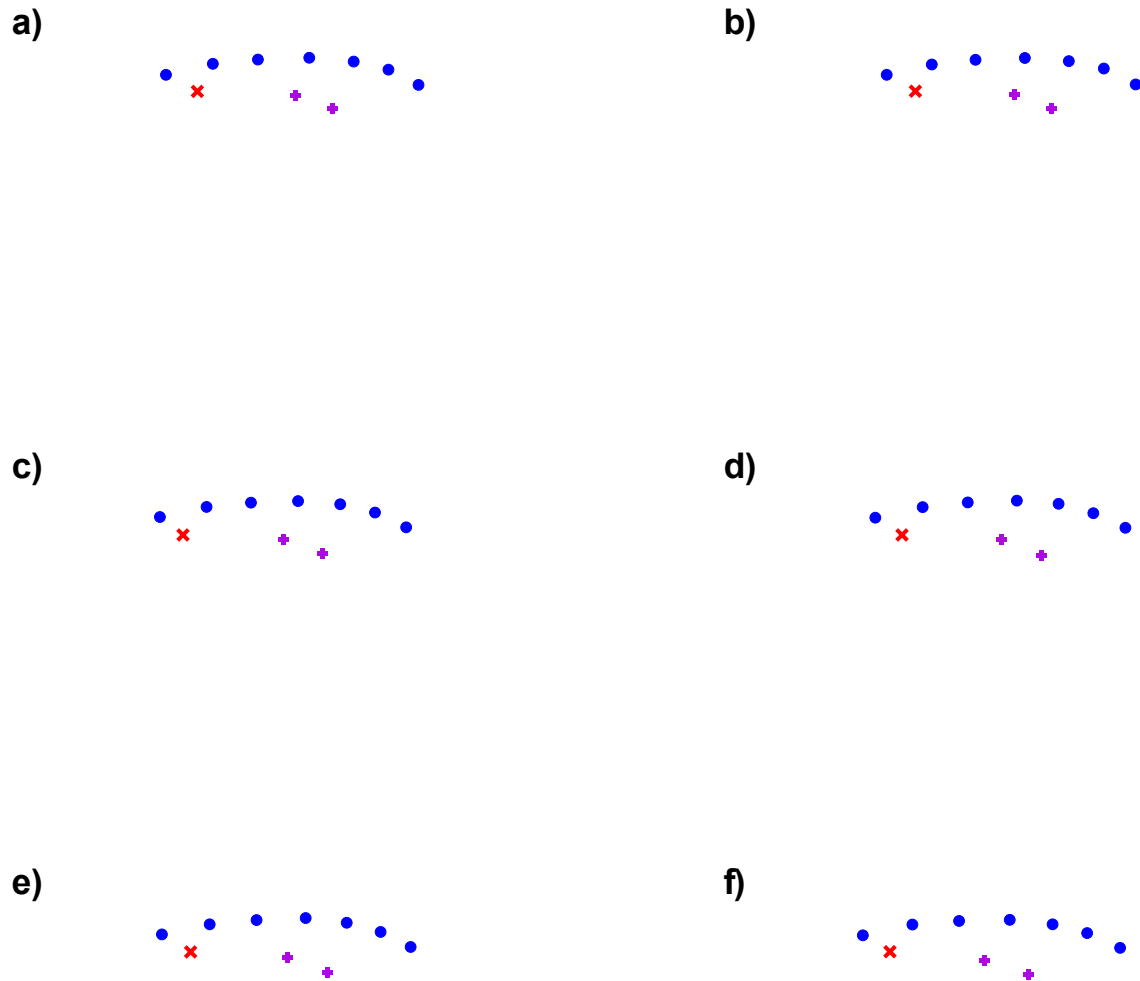


Figure F.4. Mean position of the median nerve (red x) located ulnarly to the flexor digitorum superficialis tendons of the index and middle fingers (purple +) and dorsally to the transverse carpal ligament (blue •) while ramping force down to (a) 50% MVE, (b) 40% MVE, (c) 30% MVE, (d) 20% MVE, (e) 10% MVE, and (f) 0% MVE during the chuck pinch gripping condition.

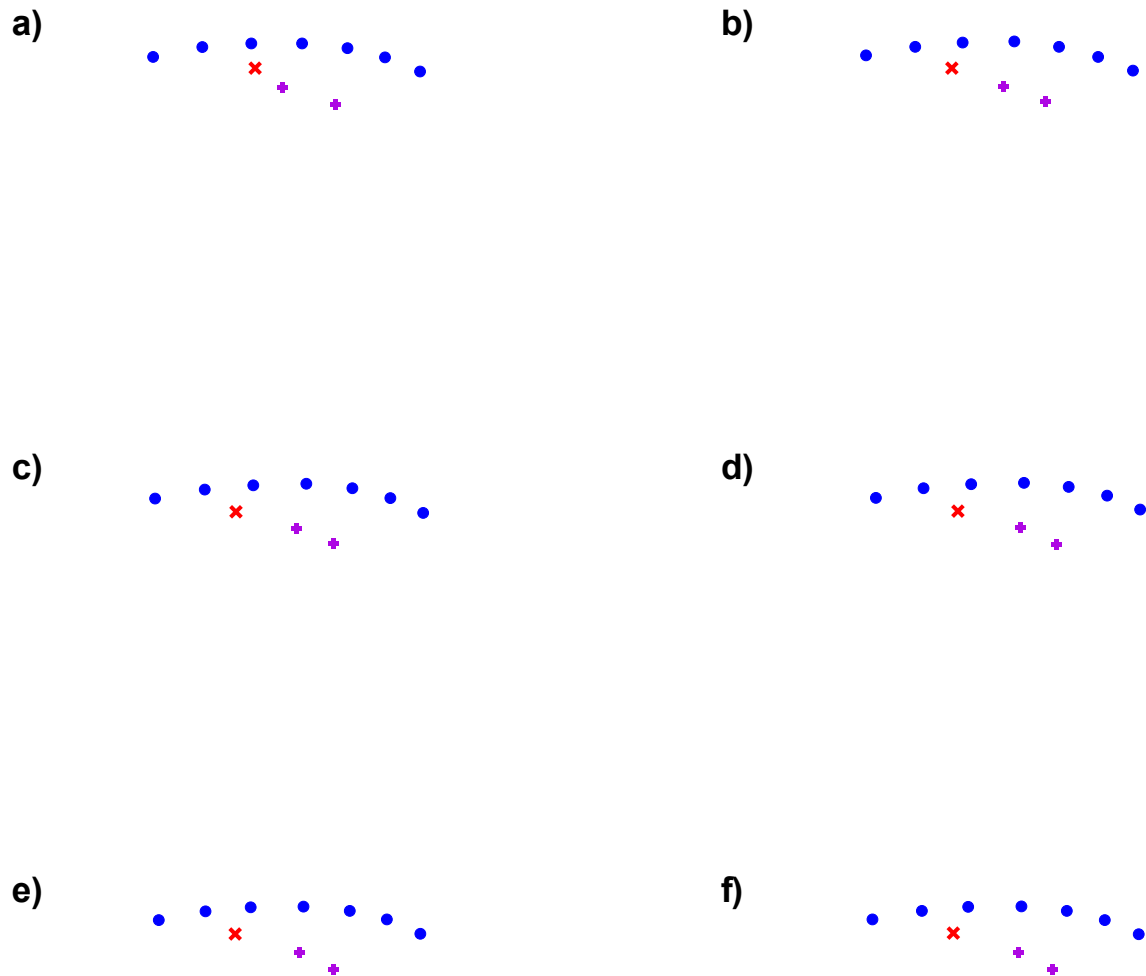


Figure F.5. Mean position of the median nerve (red x) located ulnarly to the flexor digitorum superficialis tendons of the index and middle fingers (purple +) and dorsally to the transverse carpal ligament (blue •) while ramping force up to (a) 0% MVE, (b) 10% MVE, (c) 20% MVE, (d) 30% MVE, (e) 40% MVE, and (f) 50% MVE during the power gripping condition.

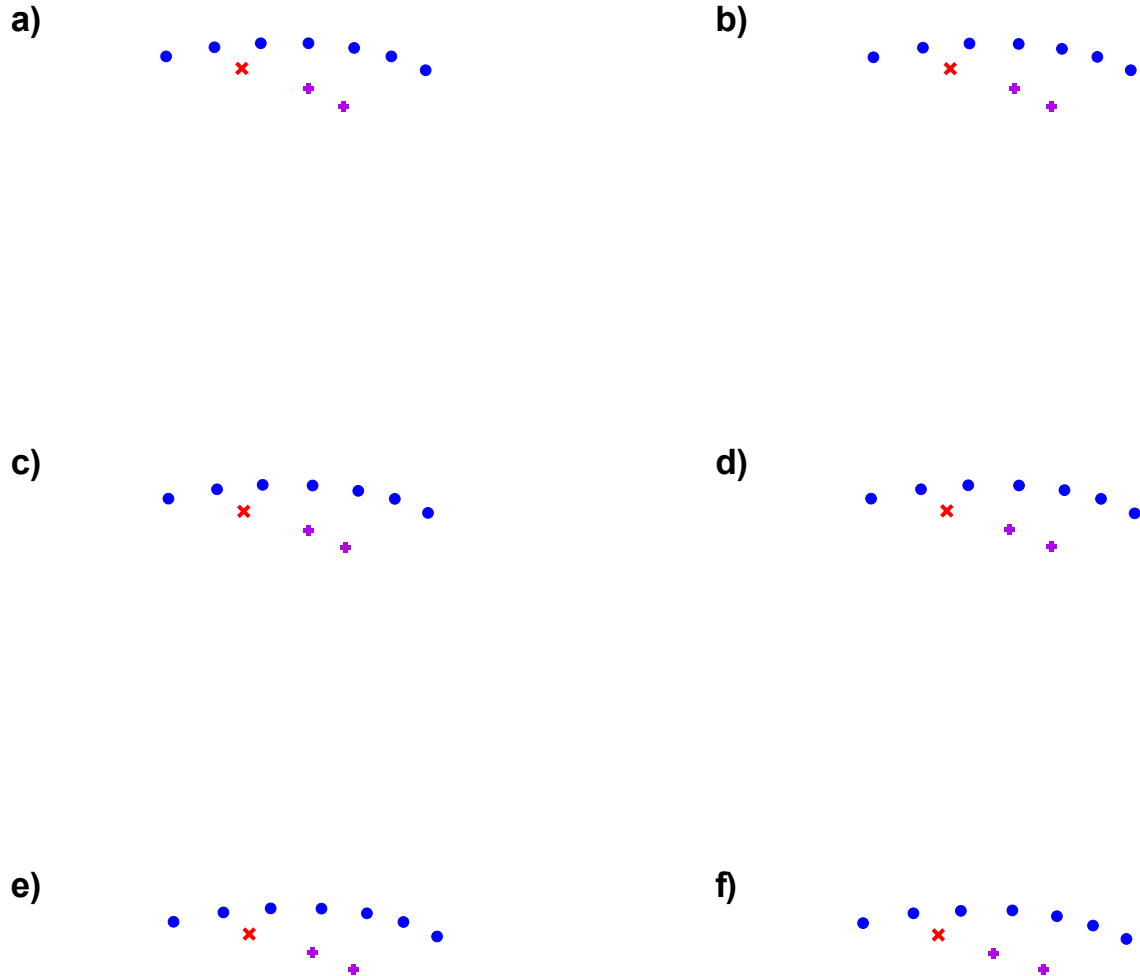


Figure F.6. Mean position of the median nerve (red x) located ulnarly to the flexor digitorum superficialis tendons of the index and middle fingers (purple +) and dorsally to the transverse carpal ligament (blue •) while ramping force down to (a) 50% MVE, (b) 40% MVE, (c) 30% MVE, (d) 20% MVE, (e) 10% MVE, and (f) 0% MVE during the power gripping condition.

Appendix G

Copyright Permission for Figure 2.1

JOHN WILEY AND SONS LICENSE TERMS AND CONDITIONS

May 11, 2021

This Agreement between Gabrielle Racine ("You") and John Wiley and Sons ("John Wiley and Sons") consists of your license details and the terms and conditions provided by John Wiley and Sons and Copyright Clearance Center.

License
Number



License date Oct 16, 2020

Licensed
Content
Publisher

John Wiley and Sons

Licensed
Content
Publication

Clinical Anatomy

Licensed
Content Title Gliding characteristics of flexor tendon and tenosynovium in carpal tunnel
syndrome: A pilot study

Licensed
Content
Author

Kai-Nan An, Megan M. O'Byrne, Peter C. Amadio, et al

Licensed
Content Date Aug 30, 2006

Licensed
Content
Volume

20

Licensed
Content
Issue

3

Licensed
Content
Pages

8

Type of use Dissertation/Thesis

Requestor
type University/Academic

Format Electronic

Portion Figure/table

Number of
figures/tables 1

Will you be
translating? No

Title MEDIAN NERVE DEFORMATION AND DISPLACEMENT INCREASE
IN CONCERT DURING GRIP TASKS IN THE TRANSVERSE PLANE OF
THE CARPAL TUNNEL

Institution
name Nipissing University

Expected
presentation
date Nov 2020

Portions Figure 1. A, Image on page 293

Gabrielle Racine
XXXXXX

Requestor
Location XXXXXX
XXXXXX
Attn: Gabrielle Racine

Tax ID

Total 0.00 USD

Terms and Conditions

TERMS AND CONDITIONS

This copyrighted material is owned by or exclusively licensed to John Wiley & Sons, Inc. or one of its group companies (each a "Wiley Company") or handled on behalf of a society with which a Wiley Company has exclusive publishing rights in relation to a particular work (collectively "WILEY"). By clicking "accept" in connection with completing this licensing transaction, you agree that the following terms and conditions apply to this transaction (along with the billing and payment terms and conditions established by the Copyright Clearance Center Inc., ("CCC's Billing and Payment terms and conditions"), at the time that you opened your RightsLink account (these are available at any time at <http://myaccount.copyright.com>).

Terms and Conditions

- The materials you have requested permission to reproduce or reuse (the "Wiley Materials") are protected by copyright.
- You are hereby granted a personal, non-exclusive, non-sub licensable (on a stand-alone basis), non-transferable, worldwide, limited license to reproduce the Wiley Materials for the purpose specified in the licensing process. This license, **and any CONTENT (PDF or image file) purchased as part of your order**, is for a one-time use only and limited to any maximum distribution number specified in the license. The first instance of republication or reuse granted by this license must be completed within two years of the date of the grant of this license (although copies prepared before the end date may be distributed thereafter). The Wiley Materials shall not be used in any other manner or for any other purpose, beyond what is granted in the license. Permission is granted subject to an appropriate acknowledgement given to the author, title of the material/book/journal and the publisher. You shall also duplicate the copyright notice that appears in the Wiley publication in your use of the Wiley Material. Permission is also granted on the understanding that nowhere in the text is a previously published source acknowledged for all or part of this Wiley Material. Any third party content is expressly excluded from this permission.
- With respect to the Wiley Materials, all rights are reserved. Except as expressly granted by the terms of the license, no part of the Wiley Materials may be copied, modified, adapted (except for minor reformatting required by the new Publication), translated, reproduced, transferred or distributed, in any form or by any means, and no derivative works may be made based on the Wiley Materials without the prior permission of the respective copyright owner. **For STM Signatory Publishers clearing permission under the terms of the [STM Permissions Guidelines](#) only, the terms of the license are extended to include subsequent editions and for editions in other languages, provided such editions are for the work as a whole in situ and does not involve the separate exploitation of the permitted figures or extracts,** You may not alter, remove or suppress in any manner any copyright, trademark or

other notices displayed by the Wiley Materials. You may not license, rent, sell, loan, lease, pledge, offer as security, transfer or assign the Wiley Materials on a stand-alone basis, or any of the rights granted to you hereunder to any other person.

- The Wiley Materials and all of the intellectual property rights therein shall at all times remain the exclusive property of John Wiley & Sons Inc, the Wiley Companies, or their respective licensors, and your interest therein is only that of having possession of and the right to reproduce the Wiley Materials pursuant to Section 2 herein during the continuance of this Agreement. You agree that you own no right, title or interest in or to the Wiley Materials or any of the intellectual property rights therein. You shall have no rights hereunder other than the license as provided for above in Section 2. No right, license or interest to any trademark, trade name, service mark or other branding ("Marks") of WILEY or its licensors is granted hereunder, and you agree that you shall not assert any such right, license or interest with respect thereto
- NEITHER WILEY NOR ITS LICENSORS MAKES ANY WARRANTY OR REPRESENTATION OF ANY KIND TO YOU OR ANY THIRD PARTY, EXPRESS, IMPLIED OR STATUTORY, WITH RESPECT TO THE MATERIALS OR THE ACCURACY OF ANY INFORMATION CONTAINED IN THE MATERIALS, INCLUDING, WITHOUT LIMITATION, ANY IMPLIED WARRANTY OF MERCHANTABILITY, ACCURACY, SATISFACTORY QUALITY, FITNESS FOR A PARTICULAR PURPOSE, USABILITY, INTEGRATION OR NON-INFRINGEMENT AND ALL SUCH WARRANTIES ARE HEREBY EXCLUDED BY WILEY AND ITS LICENSORS AND WAIVED BY YOU.
- WILEY shall have the right to terminate this Agreement immediately upon breach of this Agreement by you.
- You shall indemnify, defend and hold harmless WILEY, its Licensors and their respective directors, officers, agents and employees, from and against any actual or threatened claims, demands, causes of action or proceedings arising from any breach of this Agreement by you.
- IN NO EVENT SHALL WILEY OR ITS LICENSORS BE LIABLE TO YOU OR ANY OTHER PARTY OR ANY OTHER PERSON OR ENTITY FOR ANY SPECIAL, CONSEQUENTIAL, INCIDENTAL, INDIRECT, EXEMPLARY OR PUNITIVE DAMAGES, HOWEVER CAUSED, ARISING OUT OF OR IN CONNECTION WITH THE DOWNLOADING, PROVISIONING, VIEWING OR USE OF THE MATERIALS REGARDLESS OF THE FORM OF ACTION, WHETHER FOR BREACH OF CONTRACT, BREACH OF WARRANTY, TORT, NEGLIGENCE, INFRINGEMENT OR OTHERWISE (INCLUDING, WITHOUT LIMITATION, DAMAGES BASED ON LOSS OF PROFITS, DATA, FILES, USE, BUSINESS OPPORTUNITY OR CLAIMS OF THIRD PARTIES), AND WHETHER OR NOT THE PARTY HAS BEEN ADVISED OF THE POSSIBILITY OF SUCH DAMAGES. THIS LIMITATION SHALL APPLY NOTWITHSTANDING ANY FAILURE OF ESSENTIAL PURPOSE OF ANY LIMITED REMEDY PROVIDED HEREIN.
- Should any provision of this Agreement be held by a court of competent jurisdiction to be illegal, invalid, or unenforceable, that provision shall be deemed amended to achieve as nearly as possible the same economic effect as the original provision, and the legality, validity and enforceability of the remaining provisions of this Agreement

shall not be affected or impaired thereby.

- The failure of either party to enforce any term or condition of this Agreement shall not constitute a waiver of either party's right to enforce each and every term and condition of this Agreement. No breach under this agreement shall be deemed waived or excused by either party unless such waiver or consent is in writing signed by the party granting such waiver or consent. The waiver by or consent of a party to a breach of any provision of this Agreement shall not operate or be construed as a waiver of or consent to any other or subsequent breach by such other party.
- This Agreement may not be assigned (including by operation of law or otherwise) by you without WILEY's prior written consent.
- Any fee required for this permission shall be non-refundable after thirty (30) days from receipt by the CCC.
- These terms and conditions together with CCC's Billing and Payment terms and conditions (which are incorporated herein) form the entire agreement between you and WILEY concerning this licensing transaction and (in the absence of fraud) supersedes all prior agreements and representations of the parties, oral or written. This Agreement may not be amended except in writing signed by both parties. This Agreement shall be binding upon and inure to the benefit of the parties' successors, legal representatives, and authorized assigns.
- In the event of any conflict between your obligations established by these terms and conditions and those established by CCC's Billing and Payment terms and conditions, these terms and conditions shall prevail.
- WILEY expressly reserves all rights not specifically granted in the combination of (i) the license details provided by you and accepted in the course of this licensing transaction, (ii) these terms and conditions and (iii) CCC's Billing and Payment terms and conditions.
- This Agreement will be void if the Type of Use, Format, Circulation, or Requestor Type was misrepresented during the licensing process.
- This Agreement shall be governed by and construed in accordance with the laws of the State of New York, USA, without regards to such state's conflict of law rules. Any legal action, suit or proceeding arising out of or relating to these Terms and Conditions or the breach thereof shall be instituted in a court of competent jurisdiction in New York County in the State of New York in the United States of America and each party hereby consents and submits to the personal jurisdiction of such court, waives any objection to venue in such court and consents to service of process by registered or certified mail, return receipt requested, at the last known address of such party.

WILEY OPEN ACCESS TERMS AND CONDITIONS

Wiley Publishes Open Access Articles in fully Open Access Journals and in Subscription journals offering Online Open. Although most of the fully Open Access journals publish open access articles under the terms of the Creative Commons Attribution (CC BY) License only, the subscription journals and a few of the Open Access Journals offer a choice of Creative Commons Licenses. The license type is clearly identified on the article.

The Creative Commons Attribution License

The [Creative Commons Attribution License \(CC-BY\)](#) allows users to copy, distribute and transmit an article, adapt the article and make commercial use of the article. The CC-BY license permits commercial and non-

Creative Commons Attribution Non-Commercial License

The [Creative Commons Attribution Non-Commercial \(CC-BY-NC\) License](#) permits use, distribution and reproduction in any medium, provided the original work is properly cited and is not used for commercial purposes.(see below)

Creative Commons Attribution-Non-Commercial-NoDerivs License

The [Creative Commons Attribution Non-Commercial-NoDerivs License](#) (CC-BY-NC-ND) permits use, distribution and reproduction in any medium, provided the original work is properly cited, is not used for commercial purposes and no modifications or adaptations are made. (see below)

Use by commercial "for-profit" organizations

Use of Wiley Open Access articles for commercial, promotional, or marketing purposes requires further explicit permission from Wiley and will be subject to a fee.

Further details can be found on Wiley Online Library
<http://olabout.wiley.com/WileyCDA/Section/id-410895.html>

Other Terms and Conditions:

v1.10 Last updated September 2015

